

Dissertation in Astronomy
submitted to the
Combined Faculties for the Natural Sciences and for Mathematics
of the **Ruperto-Carola University of Heidelberg, Germany.**
for the degree of
Doctor of Natural Sciences

presented by

Licenciado D. Aday Robaina Rapisarda
born in Las Palmas de Gran Canaria, Spain

Oral examination: 25th February 2010

**Eight Gigayears of
of
Galaxy Mergers**

**Referees: Prof. Dr. Eric F. Bell
Prof. Dr. Klaus Meisenheimer**

Abstract

Galaxy interactions are expected to play a crucial role in the build-up of stellar mass in any cold dark matter cosmology. Of particular interest are the mergers between systems of a comparable mass, as they are predicted to be one of the main modes of galaxy growth and have a crucial impact in the shaping of galaxy morphologies and dynamics. In this thesis I study two key aspects of the role that mergers play in galaxy evolution: a) What is the contribution of major galaxy interactions to the star formation history of the Universe at $z < 1$?, and b) How important are galaxy interactions for the build-up of the massive end of the red sequence? To answer the first question I use photometric redshifts, stellar masses and UV star formation rates from COMBO-17, $24\mu\text{m}$ star formation rates from *Spitzer* and galaxy morphologies from two deep Hubble Space Telescope cosmological survey fields to study the enhancement in star formation activity as a function of galaxy separation. I apply robust statistical tools to find galaxies in close pairs, augmented with morphologically-selected very close pairs (unresolved in the ground-based photometry) and merger remnants from the Hubble Space Telescope imaging, finding that, on average, major galaxy interactions between galaxies more massive than $10^{10}M_{\odot}$ at $0.4 < z < 0.8$ enhance the star formation activity by a factor of less than 2. I carry out detailed modeling of the methodology using a mock galaxy catalog from the *Millenium Simulation*, finding that in the regime applicable to this work the recovered enhancement in SF rate is accurate to better than 10%, smaller than the other sources of uncertainty. Accounting for the fraction of merging and interacting systems, I integrate the enhanced star formation to demonstrate that less than 10% of star formation activity is *directly triggered* by those interactions. To answer the second question I look for close pairs of galaxies on a sample drawn from the COSMOS and COMBO-17 galaxy surveys to find that the fraction of $M_* > 5 \times 10^{10}M_{\odot}$ galaxies in close pairs (a proxy for the fraction of objects involved in an interaction) were more common 7 Gyrs ago by a factor ~ 2 . By converting this merger fraction to a merger rate I estimate that 70% of the very massive galaxies ($M_* > 10^{11}M_{\odot}$) have undergone a merger since $z = 1.2$. This merger rate is sufficient to explain the observed number density evolution of such massive galaxies in the last 7 Gyrs. Merging plays, therefore, a dominant role in the formation of massive galaxies in the Universe.

Zusammenfassung

Es wird erwartet, dass Wechselwirkungen zwischen Galaxien in jeder, auf kalter dunkler Materie aufbauenden Kosmologie eine entscheidende Rolle beim Aufbau stellarer Masse spielen. Von besonderem Interesse sind Verschmelzungen von Systemen ähnlicher Masse. Für diese wird vorhergesagt, einen der Hauptmechanismen für das Wachstum von Galaxien darzustellen und einen entscheidenden Beitrag zu leisten Morphologie und Dynamik von Galaxien zu formen. In dieser Arbeit untersuche ich zwei Schlüsselaspekte von Verschmelzungen in Bezug auf Galaxienentwicklung: a) Was ist der Beitrag der Wechselwirkungen von Galaxien ähnlicher Masse zur Sternentstehungsgeschichte des Universums bei $z < 1$?, und b) Wie wichtig sind Wechselwirkungen zwischen Galaxien um den massereichen Teil der “roten Sequenz” aufzubauen? Um die erste Frage zu beantworten benutzte ich photometrische Rotverschiebungen, stellare Massen und UV Sternentstehungsraten von COMBO-17, $24\mu\text{m}$ Sternentstehungsraten von Spitzer und Galaxienmorphologien von zwei tiefen kosmologischen Durchmusterungsfeldern des Hubble Weltraumteleskops, um die Zunahme der Sternentstehungsaktivität als Funktion des Galaxienabstands zu untersuchen. Ich wende dazu robuste statistische Methoden an, um Galaxien in engen Paaren zu finden und reiche diese Auswahl mit morphologisch ausgewählten sehr engen Paaren (nicht aufgelöst in bodengebundener Photometrie) und Galaxien in Nachverschmelzungszuständen aus Hubble Weltraumteleskop Aufnahmen an. Damit finde ich, dass im Mittel Wechselwirkungen zwischen Galaxien ähnlicher Massen oberhalb von $10^{10}M_{\odot}$ bei $0.4 < z < 0.8$ die Sternentstehungsaktivität um einen Faktor von weniger als 2 steigern. Ich führe detaillierte Modellierungen der Methodik unter der Benutzung eines künstlichen Galaxienkatalogs aus der Millenium Simulation durch und finde dabei, dass in dem in dieser Arbeit untersuchten Parameterbereich, die Erhöhung der Sternentstehungsrate mit Unsicherheiten kleiner als 10% bestimmt wird, weniger als die anderer Fehlerquellen. Unter Berücksichtigung des Anteils verschmelzender und wechselwirkender Systeme integriere ich die erhöhte Sternentstehungsrate, um zu demonstrieren, dass weniger als 10% der Sternentstehungsaktivität direkt von solchen Wechselwirkungen hervorgerufen wird. Um die zweite Frage zu beantworten, betrachte ich enge Galaxienpaare in einer Auswahl aus den COSMOS und COMBO-17 Galaxiendurchmusterungen und finde, dass der Anteil von $M_* > 5 \times 10^{10}M_{\odot}$ Galaxien in engen Paaren (stellvertretend für den Anteil von Objekten, die an Wechselwirkungen beteiligt sind) vor 7 Milliarden Jahren um einen Faktor ~ 2 grösser war. Indem ich diesen Anteil der Verschmelzungsprozesse in eine Verschmelzungsrate umwandle schätze ich ab, dass 70% der massereichsten Galaxien ($M_* > 10^{11}M_{\odot}$) seit einer Rotverschiebung von $z=1.2$ an einer Verschmelzung beteiligt waren. Diese Verschmelzungsrate ist ausreichend um die beobachtete Entwicklung der Anzahldichte solch massereicher Galaxien in den letzten 7 Milliarden Jahren zu erklären. Galaxienverschmelzungen spielen daher eine dominierende Rolle in der Entstehung massereicher Galaxien im Universum.

To Silvia, my North Star



I gazed the skies looking for the heaven, but all I found were the devil's eyes

Contents

1	Introduction	1
1.1	Galaxies in a dark Universe	1
1.1.1	Evidence for the existence of dark matter	3
1.1.2	Dark matter and hierarchical structure formation	5
1.1.3	Galaxy formation in a CDM-dominated universe	6
1.1.4	The Λ -CDM paradigm	7
1.2	Galaxy Evolution: An Empirical View	9
1.2.1	Colors and shapes: Two related problems?	11
1.3	The Role of Mergers in Galaxy Evolution	13
1.3.1	Looking for galaxy mergers	16
1.4	Galaxy Surveys	18
1.4.1	COMBO-17, GEMS, STAGES and COSMOS	19
1.5	Layout of the Thesis	20

1.5.1	Stars formed by galaxy interactions	20
1.5.2	The growth of the most massive galaxies through merging	21
2	SFR Enhancement in Galaxy Interactions	23
2.1	The Data	26
2.1.1	COMBO-17. Redshifts and stellar masses	26
2.1.2	GEMS and STAGES HST imaging data	27
2.1.3	MIPS 24 μm , total infrared emission and star formation rates	27
2.2	Sample selection and method	30
2.2.1	Projected correlation function	31
2.2.2	Visual Morphologies	33
2.3	Results	37
2.3.1	Enhancement in the Star Formation Activity	40
2.3.2	How important are mergers in triggering dust-obscured starbursts?	47
2.4	Discussion	48
2.4.1	Comparison with previous observations	49
2.4.2	What fraction of star formation is triggered by major interactions?	51
2.4.3	Comparison with theoretical expectations	55
2.5	Conclusions	57
3	Systematic Errors in Weighted 2–point Correlation Functions	59
3.1	Background	60
3.2	An idealized experiment	61

<i>Contents</i>	ix
3.3 Results	62
3.4 An example application to observations	64
3.5 Conclusions	66
4 The Merger–Driven Evolution of Massive Red Galaxies	69
4.1 Sample and method	70
4.2 Results and discussion	72
4.2.1 Comparison with previous works	74
4.2.2 The impact of galaxy merging on the creation of red $M_* > 10^{11} M_\odot$ galaxies.	76
4.3 Conclusions	78
5 Conclusions	79
Acknowledgements	83

Galaxies are clumps of stars, gas, dust and dark matter surrounded by huge volumes of relatively empty space. In our current understanding, these objects have been formed through the agglomeration of smaller clumps in a sort of dance governed by the gravitational properties of dark matter, in which all the visible components of the Universe are embedded. As the building blocks of the Universe, galaxies are one of the most important subjects of study in our effort to push the limits of our comprehension.

1.1 Galaxies in a dark Universe

In the present-day Universe, a wide variety of galaxies is within the reach of our telescopes. In an extremely simplistic view, galaxies can be assigned to one of two groups: blue objects with disk-like structures and non-prominent bulges, and red, spheroidal objects with old stellar populations. In the traditional scheme for morphological galaxy classification, first defined by Edwin Hubble back in 1926 (Hubble 1937), galaxies belonging to the first group were called ‘late type’ objects and those in the second group ‘early type’ objects. At that time, it was believed that in the galaxy formation process, the first stage was an approximately spherical, pressure supported object that would lead, given enough time, to a stage in which a disk forms and spiral arms develop. Nowadays we know this idea to be wrong, in the sense that interactions or mergers between two disk galaxies are believed to lead to the formation of an ‘elliptical’ (Toomre & Toomre 1972), and a transformation in the opposite direction is unlikely to occur (although not impossible Di Matteo et al. 2009). Mergers are not the only astrophysical process leading to changes in galaxy morphology but are clearly the most dramatic one.

In reality, the picture is more complex. Elliptical galaxies come in different flavors. There are relatively low mass early type galaxies with disk isophotes (implying some degree of rotation), which usually present an excess of light in the inner hundred of parsecs (pc). There are also very massive ellipticals with boxy isophotes and negligible rotation which display a deficit of light in the inner region (Kormendy et al. 2009). The common origin of all the galaxies in the bulge-dominated family is a matter of intense discussion nowadays (Kormendy et al. 2009; Ferrarese et al. 2006).

On the side of late-type galaxies things are not easier to describe. Although the majority of disk-dominated galaxies present non-negligible levels of star formation and blue optical colors, there is a fraction which seem to be relatively red, with little or no ongoing star formation. The relative strength of the spiral arms compared to the disk as a whole, the thickness of the stellar and gaseous disk and the ratio of stellar mass in the bulge compared to that on the disk differs dramatically from galaxy to galaxy.



Figure 1.1 *Nearby spiral galaxies. From top left to bottom right: M31 (Andromeda Galaxy), M100, M101 and NGC 4414*

As I already mentioned, the components of a galaxy that we can see in the

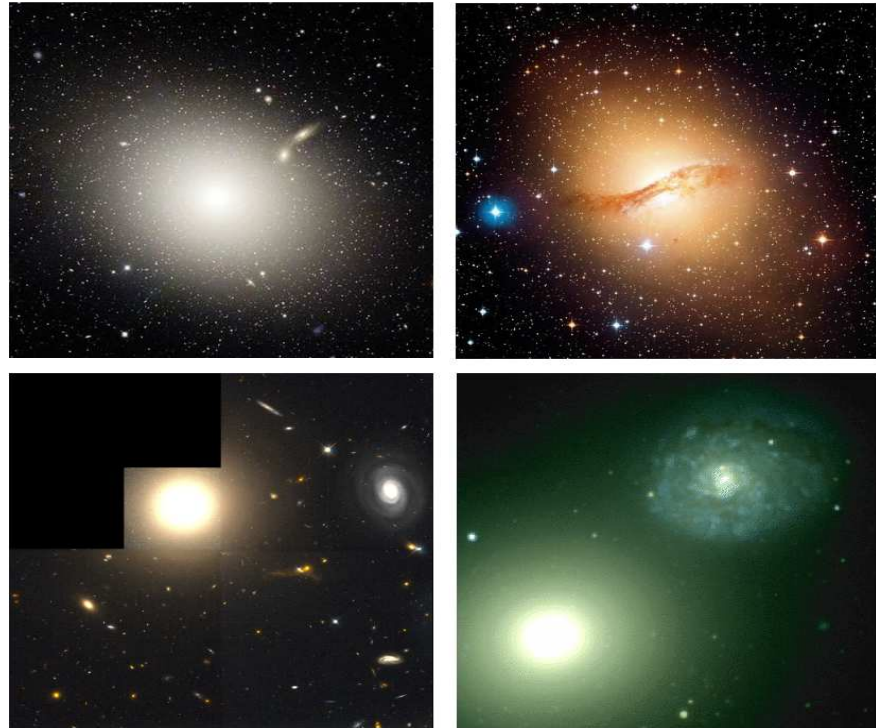


Figure 1.2 *Nearby elliptical galaxies. From top left to bottom right: M87, Centaurus A, NGC 4881 and M60 (together with the spiral NGC 4647).*

electromagnetic spectra do not sum up 100% of its composition. The dominant component, as far as gravitation is concerned, is hidden to our eyes and instruments. The stars and the gas of a galaxy are embedded in a halo of mysterious sort of matter which does not interact electromagnetically (or if it does, in an extremely weak fashion) and thus, does not emit any radiation we can detect. This unseen component of the Universe is commonly known as Dark Matter.

1.1.1 Evidence for the existence of dark matter

Since the early 30's, independent evidence for the existence of non-luminous matter in the Universe have been found, but they were not put together until the decade of the 60's, when the basic idea of the Universe was revolutionized in a way which would not be experienced again until the very end of the XX century, when an acceleration in the expansion rate of the Universe was found.

In 1933, Fritz Zwicky measured the radial velocities of clusters and large groups within the Coma supercluster, finding for some of them velocity dispersions as high as ≈ 1000 , km/s. For the first time, he applied the Virial theorem to infer the dynamical mass of the cluster, finding a value $M_{dyn}/M_{Lum} \simeq 400$ (Zwicky 1933)¹.

A particularly relevant piece of information came from the velocity curve of disk galaxies starting with the study of M31 (the Andromeda galaxy) by Babcock (1939). He found, using long-slit spectra, that the outer parts of the disk were rotating faster than what one would expect from Keplerian orbits.

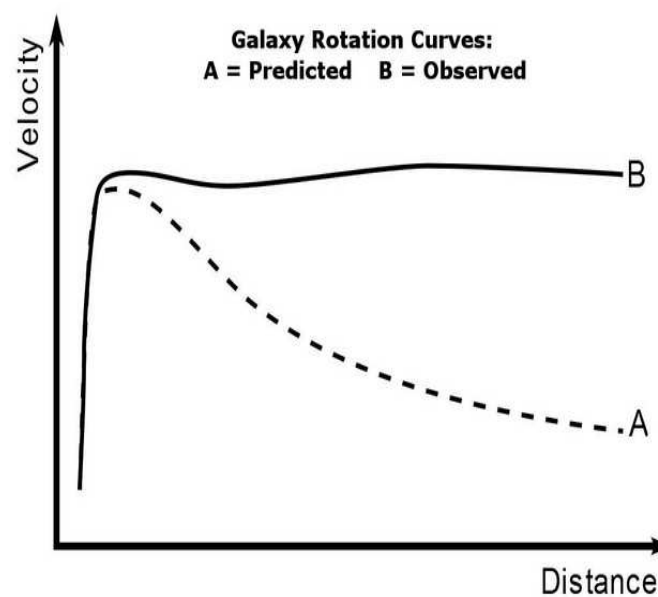


Figure 1.3 *Rotation velocity as function of the radial position in a disk galaxy. The curve A shows the expected velocity curve from Keplerian orbits when considering the luminous matter in the galaxy. The curve B shows the typical rotation curve measured in a disk galaxy.*

Further evidence comes from kinematical analysis of galaxy pairs (Kahn & Woltjer 1959), theoretical studies about the stability of galactic disks, which turn out to need the presence of a massive (unobserved) halo to reach stability (Ostriker & Peebles 1973) and the gravitational lens effect.

When all these pieces are put together, one reaches the conclusion that there are large amounts of mass in the Universe, but most of it is invisible in the

¹With a modern value for the Hubble constant H_0 one would get a value closer to 50.

electromagnetic spectrum. For this reason astronomers refer to this kind of matter as dark matter (DM).

1.1.2 Dark matter and hierarchical structure formation

Beyond the direct evidence for the existence of non luminous matter shown in the previous section, the very fact that we see structures in the Universe is pointing in the same direction.

The hierarchy of cosmic structure is assumed to have grown from primordial fluctuations (i.e., dense regions grow through the accretion of mass from its surroundings). These fluctuations are described by the density contrast δ , which is defined as the density fluctuation relative to the average density $\bar{\rho}$.

$$\delta = \frac{\rho - \bar{\rho}}{\bar{\rho}}. \quad (1.1)$$

The horizon size at the end of the radiation-dominated era (maximum distance at which two points in the Universe are causally connected) sets the limit between large structures which could grow without being suppressed during the radiation era and the small ones which could not survive. The radii of this horizon at the time of equality between matter and radiation is given by

$$r_{eq} = \frac{c}{H_0} \frac{a_{eq}^{3/2}}{\sqrt{2\Omega_{m,0}}}, \quad (1.2)$$

where a_{eq} is the scale factor of the Universe at that time, H_0 is the value of the Hubble constant nowadays and $\Omega_{m,0}$ is the dimensionless matter density at $z = 0$.

In Fourier space, the variance of the density contrast is called the power spectrum, and under the assumption that the matter contained in fluctuations of the size of r_{eq} is constant over time and that the matter is cold² (non-relativistic), the power spectrum will behave as

²Evidence for cold dark matter comes from direct observations of structure growth in the Universe. If the DM is hot, the growth scenario will be top-down, where the biggest structures are formed first and then the smallest structures. If the DM is cold the scenario would be bottom-up and the smallest structures (protogalaxies) would form first and the largest structures (superclusters) later. The observations point to a bottom-up scenario.

$$P_{\delta}(k) \propto \begin{cases} k & \text{if } k \ll k_0 \\ k^{-3} & \text{if } k \gg k_0 \end{cases} \quad (1.3)$$

with $k_0 = 2\pi r_{eq}$ being the wave number of the horizon size at the beginning of matter domination. As the size of the horizon r_{eq} was very small and increases with time, the smallest structures were formed earlier in time.

From Eq. 1.2 one can then obtain the dependency of the peak in the power spectrum (k_0) with the matter density:

$$k_0 = \frac{2\sqrt{2}\pi H_0 \sqrt{\Omega_{m,0}}}{a_{eq}^{3/2}}, \quad (1.4)$$

having into account that $a_{eq} = \Omega_{r,0}/\Omega_{m,0}$. Then, a measurement of k_0 would provide an independent measurement of $\Omega_{m,0}$.

The first successful experiments in that direction have been carried out with the *Two-Degree Field Galaxy Redshift Survey* and the *Sloan Digital Sky Survey*. By using clustering measurements which used 2–point correlation functions, these experiments have found that the total density of matter in the Universe, needed to form the observed structures is $\Omega_{m,0} = 0.24 \pm 0.02$.

From the observed ${}^4\text{He}$ abundance in the local Universe and the deuterium abundance derived from absorption systems in the spectra of high redshift quasars, the Big–Bang nucleosynthesis predicts a fraction of baryons in the Universe of $\Omega_b = 0.037 \pm 0.009$, roughly an order of magnitude smaller than the matter density needed to form the observed structures.

Direct observations of stars and cold gas in galaxies yield densities of $\Omega_{*+gas} \sim 0.0024$, which accounts only for $\sim 10\%$ of the baryon density expected from the Big–Bang nucleosynthesis predictions. The problem of where are the missing baryons is still an open question in modern Astronomy, but we believe that they are in the warm/hot gas in the intergalactic medium.

When taking together all the evidence, direct and indirect, it is clear that in order to reproduce the observed hierarchical structure growth in the Universe and the dynamics of galaxies and clusters of galaxies we need to resort to the dark matter. This dark matter has to account for roughly 80% of the matter in the Universe.

1.1.3 Galaxy formation in a CDM–dominated universe

After the radiation–dominated era, dark matter overdensities were able to collapse faster as they only had to counteract the expansion of the Universe. The first of these overdensities, which I will call haloes hereafter, were relatively small and grew through the accretion of other haloes. Still, new small haloes kept forming and being accreted by larger haloes.

As gravity is dominant interaction at these scales and dark matter dominates gravitational processes (remember that 80% of the matter in the Universe is in a non–luminous form), the baryonic content of the haloes follows the behaviour of the dark matter. On the other hand, baryons suffer electromagnetic interactions, so they act in some sense in a different way as the dark matter. Baryons which could efficiently cool collapse into a dense core in the center of the DM halo; this is what we usually call ‘galaxy’.

When the haloes merge, the galaxies in their center merge as well, therefore galaxy merging is expected to be a key process in the formation and evolution of galaxies. Furthermore, if our cosmological theories are correct, we should be able to trace the growth of dark matter haloes by the observation of galaxy mergers. In particular, mergers of galaxies of approximately equal mass are predicted to be relatively rare but easy to detect, while the much more common mergers between galaxies of very different mass are expected happen constantly but are much more difficult to observe.

1.1.4 The Λ -CDM paradigm

In the last ~ 10 years we have changed our view of the Universe. The experiments studying the redshift–distance relations from type Ia supernovae (Riess et al. 1998; Perlmutter et al. 1999) have discovered that our Universe is not only not decreasing the rate of expansion, but it is accelerating. The responsible for this acceleration is believed to be some sort of dark energy, which has the particularity of producing a negative pressure (although see Aguirre 1999; Robaina & Cepa 2007 for a discussion of the systematic uncertainties). The Cosmic Microwave Background (CMB) has also been extensively studied in this period, specially thanks to the observations from the Wilkinson Microwave Anisotropy Probe (WMAP, Spergel et al. 2007), which have pointed to a flat Universe with a significant fraction of dark matter in a

non-baryonic form. Every cosmology which takes into account the existence of dark energy (in whatever exotic form) and dark matter is usually labelled as a Λ CDM cosmology.

It is expected from cosmological simulations that dark matter haloes grow in size as the Universe ages by means of mergers of smaller units, building up the DM distribution we can infer today from wide-area galaxy surveys. Since the DM largely dominates the clustering in the Universe, it is reasonable to imagine that galaxy mergers, the topic of this thesis, will follow the trend imposed by the merging of DM haloes. As the baryons are interacting particles, they are subject to more processes than the DM, whose behaviour is largely governed by gravity, as evidenced by the lack of electromagnetic emission³. Friction, collisions and other physical processes cause the exact behaviour of a galaxy merger to deviate from that of the DM, specially in the latest phases of the interaction, when the two dark matter haloes have already merged.

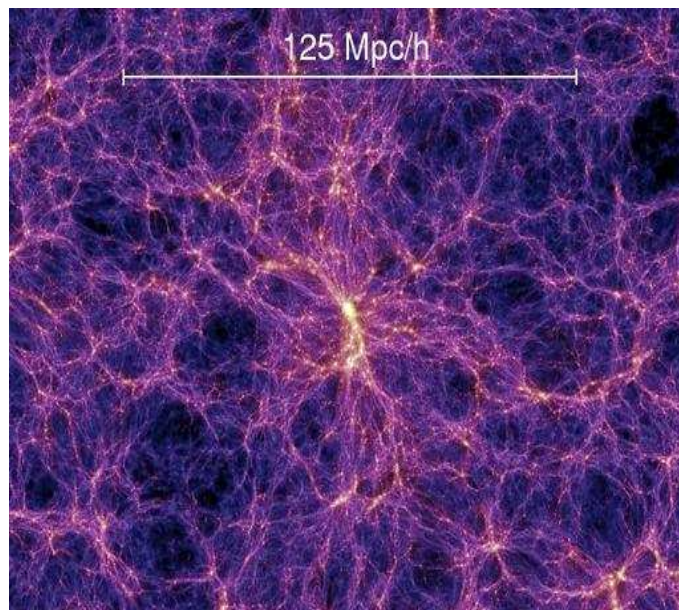


Figure 1.4 *Dark matter distribution in the Universe as predicted by the Millennium Simulation (Springel et al. 2005)*

As we lack the capability of observing DM directly, an important fraction of our knowledge about DM behavior comes from simulations. For the purpose of understanding the physics of DM halo mergers, even when extremely successful

³Also, recent studies have found very low upper limits for dark matter self-interaction cross-sections in the cluster-cluster collision known as the ‘Bullet Cluster’ (Markevitch et al. 2004).

numerical simulations as the *Millennium Simulation* (Springel et al. 2005) have been produced, the computation of huge realizations with enough resolution is prohibitively expensive. A strong alternative is to run semi-analytical models (SAM), which often base the treatment of the DM in the extended Press-Schechter formalism (Press & Schechter 1974; Bond et al. 1991). The basic idea of this formalism is the description of the mass history of particles in a hierarchical Universe with gaussian initial perturbations, and specifically it aims to provide the conditional mass function. It has been proved that merger rates and halo survival times within this formalism agree with N-body simulations (Lacey & Cole 1993, 1994), making SAMs a valuable tool for the study of mergers in the Universe.

1.2 Galaxy Evolution: An Empirical View

One particularly interesting parameter space concerning studies of galaxies is the one involving optical color and stellar mass (or luminosity). It has been known for some time that the distribution of nearby galaxies in such a diagram shows a bimodality: red galaxies appear in a relatively tight sequence (for obvious reasons known as red sequence) while blue galaxies show a wider dispersion and appear in the so-called blue cloud (e.g. Blanton et al. 2003). Other studies, like Bell et al. (2004) or Taylor et al. (2009) have found that such a bimodality is already in place at earlier times, in particular out to $z \simeq 2$. Those works (e.g., Borch et al. 2006) also show that the global stellar density of the Universe has grown by a factor of ~ 2 in the roughly 8 Gyrs between $z \simeq 1$ and $z = 0$ (see Fig. 1.6).

The intriguing aspect is that the stellar density corresponding to blue cloud galaxies (where new stars are expected to be formed) has barely been altered, implying that most of that growth has been produced in the red sequence (Bell et al. 2004; Borch et al. 2006; Faber et al. 2007). This result has a strong implication: in order to reproduce the observed evolution in the color-stellar mass diagram, galaxies have to migrate from the blue cloud to the red sequence by means of a process in which the star formation (SF) in the galaxies is quenched (Bell et al. 2007; Walcher et al. 2008)

It has also been observed that galaxies in the Universe are forming less and less stars with time. In the time interval since $z \sim 1$ the star formation density has decreased by one order of magnitude (Madau et al. 1996; Lilly et al. 1996).

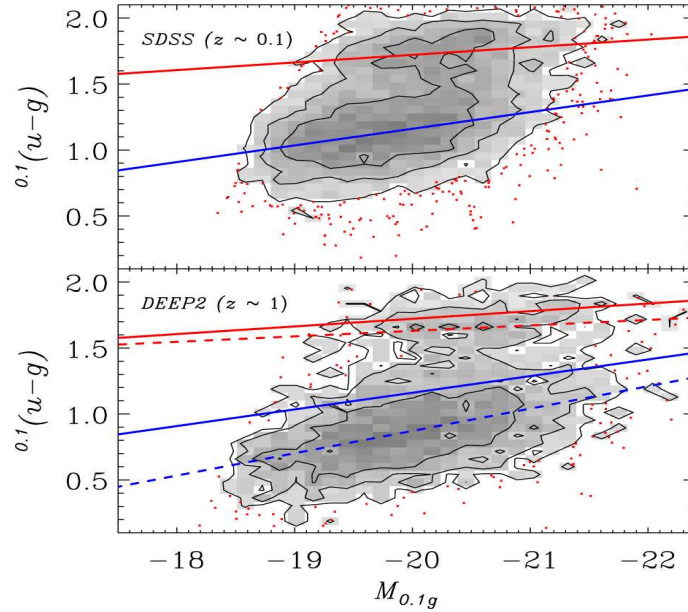


Figure 1.5 Color–magnitude diagram of galaxies. Top panel: Galaxies from the SDSS. Bottom panel: Galaxies from the DEEP2 survey. A clear bimodality is present at both redshifts. Red galaxies tend to be found in a relatively narrow region while blue galaxies show a larger dispersion. Figure taken from Blanton (2006)

Nowadays, we know that the bulk of the star formation takes place in the disk of undisturbed blue galaxies Hammer et al. (2005); Bell et al. (2005). If the majority of the stars are formed in disk galaxies at different redshifts and the number density of such objects is approximately constant, this implies that the evolution of the cosmic SFR is not only a consequence of the transition of galaxies from the blue cloud to the red sequence, but also *star forming* galaxies are also forming less and less stars as the Universe ages.

An independent point of view has been provided by the work from Noeske et al. (2007), who have shown how the star formation among star-forming galaxies scales both with the stellar mass and redshift. This is, at a given redshift, the more massive star-forming galaxies are forming stars faster than lower mass counterparts, and at a given mass, star-forming galaxies did form stars faster at higher redshift.

Another interest aspect is the evolution of the massive galaxy population, which seems to have increased considerably since $z \sim 1$. Observations have found a significant increase in the number density of $L \geq L_*$ red galaxies since $z = 1$, although systematic uncertainties in the photometry of $L > 2 - 3L_*$ galaxies

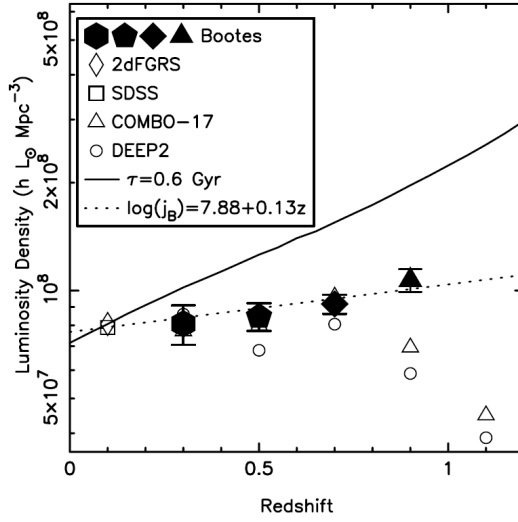


Figure 1.6 *Rest-frame B band luminosity density as a function of redshift. Points show different measurements while the solid line shows the expected luminosity density evolution taking into account passive luminosity evolution. The stellar-mass in red galaxies needs to increase by a factor of 2 since $z = 1$. Brown et al. (2007).*

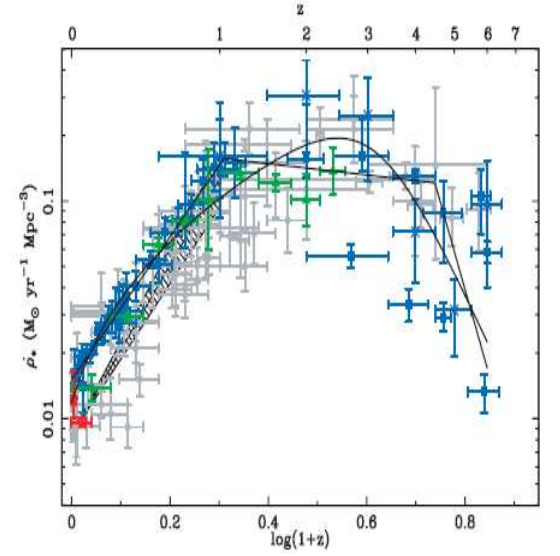


Figure 1.7 *Star formation history of the Universe. Data points show star formation density. The SFR density has decreased by one order of magnitude from $z = 1$ to $z = 0$. Figure taken from Hopkins & Beacom (2006)*

makes difficult the study of the evolution of such rare objects (Brown et al. 2007). As, by definition, quiescent galaxies do not form stars, the growth of the massive end of the red sequence has to be caused either in a process in which massive blue galaxies are rapidly transformed into red systems by the quenching of their star formation or in a process which accounts for the formation of massive galaxies from adding-up the stellar masses of lower mass objects.

Overall, we believe that galaxies are being forced to migrate from the blue cloud to the red sequence by some quenching mechanism (or mechanisms), star-forming galaxies are rapidly decreasing their star formation rate and the number of massive, quiescent galaxies is increasing.

1.2.1 Colors and shapes: Two related problems?

When studying in depth large samples of galaxies in the local Universe, many relations between different photometric and structural properties arise. A good example are the results from Blanton et al. (2003), who found relations between color, magnitude, central surface brightness and structure of the galaxies (see Fig. 1.8). Focusing on the relations between color and structure, expressed as the Sersic index of the light profile, it is evident that red galaxies tend to be spheroidal (or at least concentrated) as indicated by their high Sersic index, but also, spheroidal galaxies tend to be red in their optical colors. Moreover, recent work from van der Wel et al. (2009) has shown that in the local Universe, *all* quiescent massive galaxies are round. It is not illogical to think, then, that the process which quenches the star formation could be related to the process by which galaxies transform from disks to spheroids.

In what concerns the migration from the blue cloud to the red sequence, this is, for the quenching of the star formation, several mechanisms have been held responsible. Supernova and active galactic nuclei (AGN) feedback could produce such a behaviour through their impact on the cold gas present in the galaxy (Silk & Rees 1998). The total energy injection by those objects could be enough to heat up the gas or even to expel it from the galaxy, having the net effect of preventing the birth of new stars. Gas-heating by virial shocks of gas infalling in a massive dark matter halo (Birnboim & Dekel 2003) or gravitational heating of the gaseous disk by clumpy mass infall (Dekel & Birnboim 2008) could produce the same effect. In addition, environment-related processes like the different manifestations of Ram-pressure stripping (stripping of cold gas from the disk or hot gas from the halo, preventing subsequent cooling and infall) could also remove the cold gas from galaxies.

Some of these environment-related processes, like galaxy harassment could produce the concentration of the surface brightness profile, and also the accretion of cold gas from the cosmic web at $z > 1$ has been proposed to rapidly form massive bulges in disk-like galaxies (Dekel & Birnboim 2008). Although these processes can certainly produce the concentration of the light profile, none of them has been proved to be capable of the formation of a massive, symmetric elliptical galaxy.

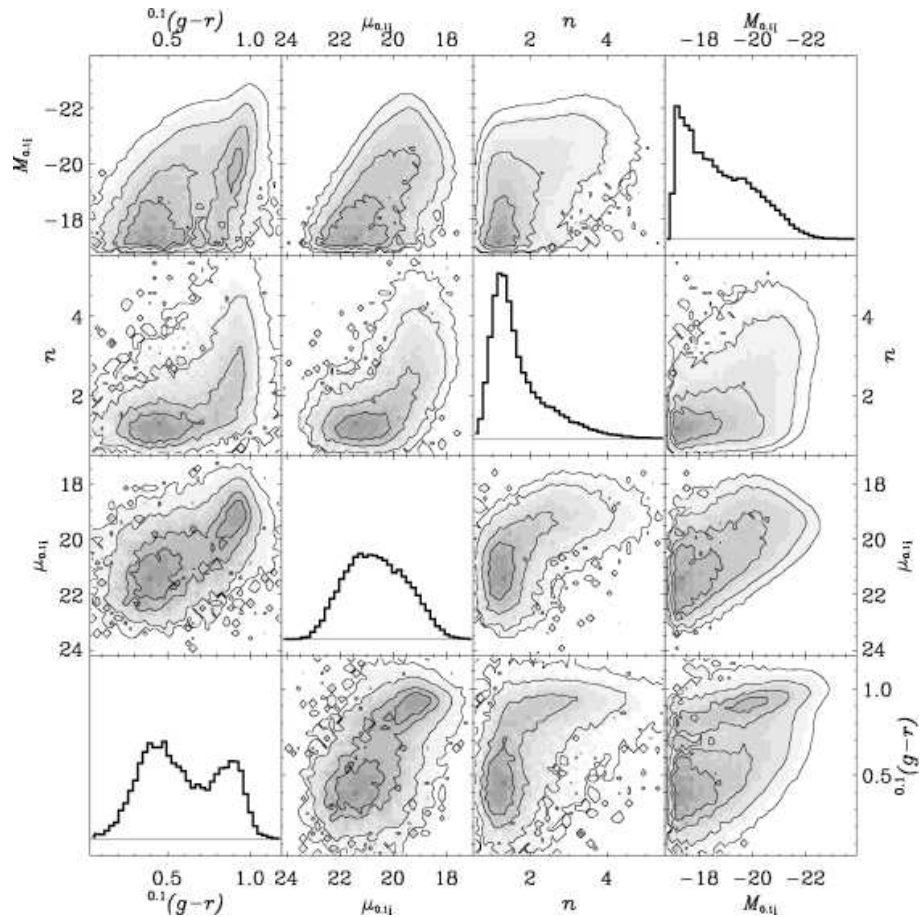


Figure 1.8 Relations between different properties of galaxies in the SDSS. $g-r$ is the optical color, μ the central surface brightness, n the sersic index and M the absolute magnitude.

1.3 The Role of Mergers in Galaxy Evolution

The first evidence for the impact of interactions on the global picture of galaxy evolution can be traced to the times of the World War II. In a pioneering work, Holmberg (1940) realized that the morphology of a galaxy depends on the number of close companions:

“This simplified scheme of distribution of nebular types suggests strongly that the type of an object is in some way dependent on the existence of physical companions. Furthermore, it suggests that the separation of the companions has some bearing on the problem of type [...]. Each passage of the components through pericenter produces, however, certain tidal effects, and consequently the orbits gradually contract [...]. The tidal effects corresponding

to successive pericenter passages may result in gradual changes in the form and the size of the nebula, just as the orbit is gradually contracted [...]. The following mechanism is suggested for the transformation of types of nebulae belonging to a double (or multiple) system, i.e., for the transformation of late spirals into early spirals or elliptical objects [...].”

Early simulations by Holmberg (1941)⁴ and Toomre & Toomre (1972) showed that collisions between disk-galaxies lead to remnants with properties similar to spheroidal galaxies, and that idea has been repeatedly used since then to explain the origin of massive galaxies, in good agreement with predictions of the Λ -CDM hierarchical cosmology. With time, the idea that mergers of disk galaxies lead to the formation of elliptical galaxies gained strength to the point that is frequently invoked as the dominant (if not unique) process capable of creating a massive, quiescent, truly red and dead, elliptical galaxy (van der Wel et al. 2009).

Although it is clear that the orbits of stars in such collisions are ‘heated’ and consequently randomized with the consequence of the transformation of disks into ellipticals, the exact process by which the star formation is quenched is still a matter of debate. Major mergers between gas-rich galaxies have been traditionally expected to trigger starbursts (Mihos & Hernquist 1996a), which could produce the depletion of the gas reservoir in a relatively short timescale. Furthermore, the starburst will produce a relatively high number of supernovae, commonly invoked to explain the heating of the cold gas, and the feedback caused by the energy deposition on the interstellar medium (ISM) by the AGN (which would be also triggered by the funnelling of gas to the central region during the interaction) would have a similar effect Kauffmann & Haehnelt (2000).

Independently of the exact mechanism responsible for the quenching of the star formation activity it is clear that galaxy interactions involving blue, gas-rich galaxies have the net effect of moving galaxies from the blue cloud to the red sequence in a color-mass diagram (e.g., Ruhland et al. 2009; Bell et al. 2007). An obvious consequence of any galaxy merger is the creation of a remnant more massive than the individual progenitors, this is, the creation of a more massive galaxy without the need of further star formation.

⁴In 1941 Erik Holmberg performed what is believed to be the first N-body simulation applied to an astronomical problem by using light-bulbes as the mass particles and the light intensity on each light-bulb as a tracer of the gravitational force.

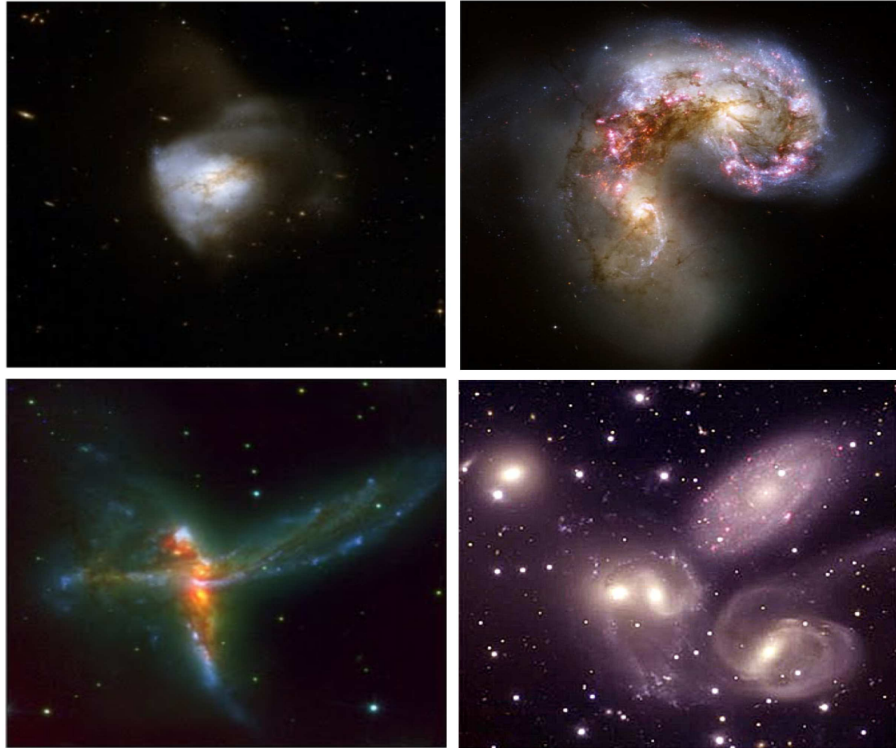


Figure 1.9 *Gas-rich galaxy mergers in the local Universe. From top left to bottom right: Arp 220, The Antennae Galaxies (NGC 4038/NGC 4039), The Bird (IRAS 19115-2124), Stephan's Quintet (NGC 7317, 18a, 18b, 19, 20).*

In addition to mergers involving blue galaxies, dry⁵ mergers between passive galaxies are yet another mechanism that could shape the color-mass diagram. As the galaxies involved in such an interaction are already quenched, and by definition red, they do not produce migration from the blue cloud to the red sequence, but re-shape the latter by moving objects within that sequence causing a tilt in the massive end and a decrease of the color dispersion (Skelton et al. 2009). Observational evidence of those interactions (van Dokkum 2005; Bell et al. 2006a) points to an scenario in which this process is very relevant for the formation of the most massive elliptical galaxies in the Universe.

Unfortunately, even when some studies have tried to quantify which fraction of red sequence/massive galaxy growth is caused by galaxy merging (e.g., Bundy et al. 2009), uncertainties related to number statistics and merging timescales make necessary a deeper study of the problem.

⁵In this context, ‘dry’ refers to the absence of cold gas, and therefore dissipation in the form of star

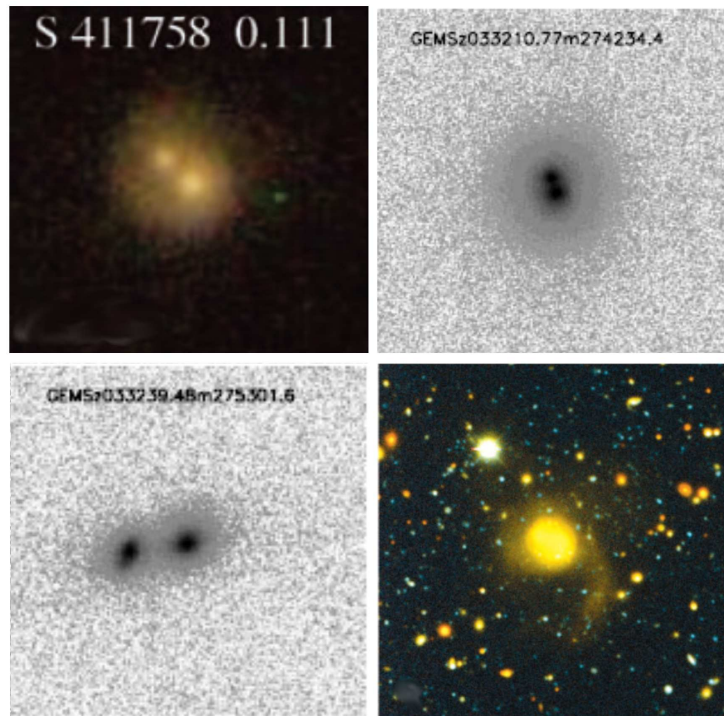


Figure 1.10 *Dissipationless (dry) mergers. The absence of prominent tidal features make these objects extremely difficult to find.*

Another interesting aspect of galaxy merging is, as opposite to the SF quenching, the already mentioned SF enhancement that they produce for a short period when two gas-rich galaxies interact (Mihos & Hernquist 1996a; Cox et al. 2008). Early studies of ultraluminous infrared galaxies (ULIRGS) in the local Universe found that $\sim 90\%$ of such extreme starbursts present evidence of a recent merger (Sanders et al. 1988), but the (wrong) interpretation that mergers could be important for the SFR in a cosmological context came a few years later. In the late 90's, it was noted that the strong decrease of the cosmic SFR density between $z = 1$ and $z = 0$ (Lilly et al. 1996, Madau et al. 1996) was not dissimilar from the relatively rapid drop in merger rate inferred (at that time) from close pairs and morphologically-selected mergers (Le Fevre et al. 2000). If much of the star formation at $z > 0.5$ were triggered by merging, the apparent similarity in evolution between SFR and merger rate would be a natural consequence. More recently, studies about the fraction of SF in morphologically-selected interacting and merging galaxies at intermediate

formation

redshifts $z < 1$ have demonstrated that, in fact, the bulk of star formation is in quiescently star-forming disk-dominated galaxies (Hammer et al. 2005, Bell et al. 2005).

Still, even when we know that galaxy mergers are not the main driver of the evolution of the cosmic SFR density, there are some key questions unanswered, like the exact amount of stellar mass that galaxy mergers add to the global mass budget of the Universe or how enhanced is the SFR in interacting galaxies when compared to objects not undergoing an interaction.

1.3.1 Looking for galaxy mergers

Overall, mergers are, potentially, an important ingredient in the recipe of galaxy evolution, so finding the exact rate at which galaxies merge is crucial to understand the global picture. Measurements of the merger rate (number of mergers per unit time or equivalently, number of mergers that a galaxy goes through in a given time) have been pursued abundantly in the literature following different methodologies and finding a variety of results, although in the latest times the results tend finally to converge.

The main problem in order to measure a merger fraction is the identification of those objects. The process of merging is long, and the galaxies undergoing a merger go through a variety of phases from the early state when they ‘feel’ the gravitational potential of the companion for the first time to the final stage in which they have coalesced and the remnant presents an spheroidal, relaxed shape.

There are mainly two approaches to find galaxy mergers: the first one is the morphological analysis of the interacting system, which typically generates clear signs of gravitational interaction like tidal tails, bridges and shells⁶ and the second is the identification of the individual galaxies as a close pair before coalescence.

A number of uncertainties come into the game of the morphological analysis. The strength of the tidal features is strongly shaped by structural parameters as the bulge-to-total ratio (B/T), gas fraction or mass ratio between the two galaxies. Orbital parameters like relative orientation of the disks or impact

⁶Although the morphological identification of dissipationless mergers is extremely hard because of the low surface brightness of tidal tails and bridges.

parameter, are also going to affect strongly the tidal debris (Di Matteo et al. 2007; Cox et al. 2008). The selection of the sample plays also a key role in the merger fraction found, as luminosity-selected samples (opposed to mass-selected) are more sensitive to issues like M/L ratio variations because of purely passive luminosity evolution or because of merger-triggered SF.

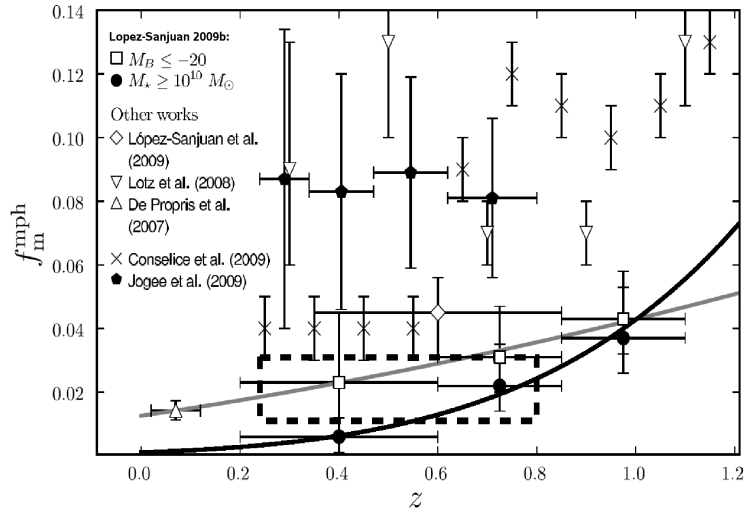


Figure 1.11 *Recent galaxy merger fractions estimated from galaxy morphologies. Dotted-line region shows the estimate for major mergers-only from Jogee et al. (2009). Figure taken from Lopez-Sanjuan et al. (2009).*

In Fig. 1.11 I show a compilation of recent results of galaxy merger fractions estimated through morphology. A variety of results have been found for both the zeropoint of the merger fraction and its evolution with redshift. This large spread between different studies is too big to be caused by cosmic variance, and it is mainly a result of different sample selection plus different identification techniques. To make it even worse, it is extremely expensive, in terms of manpower, to visually classify samples of thousands or tens of thousands of galaxies, and automated galaxy classifiers like CAS (Concentration, Asymmetry and Clumpiness, Conselice et al. 2003) or Gini/ M_{20} (Lotz et al. 2004) at intermediate and high redshift usually give as an output merger fractions higher than the visually-classified merger fractions⁷. In a recent work (Jogee et al. 2009) we have found that this is mainly due to the misclassification of lopsided or slightly irregular, non interacting disk galaxies. When one puts together

⁷The reader should remember that automated methods have been tuned to reproduce the visual classifications in the local Universe.

the poor performance of automated classifiers, the systematic uncertainties related to orbital parameters or galaxy structure and the lack of information about the progenitor galaxies, the reliability of galaxy morphologies in order to extract physical information is in jeopardy.

The other widely-used method to find galaxy mergers, is the identification of close galaxy pairs which are in an early stage of the interaction. The main advantage with respect to morphological studies is that the identification of interacting systems does not depend on orbital or structural parameters and that progenitor galaxies can be studied in detail. On the other hand, projection effects (galaxies which are relatively close on the plane of the sky but separated by large distances in the line-of-sight dimension) have been a concern for the community. This concern about projection effects has given more reliability to pair fractions from spectroscopic surveys, which produce, when compared to spectro-photometric redshift surveys, higher-quality redshift determinations.

In the last years, the projection effect issue in the spectro-photometric redshift surveys has been overcome by the use of two-point correlation function techniques applied to the study of close physical pairs, which allow astronomers to use wide-area surveys without having to deal with systematic effects present in spectroscopic surveys like fiber collisions, or in general, instrumental problems caused by the small distance (\sim galaxy size) between the two galaxies on the focal plane (Masjedi et al. 2006; Bell et al. 2006b; Masjedi et al. 2008).

1.4 Galaxy Surveys

In order to study the galaxies in the Universe, one should make use of information about all the components of a galaxy. Stars, gas, dust and accelerated particles like electrons and cosmic rays produce different electromagnetic spectra, and force the astronomers to sample the global spectra of the galaxies in as many windows of the spectra as possible.

Stars emit most of their light in the ultraviolet ($\lambda \lesssim 3800\text{\AA}$), visible (3800\AA - 7500\AA) and near-infrared (7500\AA - $6\mu\text{m}$). Dust absorbs part of the UV radiation produced by massive stars and AGNs and reemits it as mid and far-infrared ($6\mu\text{m}$ - 1mm). Cold gas like molecular hydrogen or CO is detected in the radio wavelengths, as well as the non-thermal processes involving synchrotron radiation at low energies used to trace particles accelerated by AGNs or star

forming regions. On the high energy side, some galaxies also display an spectra ranging from the soft X-rays (a few keV) to extremely energetic TeV, again produced by particles accelerated by an AGN or by processes involving extreme objects like pulsars, micro-quasars or wolf-rayet stars through physical mechanisms like inverse-compton and p-p and p- γ interactions.

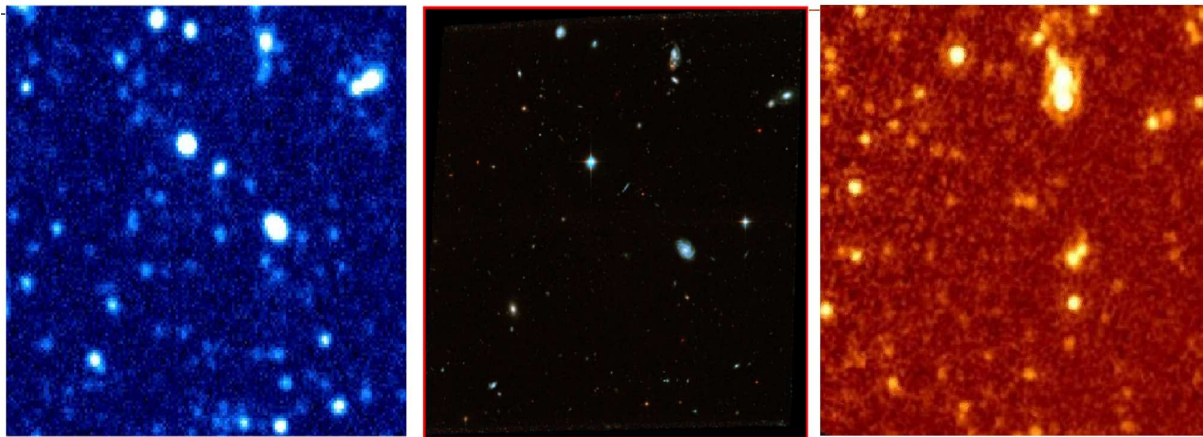


Figure 1.12 *Multiwavelength view of a tile in the GEMS field. Left: In UV as seen by Galex. Center: In visible as seen by HST. Right: In 24 μm as seen by Spitzer.*

It's clear that the observations needed are strongly shaped by the question one wants to answer. The experiments I'll carry out in the next chapters will make use, directly or indirectly, of visible and NIR light to characterize the stellar populations, UV and mid-infrared to study the SF properties (through the tracking of the dust-obscured and unobscured light from young stars) and of X-rays to track the contribution of AGNs to the heating of dust.

1.4.1 COMBO-17, GEMS, STAGES and COSMOS

The first step in order to perform an appropriate study on galaxy evolution is to get information about the spectra of galaxies. It's extremely important to know the redshift of galaxies, as a proxy for the age of the Universe at the time the radiation (this is, the information) was emitted. There are two options, either perform a spectroscopic survey to extract high resolution information and get an accurate redshift measurement or to perform a photometric survey, in which the redshift information would be acquired by the fitting of the photometric points to a set of template spectral energy distributions (SED). The first

approach has the clear advantage of the resolution, but the disadvantage of being extremely expensive in terms of telescope time, as one would have to integrate for long times in order to get an appropriate signal to noise and will be limited by the number of spectra which can be obtained simultaneously by current spectrographs placed in large enough telescopes (needed to get spectra at intermediate and high z) as VIMOS (VLT), FORS (VLT) or DEIMOS (KECK).

In this thesis I'll work with spectro-photometric redshift surveys like COMBO-17 (Wolf et al. 2003, 2004). COMBO-17 was designed to give accurate photo- z 's ($\Delta z/(1+z) \sim 0.03$ down to $m_R = 23.5$) and stellar masses (Borch et al. 2006). Observations in 5 broad bands and 12 medium bands were performed in 5 fields, giving a total of 1.25 square degrees, of which two or three fields will be used for the work presented here.

Two of the COMBO-17 fields (ECDFS and A901/2) have been also observed with the Hubble Space Telescope (HST) in the projects GEMS (Galaxy Evolution from Morphologies and SEDs) and STAGES (Space Telescope A901/902 Galaxy Evolution Survey) with the aim to study galaxy morphologies. GEMS (Rix et al. 2004) has imaged 0.25 square degrees in F606W and F850LP bands, roughly corresponding to V and Z band respectively, down to $m_{AB}(F606W) = 28.3(5\sigma)$ and $m_{AB}(850LP) = 27.1(5\sigma)$. It's still the biggest color galaxy evolution survey performed with HST and has produced more than 8000 matches for COMBO-17 galaxies. If GEMS was targeting the evolution of galaxy properties with redshift, STAGES (Gray et al. 2009) main aim is the study of the environmental dependencies of those properties. The 0.25 square degree field (in F606W band) encompasses an extremely complex multicluster system which includes the galaxy clusters A901 and A902, as well as the groups A901b and the South-West group. In §2 I'll make use of these data, together with *Spitzer* mid-IR photometry in order to study the effect of galaxy interaction on the SFR of galaxies.

COSMOS (Scoville et al. 2007) is a galaxy survey which comprises multiwavelength information from X-rays to radio including the biggest single-band mosaic taken by HST. Its large area makes of COSMOS an ideal data sample in order to perform many studies of galaxy evolution, specially those involving morphologies of galaxies at intermediate redshifts. In §4 I'll use COSMOS data in order to study the impact of major mergers on the evolution of massive, red spheroidal galaxies.

1.5 Layout of the Thesis

It is clear that galaxy mergers affect the build-up of stellar mass in galaxies in two main ways: the formation of new stellar mass (i.e., merger-triggered star formation), and the rearrangement of already-existing stars into more massive galaxies with (potentially) different structures. I study both of these modes of growth here.

1.5.1 Stars formed by galaxy interactions

As I have explained, the role played by galaxy mergers on the star formation activity of galaxies is crucial, as they can both enhance the star formation rate in the initial phases and suppress it in a more advance phase. Early studies on extremely bright IR galaxies in the local Universe (Sanders et al. 1988) had a considerably impact on the astronomical community, and for many years the idea of a cosmic star formation history driven by merger activity was seriously considered. More recently, studies showing that galaxy mergers host less than 30% of the star formation density at $z < 1$ have disproved such a scenario, but still, if galaxy interactions are *directly* responsible for all that star formation that would have large consequences on the mass distribution between the blue cloud and the red sequence. As major mergers are expected to lead to red spheroidal galaxies, an extra 30% of stellar mass would imply a dominant role of the quenching of blue galaxies over the build-up of mass from mergers between already existent red galaxies. Moreover, as the merger-induced starburst is expected to be centrally concentrated, the color, surface brightness and alpha-enhancement⁸ of merger remnants should show strong gradients. In Chapter 2 I will use photometric redshifts, stellar masses and UV SFRs from COMBO-17, $24\mu\text{m}$ SFRs from *Spitzer* and morphologies from two deep Hubble Space Telescope (HST) cosmological survey fields (ECDFS/GEMS and A901/STAGES) to study the enhancement in SFR as a function of galaxy separation and find which fraction of star formation is *directly triggered* by major galaxy interactions. In Chapter 3 I will also produce a toy-model, based on the *Millenium Simulation*, which will be used to test the statistical tools that are frequently applied to the study of the enhancement of galaxy properties as a

⁸Excess of α -elements with respect to iron expected to be present if the timescale for the star formation is shorter than ~ 1 Gyr, the time needed for type Ia supernovae to enrich the interstellar medium with iron.

function of galaxy separation.

1.5.2 The growth of the most massive galaxies through merging

The stellar mass in galaxies grows through the formation of new stars from cold gas (the mode we study in Chapters 2 and 3), and through the addition of already-formed stars to a galaxy through mergers. A cursory investigation of the properties of low-mass disk-dominated galaxies leads one to expect that the accretion of gas and formation of new stars is the dominant mode of growth for these low-mass, disk-dominated, typically rather gas-rich galaxies. Yet, high-mass galaxies tend to lack cold gas, making growth through star formation less relevant. For these galaxies, the main mode of growth may be through galaxy merging.

Unfortunately, there are very few observational studies trying to assess the real impact of galaxy mergers in the creation of massive red spheroids, and from those (e.g., Bundy et al. 2009), no conclusive evidence can be inferred. In Chapter 4 I will quantify the impact of galaxy mergers on the evolution of massive red galaxies. I will measure the fraction of galaxies in close ($r < 30$ kpc) physical pairs at $z < 1.2$ by using robust 2-point correlation function statistics on a sample of ~ 18000 $M_* > 5 \times 10^{10}$ galaxies drawn from the COSMOS and COMBO-17 surveys and I will compare the observed evolution in the number density of very massive red galaxies with the evolution implied by the measured merger rate.

Chapter 2

SFR Enhancement in Galaxy Interactions

In the previous chapter I have presented the open issues in the relation between galaxy mergers and SFR. I will extend now the motivations for the study of such relation and the possible implications.

Observational evidence from a variety of angles indicates that galaxy interactions and mergers of galaxies can lead to dramatically-enhanced star formation (Sanders et al. 1988; Barton et al. 2000; Lambas et al. 2003; Barton et al. 2007). This appears to hold true at all redshifts where one can recognize mergers through galaxy morphologies ($z \leq 1$ with rest-frame optical morphologies; Melbourne et al. 2005; Hammer et al. 2005; $1 \leq z \leq 3$ using less certain UV morphologies Chapman et al. 2004). Ultra-luminous infrared galaxies (ULIRGs), representing the highest-intensity star formation events at low redshifts, are almost invariably hosted by merging galaxies (Sanders et al. 1988). For a number of applications the quantity of interest is the *average* enhancement in star formation (SF) triggered by merging (ensemble average over the population of major mergers/interactions, or equivalently, temporal average over major merger events during a merger lifetime), not the high-intensity tail (e.g., Barton et al. 2000; Lambas et al. 2003; Lin et al. 2007; Li et al. 2008; Jogee et al. 2009). Barton et al. (2007) carefully quantified the star formation rate (SFR) enhancement in mergers in low-mass halos at low redshift, using the Two-Degree Field Galaxy Redshift Survey (Colless et al. 2001). They found that roughly 1/4 of galaxies in close pairs (separated by < 50 kpc) in low-mass halos with $M_{b_J} < -19$ have SFR enhancements of a factor of five or more¹.

It has also been noted that the strong decrease of the cosmic SFR density

¹This corresponds roughly to a mass cut of $5 \times 10^9 M_\odot$, assuming a stellar $M/L_{b_J} \sim 1$, appropriate for a star-forming blue galaxy with a Chabrier (2003) stellar IMF.

between $z = 1$ and $z = 0$ (e.g., Lilly et al. 1996; Madau et al. 1996; Hopkins 2004; Le Floc’h et al. 2005) was not dissimilar from the relatively rapid drop in merger rate inferred (at that time) from close pairs and morphologically-selected mergers (Le Fèvre et al. 2000). If much of the star formation at $z > 0.5$ were triggered by merging, the apparent similarity in evolution between SFR and merger rate would be a natural consequence. More recently, studies of the fraction of star formation in morphologically-selected interacting and merging galaxies at intermediate redshifts $z < 1$ have demonstrated that, in fact, the bulk of star formation is in quiescently star-forming disk-dominated galaxies (Hammer et al. 2005; Wolf et al. 2005; Bell et al. 2005; Jogee et al. 2009).

Similarly, it has long been argued that early-type (elliptical and lenticular) galaxies are a natural outcome of galaxy mergers (e.g., Toomre & Toomre 1972; Schweizer & Seitzer 1992). In any hierarchical cosmogony mergers are expected to play a large role; a wide range of work — observations of the increasing number density of non-star-forming early-type galaxies from $z = 1$ to the present (Bell et al. 2004; Brown et al. 2007; Faber et al. 2007), the kinematic and stellar populations of local early-type galaxies (Trager et al. 2000; Emsellem et al. 2004), or the joint evolution of the stellar mass function and star formation rates of galaxies (Bell et al. 2007; Walcher et al. 2008; Pérez-González et al. 2008) — has given support to the notion that at least some of the early-type galaxies assembled at $z < 1$ have done so through galaxy merging. In such a picture, the average SFR enhancement from merging is of interest for interpreting the SF and chemical enrichment history of early-type galaxies, inasmuch as it gives an idea of what kind of fraction of stars in present-day early-type galaxies we can expect to have formed in the burst mode, and what fraction we can expect to have formed in a quiescent mode in the progenitor galaxies.

Direct observational constraints on the enhancement in SFR caused by merging provide an important calibration for modeling triggered star formation in cosmologically-motivated galaxy formation models. Hydrodynamic simulations of interacting galaxies in which gas and star formation are explicitly modeled have demonstrated that torques resulting from the merger can efficiently strip gas of its angular momentum, driving it to high densities and leading to significant enhancement in star formation (e.g., Barnes & Hernquist 1996; Mihos & Hernquist 1996b; Cox et al. 2006, 2008; Di Matteo et al. 2007). However, state-of-the-art cosmological simulations lack the dynamic range to accurately simulate the internal structure of galaxies in significant

volumes, so estimates of the global implications of merger-driven star formation enhancement have had to rely on semi-analytic calculations (e.g. Somerville et al. 2001; Baugh et al. 2005; Somerville et al. 2008). Furthermore, as the progenitor properties play a key role in the simulated SFR enhancements (e.g., Di Matteo et al. 2007; Cox et al. 2008), inaccurate progenitor property values (e.g., incorrect gas fraction or internal structure) will lead to incorrect estimates for the average fraction of SF in mergers even if the SF in each individual merger were modeled perfectly.

Therefore, to constrain galaxy evolution models and to understand the physical processes responsible for the main mode of star formation at $z < 1$, it is of interest to determine observationally the typical enhancement² in SFR averaged over the duration of the entire major (stellar-mass ratio between 1:1 and 1:4) galaxy merger or interaction and to constrain the overall fraction of SF triggered by mergers/interactions at intermediate redshift. In a recent work (Jogee et al. 2009) we focus on the rate of merging and also present a preliminary exploration of the average change in the SFR caused by late-stage major and minor merging (see also Kaviraj et al. 2009), finding an average mild enhancement within the restrictions imposed by the sample size. In this chapter I present a statistically-robust analysis of the properties of star-forming galaxies at $0.4 < z < 0.8$ including all relevant merger phases and aimed at providing a satisfactory answer to two key questions. What is the average enhancement in star formation rate as a function of galaxy pair separation compared to their SFR before the interaction? What fraction of star formation is directly triggered by major mergers and interactions?

There are a number of conceptual and practical challenges in such an experiment. Enhancements in SFR produce both a boost in luminosity, but also increase dust content and extinction. At a minimum, one therefore needs dust-insensitive SFR indicators. In addition, simulations have indicated that SF can be enhanced at almost all phases of an interaction from first passage through to after coalescence (e.g., Barnes & Hernquist 1996; Di Matteo et al. 2007); although close pairs will inevitably include some fraction of galaxies before first pass and galaxies with unbound orbits. Therefore, an analysis needs to include both close pairs of galaxies (those before coalescence) and morphologically-classified mergers (primarily those near or after coalescence). Morphological classification is not a straightforward art (see Jogee et al. 2009 for

²When I refer to SFR enhancement, I define this as the ratio of SFR in some subsample (e.g., close pairs) to the average SFR of all systems in that mass bin.

a comparison between automated classifications and visual morphologies), even in ideal cases (Lisker 2008). Finally, galaxy mergers are rare and short-lived, necessitating large surveys to yield substantive samples of mergers.

In this work, I address these challenges as far as possible (see also Lin et al. 2007 and Li et al. 2008). I use estimates of redshift and stellar mass from the COMBO-17 survey (Wolf et al. 2003; Borch et al. 2006) to define and characterize the sample. Stellar mass selection should limit the effect of enhanced star formation and dust content on the sample definition. I use SFR indicators that are constructed to be dust extinction insensitive, by combining ultraviolet (UV; direct, unobscured light from young stars) and infrared (IR; thermal emission from heated dust, powered primarily by absorption of UV light from young stars) radiation (Bell et al. 2005). Finally, I study a very well-characterized sample of galaxy pairs at $0.4 < z < 0.8$ using weighted projected two-point correlation functions (Skibba et al. 2006; Li et al. 2008), supplementing them at very small separations < 15 kpc with very close pairs or merger remnants morphologically selected from two wide HST mosaics, GEMS (Rix et al. 2004) and STAGES (Gray et al. 2009), in an attempt to account for all stages of galaxy interactions.

The plan of this chapter is as follows. In §2.1 I discuss the data and the methods used to estimate the stellar masses and the SFRs. In §2.2 I describe the sample selection and the method used for the analysis. In §2.3 I present my estimates of the enhancement in SFR as a function of projected separation. In §2.4, I compare with previous observations, constrain the fraction of SF triggered by major mergers and interactions at $0.4 < z < 0.8$, and compare with simulations of galaxy merging. Finally in §2.5 I summarize the main findings of this chapter. All the projected distances between the pairs used here are proper distances. I assume $H_0 = 70 \text{ km s}^{-1} \text{ Mpc}^{-1}$, $\Omega_{\Lambda 0} = 0.7$ and $\Omega_{m0} = 0.3$.

2.1 The Data

2.1.1 COMBO-17. Redshifts and stellar masses

COMBO-17 has to date fully surveyed and analyzed three fields to deep limits in 5 broad and 12 medium pass-bands (Extended Chandra Deep Field South (ECDFS), A901/2 and S11, see Wolf et al. (2003) and Borch et al. (2006)).

Using galaxy, star and quasar template spectra, objects are classified and redshifts assigned for $\sim 99\%$ of the objects to a limit of $m_R \sim 23.5$ (Wolf et al. 2004). The photometric redshift errors can be described as

$$\frac{\sigma_z}{1+z} \sim 0.007 \times [1 + 10^{0.8(m_R-21.6)}]^{1/2}, \quad (2.1)$$

and rest frame colors and absolute magnitudes are accurate to ~ 0.1 mag (accounting for distance and k -correction uncertainties). The astrometry is accurate to $\sim 0.1''$ and the average seeing is $0.7''$. It is worth noting that Eq. 2.1 leads to typical redshift errors of $\sigma_z \simeq 0.01$ for bright ($m_R < 21$) and $\sigma_z \simeq 0.04$ for faint ($21 < m_R < 23.5$) galaxies in the $0.4 < z < 0.8$ interval.

The stellar masses were estimated in COMBO-17 by Borch et al. (2006) using the 17-passband photometry in conjunction with a non-evolving template library derived using the PEGASE stellar population model (see Fioc & Rocca-Volmerange 1997, 1999) and a Kroupa et al. (1993) initial mass function (IMF). Note that the results assuming a Kroupa (2001) or a Chabrier (2003) IMF yield similar stellar masses to within $\sim 10\%$. The reddest templates have smoothly-varying exponentially-declining star formation episodes, intermediate templates have a contribution from a low-level constant level of star formation, while the bluer templates have a recent burst of star formation superimposed.

The masses are consistent with those using M/L estimates based on a single color (e.g., Bell et al. 2003). Random stellar mass errors are < 0.3 dex on a galaxy-by-galaxy basis, and systematic errors in the stellar masses were argued to be at the 0.1 dex level (see Borch et al. 2006 for more details). Bell & de Jong (2001) argued that galaxies with large bursts of recent star formation could produce stellar M/L values at a given color that are lower by up to 0.5 dex; this uncertainty is more relevant in this work than is often the case. While this will inevitably remain an uncertainty here, I note that the Borch et al. (2006) templates do include bursts explicitly, thus compensating for the worst of the uncertainties introduced by bursting star formation histories. In §2.3.1 I will explicitly study the impact that such uncertainties have on my results.

In what follows, I use COMBO-17 data for two fields: the ECDFS and Abell 901/902 fields, because of their complementary data: deep HST/ACS imaging from the GEMS and STAGES projects respectively (allowing an investigation of morphologically-selected merger remnants and very close pairs), and deep $24\mu\text{m}$ imaging from the MIPS instruments on board *Spitzer*, required to measure

obscured SF.

2.1.2 GEMS and STAGES HST imaging data

F606W (V-band) imaging from the GEMS and STAGES surveys provides 0.1" resolution images for my sample of COMBO-17 galaxies. Using the Advanced Camera for Surveys (ACS; Ford et al. 2003) on board the Hubble Space Telescope (HST), areas of $\sim 30' \times 30'$ in each of the ECDFS and the A901/902 field have been surveyed to a depth allowing galaxy detection to a limiting magnitude of $m_{lim}^{AB}(F606W) = 28.5$ (Rix et al. 2004; Gray et al. 2009; Caldwell et al. 2008). These imaging data are later used to visually classify galaxies, allowing very close pairs (separations $< 2''$) and merger remnants to be included in this analysis. I choose not to use F850LP HST data available for the GEMS survey in order to be consistent in my classification between the two fields (only F606W is available from STAGES).

2.1.3 MIPS 24 μm , total infrared emission and star formation rates

The IR observatory Spitzer has surveyed two of the COMBO-17 fields: a $1^\circ \times 0.5^\circ$ scan of the ECDFS (MIPS GTO), and a similarly-sized field around the Abell 901/902 galaxy cluster (MIPS GO-3294: PI Bell). The final images have a pixel scale of $1''.25/\text{pixel}$ and an image PSF FWHM of $\simeq 6''$. Source detection and photometry are described in depth in Papovich et al. (2004) and catalogue matching in Bell et al. (2007)³. Based on those works, I estimate that my source detection is 80% complete at the 5σ limit of $83\mu\text{Jy}$ in the $24\mu\text{m}$ data in the ECDFS for a total exposure of $\sim 1400 \text{ s pix}^{-1}$. The A901/902 field has similar exposure time, but owing to higher (primarily zodiacal) background the 5σ limit (80% completeness) is $97\mu\text{Jy}$, with lower completeness of 50% at $83\mu\text{Jy}$. I use both catalogs to a limit of $83\mu\text{Jy}$.

To include both obscured and unobscured star formation into the estimate of the SFR of galaxies in my sample, I combine UV emission with an estimate of the total IR luminosity in concert. As the total thermal IR flux in the

³In this work, I am interested in SFR enhancements in close pairs of galaxies, where the closest pairs may fall within a single *Spitzer*/MIPS PSF. Accordingly, in this work I choose to explore the total SFR in the pair (avoids deblending uncertainties) rather than the individual SFR occurring in both galaxies.

8–1000 μm range is observationally inaccessible for almost all galaxies in my sample, I have instead estimated total IR luminosity from the observed 24 μm flux, corresponding to rest-frame 13–17 μm emission at the redshifts of interest $z = 0.4 - 0.8$. For this exercise, I adopt a Sbc template from the Devriendt et al. (1999) SED library (Zheng et al. 2007b; Bell et al. 2007). The resulting IR luminosity is accurate to a factor of $\lesssim 2$: local galaxies with IR luminosities in excess of $> 10^{10}L_{\odot}$ show a tight correlation between rest-frame 12–15 μm luminosity and total IR luminosity (Spinoglio et al. 1995; Roussel et al. 2001; Papovich & Bell 2002) with a scatter of ~ 0.15 dex. Furthermore, Zheng et al. (2007b) have stacked luminous ($L_{TIR} > 10^{11}L_{\odot}$) $z \sim 0.7$ galaxies at 70 μm and 160 μm , finding that their average spectrum is in good agreement with the Sbc template from Devriendt et al. (1999), validating at least on average my choice of IR SED used for extrapolation of the total IR luminosity.

I estimate the SFR by using both directly observed UV-light from massive stars and dust-obscured UV-light measured from the mid-infrared. As in Bell et al. (2005) I estimate the SFR ψ by means of a calibration derived from PEGASE synthetic models assuming a 100 Myr-old stellar population with constant SFR and a Chabrier (2003) IMF:

$$\psi / (\text{M}_{\odot} \text{yr}^{-1}) = 9.8 \times 10^{-11} \times (L_{TIR} + 2.2L_{UV}). \quad (2.2)$$

Here L_{TIR} is the total IR luminosity and $L_{UV} = 1.5\nu l_{\nu,2800}$ is a rough estimate of the total integrated 1216 \AA –3000 \AA UV luminosity. This UV luminosity has been derived from the 2800 \AA rest-frame luminosity from COMBO-17 $l_{\nu,2800}$. The factor of 1.5 in the 2800 \AA -to-total UV conversion accounts for UV spectral shape of a 100 Myr-old population with constant SFR, and the UV flux is multiplied by 2.2 to account for the light emitted longwards of 3000 \AA and shortwards of 1216 \AA by the unobscured stars belonging to the young population.

For all galaxies detected above the 83 μJy limit, I have used the IR and UV to estimate the total SFR. For galaxies undetected at 24 μm , or detected at less than 83 μJy , I use instead UV-only SFR estimates.

IR emission from AGN-heated dust

Possible contamination of mid-IR-derived SFRs from AGN heated dust is often addressed by estimating the fraction of star formation held in X-ray detected sources. In my case $< 15\%$ of the star forming galaxy sample were detected in X-rays, in good agreement with the results found by i.e. Silva et al. (2004) or Bell et al. (2005).

Yet, there are two limitations of this estimate. Firstly, this does not account for any contribution from X-ray undetected Compton-thick AGN, which could drive up the expected contribution from AGN in my sample. For example, applying an $m_R = 24$ cut to the sample of Alonso-Herrero et al. (2006), I estimate the fraction of X-ray undetected AGN to be $\sim 30\%$, while Risaliti et al. (1999) find $\sim 50\%$ of local AGN to be Compton thick. On this basis, it is conceivable that up to 30% of $24\mu\text{m}$ luminosity is from galaxies with AGN⁴.

Secondly, even in galaxies with AGN, not all of the IR emission will come from the AGN. Although the data does not currently exist to answer this question conclusively, it is possible to make a rough estimate of the effect. In order to estimate the fraction of mid-IR light that comes from the AGN (as opposed to star formation in the host), I have made use of the results of Ramos Almeida et al. (2007), who attempted to structurally decompose mid-infrared imaging from *Infrared Space Observatory* for a sample of both Seyfert 1 and 2 AGN in the local Universe, some of which are very highly-obscured in X-rays. Analyzing the results in Tables 2 and 3 of Ramos Almeida et al. (2007), I have found that only a small fraction of the IR radiation at $\sim 10\mu\text{m}$ (in this chapter I work at rest-frame $13\text{-}17\mu\text{m}$) comes from the central parts of the galaxies in the Seyfert 2 population, finding a total contribution of:

$$\frac{F_{IR}^{AGN}}{F_{IR}^{total}} = 0.26 \pm 0.02. \quad (2.3)$$

This result should be viewed as indicative only: obviously, the systems being studied will be different in detail from those in my sample. Furthermore, the $10\mu\text{m}$ luminosities of the nuclei will be preferentially affected by silicate absorption, making it possible that my value of $F_{IR}^{AGN}/F_{IR}^{total}$ is a lower limit.

⁴Although note that in a recent investigation of X-ray undetected IR-bright galaxies in the CDFS, Lehmer et al. (2008) found that radio-derived (1.4GHz) SFRs agree with the UV+IR-derived ones. This implies that the relative strength of any AGN component is not dominant when compared to the host galaxy.

Despite the various levels of uncertainty, taking the different lines of evidence together demonstrates that $< 30\%$ of the IR luminosity in my sample comes from systems that may host an AGN, and that it is likely that $< 10\%$ of the IR luminosity of my sample is powered by accretion onto supermassive black holes. Given the other uncertainties in my analysis, I choose to neglect this source of error in what follows.

2.2 Sample selection and method

The goal of this chapter is to explore the star formation rate in major mergers between massive galaxies, from the pre-merger interaction to after the coalescence of the nuclei. I chose a stellar mass-limited sample with $M_* \geq 10^{10} M_\odot$ in the redshift slice of $0.4 < z \leq 0.8$ (see Fig. 1). This roughly corresponds to $M_V = -18.7$ for galaxies in the red sequence and $M_V = -20.1$ for blue objects. I only included galaxies that fall into the footprint of both the ACS surveys GEMS and STAGES and of existing *Spitzer* data. These criteria resulted in a final sample of 2551 galaxies.

Given the flux limit $m_R \lesssim 23.5$ for which COMBO-17 has reasonably complete redshifts (Wolf et al. 2004) I am complete for $M_* > 10^{10} M_\odot$ blue cloud galaxies over the entire redshift range $0.4 < z < 0.8$. For red sequence galaxies, the sample becomes somewhat incomplete at $z > 0.6$, and at $z = 0.8$, the limit is closer to $2 \times 10^{10} M_\odot$. I chose to adopt a limit of $10^{10} M_\odot$ in what follows, despite some mild incompleteness in the red sequence, for two reasons. First, adopting a cut of $2 \times 10^{10} M_\odot$ across the whole redshift range reduces the sample size by a factor of 30%, leaving too small a sample for the proposed experiment. Second, the vast majority of the star forming galaxies are blue cloud galaxies (83% of the star formation is occurring in blue galaxies), making the modest incompleteness in the red sequence of minor importance.

Later, I will use a subsample composed of star forming galaxies. I will refer to 'star formers' as galaxies defined by having either blue optical colors or having been detected in the MIPS $24\mu\text{m}$ band. I select optically-blue galaxies adopting a stellar mass-dependent cut in rest-frame $U - V$ color, following Bell et al. (2007): $U - V > 1.06 - 0.352z + 0.227(\log_{10} M_* - 10)^5$ (see Fig. 2.1). I include

⁵Due to minor magnitude and color calibration differences between the two fields, the red sequence cut is slightly field dependent, with the intercept at $10^{10} M_\odot$ and $z=0$ being $U-V=1.01$ and 1.06 for the ECDFS and the A901/902 fields.

all objects detected above the $24\mu\text{m}$ limit of $83\mu\text{Jy}$ as star-forming.

In order to track star formation in very close pairs ($< 2''$ and hence unresolved by the ground-based COMBO-17 data) and merger remnants, I include only merging systems (from the ACS data) with $M_* > 2 \times 10^{10} M_\odot$: i.e. the minimum possible mass for a merger between two galaxies in my sample.

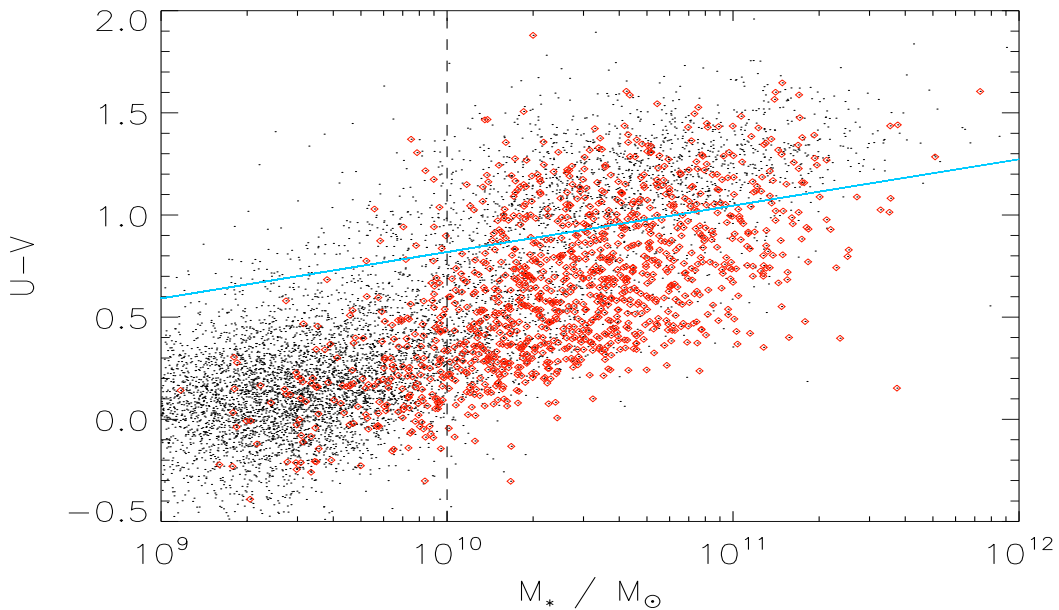


Figure 2.1 *Stellar mass vs. color distribution of COMBO-17 selected galaxies in the ECDFS and A901/2 field with $0.4 < z < 0.8$. The vertical line shows the mass limit $M_* > 10^{10} M_\odot$ used to select my sample. This mass selected sample is complete except for red sequence galaxies at $z > 0.6$. The blue line shows the cut used to separate red sequence and blue cloud galaxies. Red symbols denote $24\mu\text{m}$ detected galaxies with $\geq 83\mu\text{Jy}$.*

2.2.1 Projected correlation function

The correlation function formalism is a convenient and powerful tool to characterize populations of galaxy pairs (e.g. Davis & Peebles 1983). Here, I use weighted projected two-point correlation functions because redshift uncertainties (1-3%) from COMBO-17 translate to line-of-sight distance errors of ~ 100 Mpc, necessitating the use of projected correlation functions to explore the properties of close physical pairs of galaxies (Bell et al. 2006b). For my

sample at hand, I estimate the weighted (or marked) two-point correlation function (Boerner et al. 1989; Skibba et al. 2006; Skibba & Sheth 2009), using both the SFR and the specific SFR (SFR per unit stellar mass) as the weight.

The projected correlation function $w(r_p)$ is the integral along the line of sight of the real-space correlation function:

$$w(r_p) = \int_{-\infty}^{\infty} \xi([r_p^2 + \pi^2]^{1/2}) d\pi, \quad (2.4)$$

where r_p is the distance between the two galaxies projected on the plane of sky and π the line-of-sight separation. A simple estimator for this unweighted correlation function is $w(r_p) = \Delta(DD/RR - 1)$, where Δ is the path length being integrated over, $DD(r_p)$ is the histogram of separations between real galaxies and $RR(r_p)$ is the histogram of separations between galaxies in a randomly-distributed catalogue (this is the same estimator used in Bell et al. 2006b). Basically, the aim is to find the excess probability (compared to a random distribution) of finding a galaxy at a given distance of another galaxy. This estimator accomplishes that by subtracting the random probability of finding two galaxies at a given separation from the probability in the real data sample and normalizing to the probability in the random case. Other estimators (i.e. $\Delta[(DD-DR)/RR]$ or $\Delta[(DD-2DR+RR)/RR]$) for the 2-point correlation function give results different by $< 5\%$ (less than other sources of uncertainty). Thus:

$$DD(r_p) = \sum_{ij} D_{ij}$$

$$RR(r_p) = \sum_{ij} R_{ij}$$

where the sum is over all non-repeated pairs in the sample, and D_{ij} (R_{ij}) equals 1 only if the pair selection criteria are satisfied in the real (random) galaxy catalogue, and is equal to 0 otherwise. The first criterion is that the stellar-mass ratio falls between 1:1 and 1:4. I further only allow a maximum redshift difference $\Delta z = \Delta = \sqrt{2}\sigma_z$, where σ_z is the error in redshift of the primary galaxy (see Equation 2.1), and, depending on the case, either the primary or both galaxies in the pair have to be star formers (see §2.3).

I can then study the possible enhancement of (specific) star formation rate by means of a projected marked (or weighted) correlation function, which can be defined:

$$E(r_p) = \frac{1 + W(r_p)/\Delta}{1 + w(r_p)/\Delta}, \quad (2.5)$$

where $W(r_p) = \Delta(PP/PP_R - 1)$ and,

$$PP(r_P) = \sum_{ij} P_{ij} D_{ij}$$

$$PP_R(r_P) = \sum_{ij} P_{ij} R_{ij}.$$

P_{ij} is the mark (or weight). I adopt two different weights P_{ij} in what follows, one is the SFR of the pair of galaxies:

$$P_{ij} = S_{ij} = SFR_{ij} = SFR_i + SFR_j,$$

and the other is the specific SFR of the galaxy pair:

$$P_{ij} = s_{ij} = \text{Specific } SFR_{ij} = \frac{SFR_i + SFR_j}{M_{*,i} + M_{*,j}}.$$

Then, the estimator that I use for $E(r_p)$ is:

$$E(r_p) = \frac{PP/DD}{\langle P_{ij} \rangle}, \quad (2.6)$$

where $\langle P_{ij} \rangle$ is the average value of the weight used (SFR, or specific SFR) across the sample. This normalization is the average value of pair SFR or SSFR for the actual pair samples used in this analysis, out to a projected separation of 8 Mpc, in order to probe galaxy pairs sampling different environments to build a representative cosmic-averaged weight. The SFRs or SSFRs of individual galaxies used to find the normalization are exactly the same as for the numerator, as described in § 2.1.3. It is worth noting that with my definition of the enhancement given in eq. 5 the random histograms RR and PP_R cancel in the process of obtaining the expression in eq. 6, so they are not used in the computation of my enhancement.

In the present work I perform two analyses: the cross-correlation of star forming galaxies (as defined above) as primary galaxies with all galaxies as secondaries, and the autocorrelation of star-forming galaxies. I will estimate the errors in my mark by means of bootstrapping resampling.

2.2.2 Visual Morphologies

A particular challenge encountered when constructing a census of star formation in pairs and mergers is accounting for systems with separations of $< 2''$ (which corresponds to < 15 kpc, the radius within which I can no longer separate two massive galaxies using COMBO-17; Bell et al. 2006b). In order to pick up the SF in all the stages of the interaction, I need to have an estimate of the SFR not only in galaxy pairs with separations > 15 kpc but also in extremely close pairs and in recent merger remnants. I conduct my census of such close physical pairs by including in the < 15 kpc range sources that are not resolved by COMBO-17, but appear to be interacting pairs or merger remnants on the basis of visual classification of the $\sim 0.1''$ resolution ACS images. I try to recover visually all < 15 kpc separation pairs of two $M_* > 10^{10} M_\odot$ galaxies with a mass ratio between 1:1 and 1:4 missed by COMBO-17. In addition to those extremely close pairs, I also account for the SF in recent merger remnants $M_* > 2 \times 10^{10} M_\odot$ (two times the minimum mass of a galaxy in the sample and the minimum possible mass of a galaxy pair as defined before).

Discussion of visual classifications

My goal is to include very close pairs or already-coalesced major merger remnants into the census of ‘mergers’ in order to account for any SF triggered by the merger/interaction process⁶. I do so on the basis of visual classification of the sample. The motivation for visual classification is a pragmatic one: while a number of automated morphological classification systems have been developed in the last 15 years (i.e. Abraham et al. 1996; Conselice et al. 2003; Lotz et al. 2004 etc.), it seems that the sensitivity of the observables used (asymmetry, clumpiness, Gini coefficient, second order moment of the 20% brightest pixels) is insufficient for matching the performance of visual classification in current intermediate redshift galaxies with the same level of precision that they display in the local Universe samples used for their calibration (Conselice et al. 2003; Lisker 2008; Jogee et al. 2009).

Yet, there is a degree of subjectivity to what one deems to be a major merger remnant. Many factors shape the morphology of a galaxy merger that are

⁶Note that a consistent comparison with the projected correlation function sample requires the inclusion of all non-interacting pairs that are physically-associated (in the same cluster, filament, etc), are seen to be close projected pairs on the sky, but may be separated by as much as a few Mpc along the line of sight.

beyond the control of the classifier. Bulge-to-total (B/T) mass ratios have an strong effect on both the intensity of the SFR enhancement and the time at which the intensity peak shall occur (e.g., Mihos & Hernquist 1996b). Orbital parameters strongly shape the development of easily recognizable tidal tails and bridges (coplanar or not, retrograde vs. prograde, etc). Prior dust and gas content of the parent galaxies (‘dry’ vs. ‘wet’ mergers) will make a difference to the appearance of the final object during the coalescence. Furthermore, merging timescales will depend on whether the galaxies are undergoing a first passage or are in the final stages of the merger. Finally, there is a degeneracy between all these parameters and the relative masses of the galaxies undergoing the interaction, which makes difficult in some cases to distinguish the morphological signatures of a major merger from those of a minor merger.

Some of these factors (e.g. gas fraction, B/T ratios, etc) will also affect the enhancement of the SFR during the interaction (e.g. Di Matteo et al. 2007, 2008; Cox et al. 2008). While there is considerable merger-to-merger scatter, encounters of two gas rich disk galaxies with parallel spins tend to develop, on average, the strongest morphological features, but at the same time are more likely to throw out large amounts of cold gas in tidal tails, preventing the funneling of this gas to the central regions. Thus, samples selected to have the strongest morphological features may have an average SFR enhancement different from the actual mean enhancement⁷.

One practical issue is that of passband choice and shifting. I choose to classify the F606W images of the GEMS and STAGES fields (in STAGES because that is the only available HST passband and in GEMS for consistency and because F606W has higher S/N than the F850LP data). This corresponds to rest-frame $\sim 430(330)nm$ at redshift 0.4(0.8). In previous papers (Wolf et al. 2005; Bell et al. 2005; Jogee et al. 2009), it has been assessed whether the morphological census derived from GEMS/STAGES would change significantly if carried out data a factor of 5 deeper from the GOODS project (testing sensitivity to surface brightness limits), or if carried out at F850LP (always rest-frame optical at these redshifts). We found that the population does not show significantly different morphologies between our (comparatively) shallow F606W data and the deeper/redder imaging data from GOODS (see Fig. 5 in Jogee et al. 2009).

⁷This bias might also be present in the case of studies looking for signs of interactions in the host galaxies of AGNs, attempting to assess whether the AGN activity is preceded by a merger.

Method

An independent visual inspection of the galaxy sample has been carried out by four classifiers, A.R.R., E.F.B., R.E.S. and D.H.M. in order to identify morphological signatures of major gravitational interactions. Each classifier assigned every one of the ~ 2500 sample members to one of the three following groups:

1. **Non-major interactions:** The bulk of galaxies in this bin show no signatures of gravitational interactions. Asymmetric, irregular galaxies with patchy star formation triggered by internal processes lie in this category. A small fraction of galaxies in this bin show a clearly recognizable morphology (e.g. spiral structure) but also signatures of an interaction (such as tidal tails, or warped, thick or lopsided disks) but have no clear interaction companion; note that these objects could be interacting systems where the companion is now reasonably distant and/or faint and more difficult to identify. The tidal enhancement of SF from such systems will *not* be missed by putting them in this bin; rather, it will be measured statistically and robustly from the two point correlation function analysis. Minor mergers and interactions (interactions where the secondary is believed, on the basis of luminosity ratio, to be less than $1/4$ of the mass of the primary) also belong to this category.
2. **Major close interactions:** Close pairs resolved in HST imaging but not in ground-based COMBO-17 data, consisting of two galaxies with mass ratios between 1:1 and 1:4 based on relative luminosity, and clear signatures of tidal interaction such as tidal tails, bridges or common envelope (see Fig. 2.2). From now on I shall refer to objects classified in this group as "very close pairs".
3. **Major merger remnants:** Objects that are believed to be the coalesced product of a recent major merger between two individual galaxies. Signposts of major merger remnants include a highly-disturbed 'train wreck' morphology, double nuclei of similar luminosity, tidal tails of similar length, or spheroidal remnants with large-scale tidal debris (see Fig. 2.3). Galaxies with clear signs of past merging but a prominent disk (e.g., highly asymmetric spiral arms or one tidal tail) were deemed to be minor merger remnants and were assigned into the group 1. Naturally there is some uncertainty and subjectivity in the assignment of this class,

in particular; such uncertainty is taken into account in my analysis by the Monte Carlo sampling of all four classifications in order to properly estimate the dispersion in the opinions of the individual classifiers (see below).

Table 2.1 Results from the morphological classification

Lower mass limit	Sample size	Group 1	Group 2	Group 3
$10^{10} M_{\odot}$	2551	$2380 \pm 37 \pm 49$	$106 \pm 7 \pm 10$	$72 \pm 7 \pm 8$
$2 \times 10^{10} M_{\odot}$	1749	$1640 \pm 32 \pm 40$	$69 \pm 6 \pm 8$	$44 \pm 5 \pm 7$

Note. — Galaxy and interaction sample. Group 1: Isolated objects and minor interactions. Group 2: Extremely close pairs ($r_P < 15$ kpc). Group 3: Merger remnants. The first error bar represents classifier-to-classifier scatter while the second one represents Poisson noise.

I then assign the objects in the groups 2 and 3 (very close pairs with morphological signatures of interaction and merger remnants respectively) to a small projected separation and treat every one of them as a galaxy pair in order to combine them with the correlation function analysis result for pairs with separations $> 2''$. All objects in Group 2 (extremely close pairs with projected separations < 15 kpc as measured by centroids in HST imaging) are assigned to a separation of 10 kpc and all objects in Group 3 (merger remnants) are assigned to a separation of 0 kpc. I have checked for duplicate pairs in both the visually selected sample and the COMBO-17 catalog in order to avoid repeated pairs. Galaxies in group 1 are already included in the two point correlation function analysis, and any SF triggered by major interactions or early-stage major merging is accounted for by that method. As I have four different classifications for every object (one given by each human classifier), I randomly assign one of them, calculate the average value of the weight I am using and repeat the process a number of times. As by definition objects in groups 2 and 3 are considered to be a galaxy pair by themselves, I remove in every Monte Carlo realization the objects assigned to those groups before I run the weighted correlation function. This approach presents two clear advantages: a) the resultant bootstrapping error not only represents the statistical dispersion but also the different criteria of the four human classifiers, and b) the morphology of every object is weighted with *the four* classifications given. This means that objects with discrepant classifications are not just assigned to one category when I calculate the SFR (or specific SFR) enhancement; rather, any dispersion in classifications is naturally accounted for (e.g. minor/major criteria). The

numbers of such systems and their uncertainties, estimated from the classifier-to-classifier scatter, are given in Table 2.1.

2.3 Results

I am now in a position to quantify the triggering of star formation in galaxy interactions and mergers in the redshift interval $0.4 < z < 0.8$, in the cases where each galaxy has $M_* > 10^{10} M_\odot$ and the pair has a stellar mass ratio between 1:1 and 1:4. My primary analysis is based on a marked cross-correlation between star-forming galaxies, as defined in §3, and all galaxies in the sample. For morphologically-selected very close pairs or interactions (unresolved by COMBO-17), I also require them to be blue or detected by Spitzer to be considered as part of the star-forming sample⁸, with a mass of $M_* > 2 \times 10^{10} M_\odot$.

I perform two analyses in this chapter: the cross-correlation of star-formers as primary galaxies with all galaxies as secondaries (my default case), and the autocorrelation of star-forming galaxies. While the first analysis is a rather more direct attack on the question of interest, I show results from the autocorrelation of star-forming galaxies to illustrate the effects of making different sample choices on the final results.

2.3.1 Enhancement in the Star Formation Activity

My main results are shown in Fig. 2.4, which shows the enhancement of the specific star formation rate (SSFR) in pairs as a function of their projected separation. As explained in §2.1.3 I use UV+IR SFRs for the objects detected in 24 μm and only UV SFRs for those undetected. For the whole sample, 38% of the galaxies were detected by *Spitzer* above the 83 μm limit, while if I restrict to the groups 2 and 3 in my morphological classification I find a detected fraction of 60%. Fig. 2.4 shows a clear enhancement in the SSFR for projected pair separations $r_P < 40$ kpc. It could be argued that the SSFR is a better measure of the SF enhancement than the SFR-weighted estimator, because the strong scaling of SFR with galaxy mass is factored out. The figure shows both the cross-correlation between star-forming primaries and all secondaries (SF–All,

⁸All galaxies, irrespective of their color or IR flux, were classified; the star-forming galaxies are simply a subsample of this larger sample.

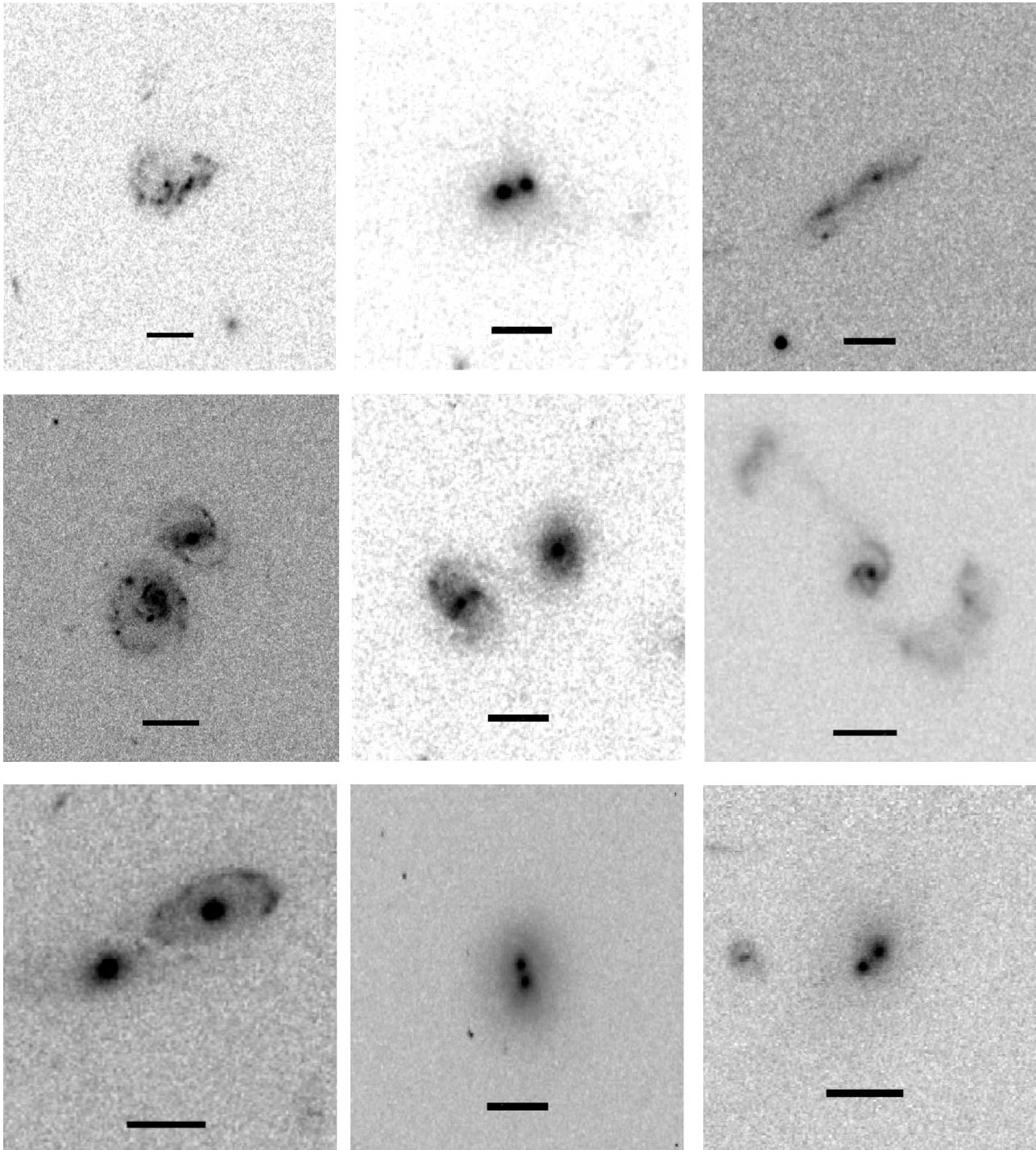


Figure 2.2 *Objects classified in group 2: Major close interactions. The presence of two galaxies and signs of interaction are required. The classifier believes the mass ratio is between 1:1 and 1:4. At this stage of the interaction, dry mergers are still recognizable as seen in panels at top center, bottom center and bottom right. The black bar at the bottom of every panel shows a proper distance of 20 kpc at the redshift of the object. Some of the objects classified in this group were also separated as two galaxies in the ground-based catalog and treated in consequence.*

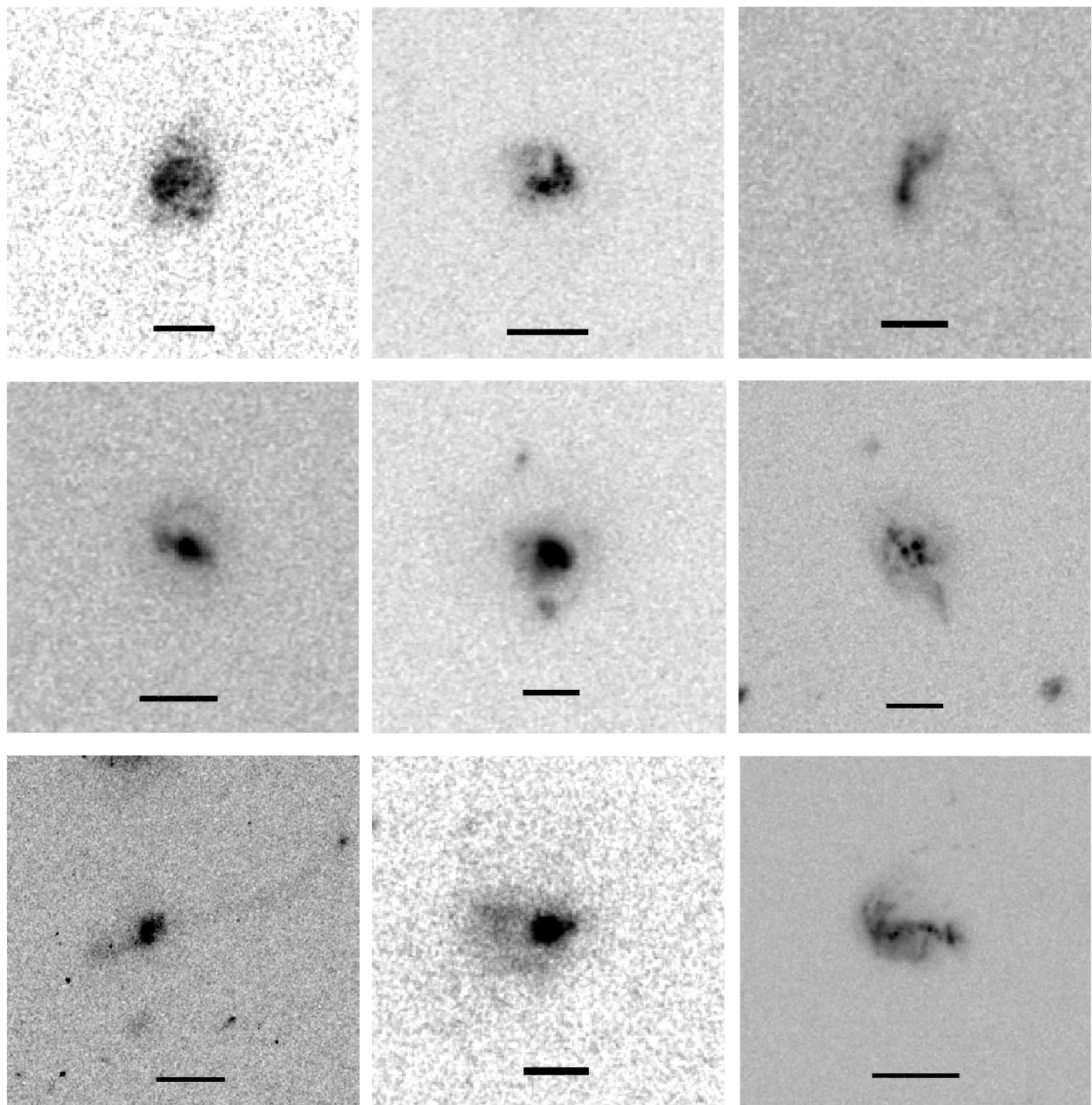


Figure 2.3 *Objects classified in group 3: Major merger remnants. The black bar at the bottom of every panel shows a proper distance of 20 kpc at the redshift of the object*

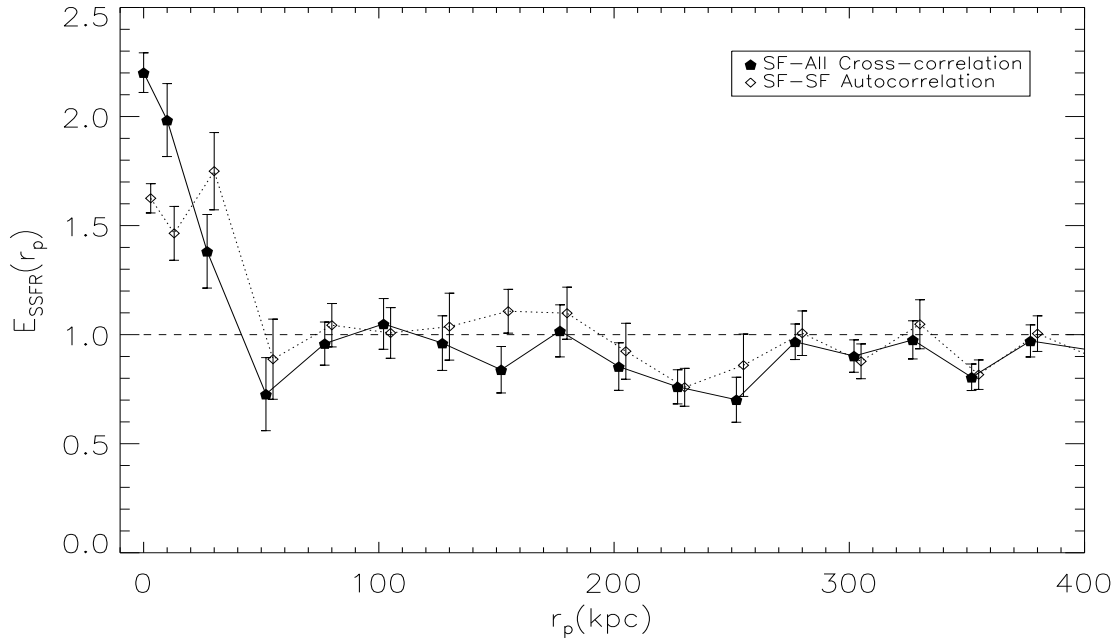


Figure 2.4 *Pair specific SFR enhancement as function of the projected separation between two galaxies. The two smallest radii bins are derived from morphologically-selected very close pairs (shown with $r_p \sim 10$ kpc) and merger remnants (shown with $r_p = 0$); enhancements at larger radii are determined using weighted two-point correlation functions. A statistically significant enhancement is present in galaxy pairs and mergers below 40 kpc in both the cross-correlation between star forming galaxies as primaries and all galaxies as secondaries (black filled symbols) and the autocorrelation of star-forming galaxies (empty diamonds). Error bars have been calculated by bootstrapping.*

solid line) and the star-forming galaxy autocorrelation (SF-SF, dotted line). The two bins at $r_p \leq 15$ kpc are calculated from morphologically-selected very close pairs ($r_p = 10$ kpc) and merger remnants ($r_p = 0$). All the errors in E_{SSFR} have been computed by bootstrap resampling. This approach allows us to treat both the morphologically-selected objects and the galaxy pairs exactly in the same way, having as a result a coherent display of the error bars.

There are two reasons why this excess in E_{SSFR} in close pairs and remnants is likely a sign that interactions induce additional star formation, rather than being due to a correlation with some other unidentified quantity: a) It is well known from simulations (Mihos & Hernquist 1996b; Di Matteo et al. 2007; Cox et al. 2008) that a burst of star formation is expected in the collisions of gas-rich galaxies, and b) the observed effect is in the opposite sense of the usual

SFR–density relation (e.g., Balogh et al. 2002), which says that galaxies in dense environments (where preferentially close galaxy pairs tend to be found, as shown in Barton et al. 2007) have, on average, weaker star formation activity than galaxies in less dense regions.

Even when I consider my morphological classification and further Monte Carlo resampling method to be very robust, potential classification errors could act in two different directions. Interacting systems misidentified as non-interacting will be diluted into the background star formation as single galaxies contributing to pairs at random separations. While this SF should be lost to the interacting bin, the effect on the average SFR would be minimal. On the other hand, isolated galaxies misidentified as interacting systems because of internal instabilities or stochastic star formation would act to reduce the enhancement.

As mentioned before, the SFR for the objects undetected at $24\ \mu\text{m}$ has been calculated based only on the UV. In the $24\ \mu\text{m}$ detected objects, I have found no clear trend in both the UV vs. UV+TIR SFRs and in the TIR/TUV vs. optical dust attenuation but found instead a constant correction factor with a large scatter (4.1 ± 2.4 as estimated from the relation between TIR/TUV vs optical attenuation.) I have checked the effects of such a dust-correction of the UV-only SFRs: the results differ in all bins by $\lesssim 10\%$, comparable to or smaller than other sources of systematic uncertainty.

Yet, in order to understand the degree of obscuration in galaxy interactions I have repeated my analysis including *only* UV–derived SFRs, this is, excluding the TIR component in Eq. 2.2 for $24\ \mu\text{m}$ detections. The result of this analysis is shown in Fig. 2.5. The enhancement in the unobscured SSFR measured for close pairs ($r_P < 40\ \text{kpc}$) in this case is dramatically smaller than the enhancement including the dust-obscured (IR-derived) star formation rate. This is more apparent in the very close pairs and merger remnants, where the excess in the SSFR even disappears completely in the case of the SF–SF autocorrelation ($E(r_P < 15\ \text{kpc}) \simeq 1$). This implies that most of the directly triggered star formation is dust obscured, in good agreement with the expectations from Mihos & Hernquist (1994, 1996b), Di Matteo et al. (2007), Cox et al. (2008) and the detailed models by Jonsson et al. (2006). In these simulations most of the star formation is triggered in the central regions of the galaxy after the cold gas has been funneled to the inner kpc.

This scenario is also supported by my measurement of the mean ratio between the total SFR and the UV-derived, which gives an idea of the degree of dust-

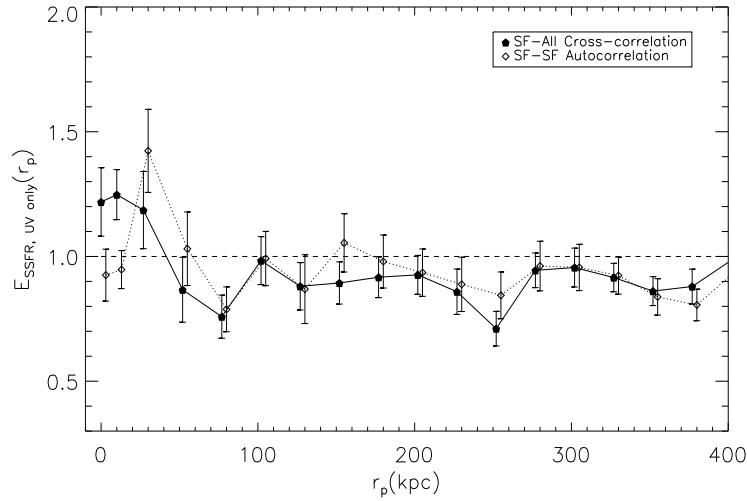


Figure 2.5 Same as Fig. 2.4 but tracing only unobscured (*UV*-derived) star formation. The unobscured SSFR enhancement found in galaxy pairs with separations $r_P < 40$ kpc and mergers remnants is dramatically reduced with respect to the case in which the obscured star formation is taken into account (Fig. 2.4).

obscuration (SFR_{IR+UV}/SFR_{UV}). I find 6.64 ± 0.66 in the case of the merger remnants (Group 3 in §2.2.2) and 6.63 ± 0.64 in the case of the very close pairs (group 2), compared to 3.15 ± 0.53 for all objects in the sample.

Star formation rate vs. specific star formation rate

To study the fraction of the global star formation *directly triggered* by galaxy–galaxy interactions the enhancement in the SFR (rather than in the SSFR) is a better quantity to consider.

I show in Fig. 2.6 the enhancement in the SFR ($E_{SFR}(r_p)$) as a function of the projected pair separation. For the cross–correlation function (my default case) the enhancement in the SFR is similar to the one found in the SSFR at all separations except for the merger remnants ($r_p = 0$), in which the excess above the whole population is $\sim 50\%$ lower. The SFR–weighted autocorrelation of star forming galaxies matches that of the SSFR–weighted one for $r_p < 40$ kpc but differs beyond: $E_{SFR} = 1.25$ for $40 < r_P < 180$ kpc. While most of these points in Fig. 2.6 are individually compatible with the error bars shown in Fig. 2.4, taken together they represent a $\sim 2\sigma$ significant difference between

E_{SSFR} and E_{SFR} for the entire region $40 < r_p < 180$ kpc.

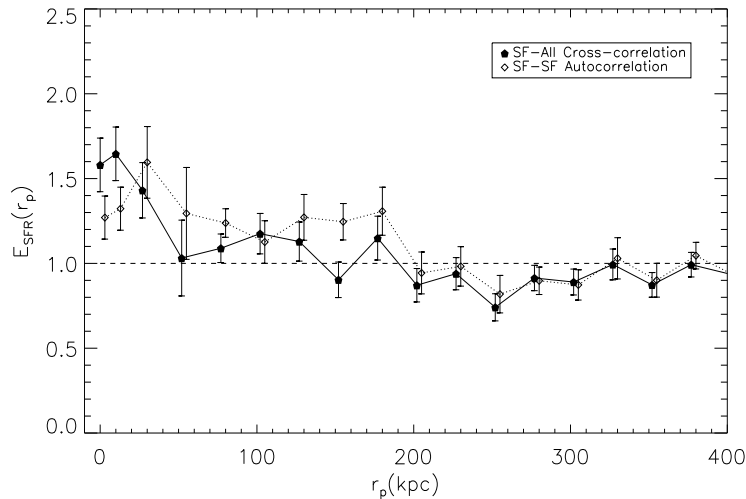


Figure 2.6 *SFR enhancement in galaxy interactions. The two smallest radii bins are derived from morphologically-selected extremely close pairs ($r_p \sim 10$ kpc) and merger remnants (shown with $r_p = 0$); enhancements at larger radii are determined using weighted two-point correlation functions. There is a clear enhancement at $r_p < 40$ kpc for the cross-correlation analysis (black-filled symbols) which is compatible with E_{SSFR} (Fig. 2.4) except for the merger remnants, where the excess is $\sim 50\%$ lower. The autocorrelation of star forming galaxies (empty symbols) presents an unexpected behavior, showing a very mild enhancement at $r_p < 180$ kpc.*

A potential driver of the SFR enhancement in the regime $40 < r_p < 180$ kpc is the fact that more massive galaxies tend to be both more clustered and have higher SFR (Noeske et al. 2007); this could translate into a weak enhancement in the SFR in galaxy pairs living in dense environments (see Barton et al. 2007 for a thorough discussion on the relation between galaxy pairs and environment) which will not be present in the SSFR, because the normalization by galaxy mass factors out this dependence. To test the relevance of this systematic effect, I randomized the SFRs among galaxies of similar mass 500 times in the sample and repeated the analysis. I show the results of this exercise in Fig. 2.7, where I can see a tail of enhancement with a behavior similar to the one seen in Fig. 2.6. I believe that a combination of the density–mass–SFR relation plus noise is driving $E_{SFR} > 1$ (autocorrelation) between 40 and 180 kpc.

It is clear that most of this extra enhancement at large separations is driven

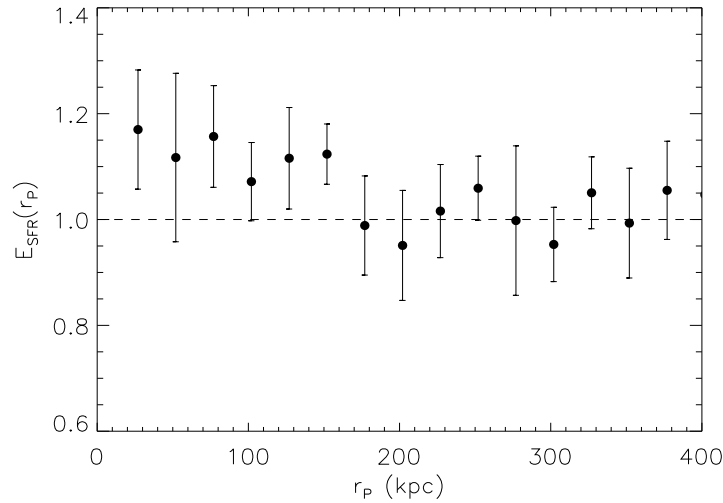


Figure 2.7 SFR enhancement measured after randomizing the SFR between galaxies of similar stellar mass. A mild enhancement is found out to separations of ~ 160 kpc. I show the points corresponding to the SF-SF autocorrelation at distances > 15 kpc, where no morphological information is used.

by the relation between SFR and clustering properties of massive galaxies, but there is yet another possible source of uncertainty: If one galaxy turns out to be in the same group or cluster where a galaxy interaction is taking place, some of the enhancement will be ‘lifted’ and shifted to larger separations. In Chapter 3 I will develop a toy model in order to check for this effect.

Accordingly to the results I show in Fig. 2.7, I consider only the enhancement at $r_p < 40$ kpc as produced by major merging in what follows, and use the differences between the SFR and SSFR enhancement on < 40 kpc scales as a measure of systematic uncertainty. Under those assumptions, I find a weak enhancement of star formation at $r_p < 40$ kpc of $\epsilon = 1.50 \pm 0.25$ in the SF-SF autocorrelation and $\epsilon = 1.80 \pm 0.30$ in the SF-All cross-correlation. These values have been computed as the average of the enhancement in the bins $r_p < 40$ kpc together in E_{SSFR} and E_{SFR} . These (conservative) error bars include both the statistical uncertainties and the systematics driving the differences between the SFR and the SSFR.

Further Uncertainties

As I have briefly mentioned in §2.1, there are some uncertainties which need to be estimated in the process of calculating the enhancement in the SF activity. Here I try to estimate the impact of the stellar-mass and IR SED selection uncertainties. Through this section I will focus in my default case, the SF-All cross-correlation.

Random errors in stellar masses in Borch et al. (2006) are < 0.1 dex (with 0.3 dex in cases with large starbursts (Bell & de Jong 2001)) on a galaxy-by-galaxy basis, and systematic errors non related to the choice of an universally-applied stellar IMF are 0.1 dex. In addition, M/L ratios in starbursting galaxies can be biased to produce unrealistic high stellar masses (Bell & de Jong 2001). Those effects would have certain impact in the calculation of the SSFR, and thus, in the enhancement of that quantity. In order to estimate how those mass uncertainties affect my results, I have run two additional Monte Carlo shufflings. In Fig. 2.8 I show the result of this exercise. I have randomly added a gaussian error with $\sigma = 0.1$ dex to the stellar masses of all galaxies and repeated the process 500 times, finding an average output value similar to the one presented in Fig. 2.4 but with larger errors. The impact of the new errors on the average enhancement (taking into account also the enhancement in the SFR, as I did in the previous section) is negligible.

In order to estimate the uncertainties introduced by systematics in the M/L ratio of starbursts, I have performed a similar exercise but using an error which includes a systematic shift down of 0.1 dex, $\sigma = 0.2$ dex and a tail to the lower masses defined by an inverted lognormal distribution. I have applied this new error to objects with $SFR > 16M_{\odot}yr^{-1}$, which roughly corresponds to twice the average SFR in my sample of *star forming* galaxies, and the symmetric error described above to galaxies with $SFR < 16M_{\odot}yr^{-1}$. The result (dash-dotted in Fig. 2.8) shows some extra enhancement in this case, which leads to an average enhancement in the SF activity $\epsilon = 1.85 \pm 0.35$, barely changing the result already found.

Another potential source of uncertainty is the stellar masses of pairs of galaxies not resolved in the ground-based photometry catalog (i.e., my very close pairs group). In order to test the impact of this underdeblending on the galaxy masses, I take U and V rest-frame fluxes of galaxies widely separated, add them together and check what stellar mass would result in the case of applying the Borch et al. (2006) method to a galaxy with exactly the same color as

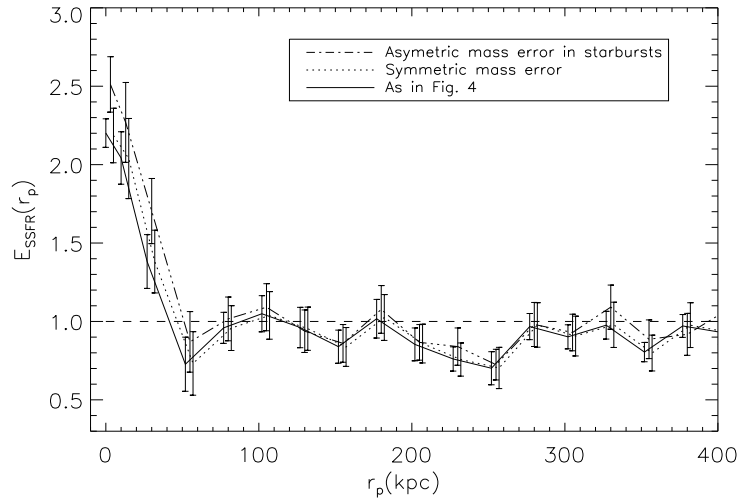


Figure 2.8 *Enhancement in the SSFR including estimates for the errors in the stellar masses. Dotted line: Gaussian error with $\sigma = 0.1$ dex. Dash-dotted line: Non star forming galaxies with gaussian error with $\sigma = 0.1$ dex and starburst galaxies ($SFR > 16M_{\odot}yr^{-1}$) with errors following an inverted lognormal distribution to produce a tail to the lower masses, with a shift of 0.1 dex also to the lower masses and $\sigma = 0.2$ dex. Solid line: Enhancement in the SSFR as in Fig.2.4, for comparison.*

the combination of the two galaxies, and compare with the sum of the two original masses. I find that for pairs of galaxies of all kinds (all-all, SF-SF and SF-all) there is a < 0.01 dex offset and 0.08 dex scatter between the two sets of masses. I.e., masses from combined luminosities are the same as the sum of the individual masses to 0.08 dex, what means that my stellar masses are extremely robust against underdeblending issues.

Together with the stellar-masses, the main source of uncertainty in my analysis is the conversion between observed $24\mu m$ and TIR in the process of obtaining the SFRs. Zheng et al. (2007b) have demonstrated that the Sbc template used here is an appropriate choice for this dataset at all IR luminosities, but in order to find an absolute upper limit for the final results I will show in §2.4.2 I estimate the different results I would obtain if considering an Arp220 template in some cases.

I find that at a given $24\mu m$ flux, the use of an Arp220 template gives a TIR luminosity which is higher than that derived using a Sbc template by a factor of 2. I apply this factor of 2 correction to the TIR luminosity of all the galaxies that I define as starburst for this purpose ($SFR > 16M_{\odot}yr^{-1}$) and show the

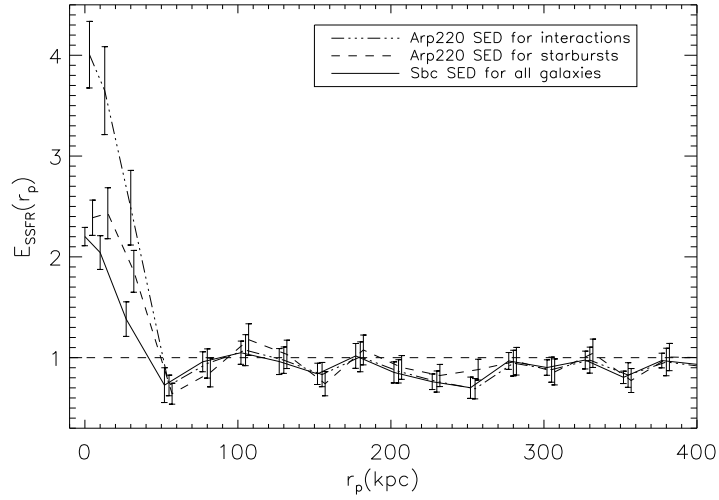


Figure 2.9 *Impact on the SSFR enhancement when using an Arp220 template in the conversion between observed $24\ \mu\text{m}$ and TIR luminosity for certain objects. Red line: Extreme case in which I apply an Arp220 template to all interacting systems (and Sbc template to everything else). Green line: Arp220 template applied to objects with $\text{SFR} > 16M_{\odot}\text{yr}^{-1}$ (and Sbc template to everything else). Black line: Same as in Fig. 2.4, for comparison. Red and green lines include the asymmetric stellar mass errors applied in Fig. 2.8.*

result as the green line in Fig. 2.9. The enhancement found in this case is $\epsilon = 2.1 \pm 0.4$, consistent with, by higher than the $\epsilon = 1.8 \pm 0.3$ found in §2.3.1.

I also want to test the extreme case in which the IR SED of all galaxies undergoing an interaction follows an Arp220 SED, independently of their level of SFR. This is clearly an unrealistic case as I know that some of my galaxies in close pairs and remnants have SFRs as low as $4\text{-}5M_{\odot}\text{yr}^{-1}$ (factor of 10 less SFR than Arp220), and I know also that the average IR SED of $z \sim 0.6$ galaxies with $\text{SFRs} \geq 10M_{\odot}\text{yr}^{-1}$ is similar to the Sbc template adopted here (Zheng et al. 2007a), but it is useful in the sense that it provides a strong upper limit beyond the uncertainties of my data and method. The result found in this case can be seen as the red line in Fig. 2.9. Clearly, a much stronger enhancement is present as a consequence of this overestimation of the TIR luminosity, that leads, when taken together with the SFR enhancement calculated in the same way, to $\epsilon = 3.1 \pm 0.6$.

2.3.2 How important are mergers in triggering dust-obscured starbursts?

I have demonstrated that when averaged over all events and all event phases there is a relatively modest SFR enhancement from major galaxy merging and interactions. It is of interest to constrain how the distribution of SFRs differs between the non-interacting and interacting galaxies. Here I present a preliminary result on one aspect of the issue, namely the fraction of infrared-luminous galaxies that are in close pairs $r_p < 40$ kpc or were visually classified as merging systems.

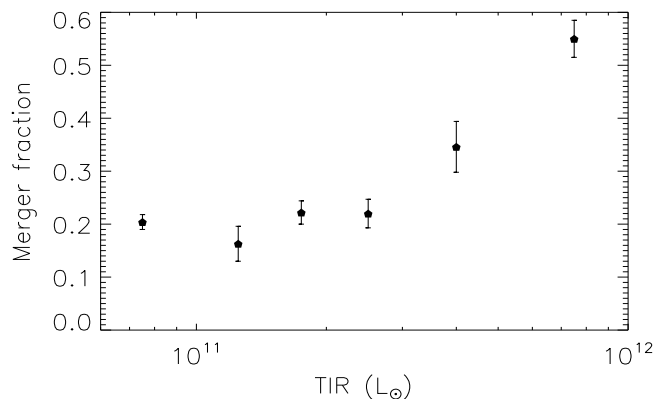


Figure 2.10 *The fraction of systems in close projected pairs $r_p < 40$ kpc or in visually identified mergers as function of the total IR luminosity of all $24\mu\text{m}$ detected galaxies in the sample. The merger fraction is $\sim 20\%$ from my luminosity limit of $6 \times 10^{10} L_{\odot}$ to $3 \times 10^{11} L_{\odot}$. Higher than this luminosity, the merger fraction begins to grow to 55% just below $10^{12} L_{\odot}$.*

In Fig. 2.10 I show how the fraction of galaxies that are either in close pairs ($r_p < 40$ kpc) or in morphologically-classified merger remnants varies as a function of their total IR luminosity. This fraction is constant ($\sim 20\%$) for $6 \times 10^{10} L_{\odot} < L_{TIR} < 3 \times 10^{11} L_{\odot}$. At higher luminosities, the merger fraction increases as a function of the IR luminosity, reaching 55% just below $L_{TIR} = 10^{12} L_{\odot}$. The lower IR limit of $6 \times 10^{10} L_{\odot}$ was chosen to ensure a flux of $83\mu\text{Jy}$ over the entire redshift range. The increase in merger fraction at high IR luminosity is in accord with previous results at both low and intermediate redshift (e.g., Sanders et al. 1988). This suggests that merging and interactions are an important trigger of intense, dust-obscured star formation. Apparently,

high IR luminosities are difficult to reach without an interaction.

A key point, however, is that *not all* mergers have high IR luminosity. While mergers can produce enormous SFRs, and also $L_{TIR} > 10^{12}L_{\odot}$ is best reached by merging, the typical SFR enhancement in mergers is modest.

2.4 Discussion

I have assembled a unique data set for galaxies at $0.4 < z < 0.8$ that combines redshifts, stellar masses, SFRs and HST morphologies to explore the role of major mergers and interactions in boosting the SFR. In practice, I have combined projected correlation-function and morphological techniques to estimate the average enhancement of star formation in star-forming galaxies with $M_* > 10^{10}M_{\odot}$ and $0.4 < z < 0.8$, where the average is taken over most merging phases and all mergers. I find a SF enhancement by a modest factor of ~ 1.8 for separations of < 40 kpc in both the SFR and the SSFR. How does this compare with previous observations and models? What implications does this mild enhancement have on the contribution of major mergers to the cosmic SF history?

2.4.1 Comparison with previous observations

My analysis is most directly comparable to estimates of star formation rate enhancement in galaxy close pairs by Li et al. (2008) using the SDSS at $z \sim 0.1$ because of the similarities between our methods. Using a cross-correlation between star-forming and all galaxies, they found an enhancement of $\simeq 1.45$ for an average galaxy mass of $\langle \log(M_*/M_{\odot}) \rangle = 10.6$ within a radius of 15 to $\sim 35 - 40$ kpc. In Fig. 4.2, I show the comparison between their present-epoch measurements and mine (average galaxy mass $\sim 10^{10.5}M_{\odot}$, SF-all cross-correlation) revealing reasonable quantitative agreement. Both the projected separation scale ($\lesssim 40$ kpc) and the overall amplitude at small projections ($\times 1.5 - 2$) agree. The enhancement found here also agrees (given the error bars) with the enhancement found at $0.75 < z < 1.1$ in Lin et al. (2007). My results are similar to those at both $z = 0.1$ and at $z = 1$, despite the factors of several difference between the typical star formation rates of galaxies between $z = 1$ and $z = 0$ (see, e.g., Zheng et al. 2007a). This is interesting, and points to

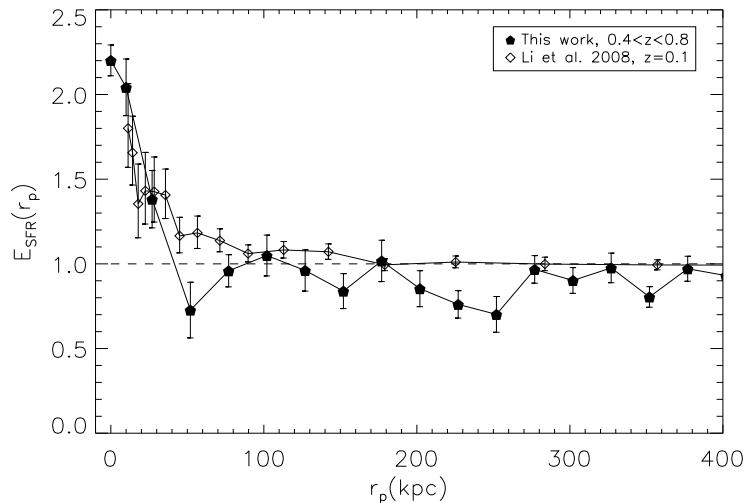


Figure 2.11 Comparison between the enhancement found in this work (black filled points) and the one found in Li et al. (2008) at $z \simeq 0.1$ (open diamonds). In both cases, a cross-correlation SF-all is shown. Both works show a statistically significant enhancement of the SSFR at $r_P < 40$ kpc.

a picture in which at least the average enhancement of star formation in galaxy interactions appears to be independent of the ‘pre-existing’ star formation in the population.

Lin et al. (2007) also measured an enhancement in the TIR emission in galaxy pairs and mergers in the $0.4 < z < 0.75$ range. They find that the infrared luminosity of close pairs with both members selected to be blue is 1.8 ± 0.4 times that of control pairs, similar to my value 1.75 ± 0.18 for close pairs in the bin $15 \text{ kpc} < r_P < 40 \text{ kpc}$ from the SF-SF autocorrelation. For late-phase mergers, they measure 2.1 ± 0.4 , marginally consistent with my 1.54 ± 0.08 from the SF-SF autocorrelation at $r_P = 0$ kpc. Slight differences in that number may be attributed to differences in the ‘merger’ classification. For example, many of the remnants that I include in this study may not be detected by automated methods based on the intensity-weighted Gini- M_{20} or asymmetry parameters. As shown in recent work (Jogee et al. 2009; Miller et al. 2008), automated methods based on CAS asymmetry parameters tend to capture only a fraction (typically 50% to 70%) of the visually-identified merger remnants and often pick up a dominant number of non-interacting galaxies that have small-scale asymmetries associated with dust and star formation.

In related work (Jogee et al. 2009), we recently estimated the overall merging rate and also addressed the SFR enhancement at $0.24 < z < 0.8$. For the subsample of systems with $M_* > 2.5 \times 10^{10} M_\odot$ I find that the average SFR of late stage mergers with mass ratio between 1:1 and 1:10 (both major and minor mergers) are only enhanced by a modest factor (1.5-2 from their Fig. 15) with respect to non-interacting galaxies. There are three differences that make it difficult to perform an exact comparison between our works: a) In the present study I try to isolate the contribution from major interactions (mass ratio 1:1 to 1:4) while in Jogee et al. (2009) I focused on both major and minor interactions (mass ratio from 1:1 to 1:10). b) The normalization is slightly different because in the present work I compare the SFR in mergers with the SFR in the pair of progenitors, while in Jogee et al. (2009) we compare with the SFR of individual galaxies with mass similar to the interacting system. As the average SFR is a function of the galaxy stellar mass, $2 \times \text{SFR}_{M > 10^{10}, \text{progenitor}} \neq \text{SFR}_{M > 2 \times 10^{10}, \text{descendant}}$. c) In the present work I attempt to target both early and late phases of the interaction, while in Jogee et al. (2009) we focus on the later phase. Nonetheless, it is encouraging that the two studies agree qualitatively in finding a modest enhancement in the average SFR in galaxy interactions.

Taken together, I argue that my results are consistent with those of previous works. I have used a bigger sample of galaxies with both HST/ACS and *Spitzer*/MIPS coverage than previous works at $z \geq 0.4$ and I tried to trace the SFR enhancement in all the stages of the interaction with a consistent treatment of ground-based selected galaxy pairs and morphologically-selected pairs and remnants. I view it as extremely encouraging that where the works are the most robust (close pairs), the results are highly consistent (comparing my work with Li et al. 2008 and the pairs from Lin et al. 2007). It is clear that robustly assessing the star formation enhancement in advanced-stage mergers, identifiable using only high-resolution data and morphological techniques, is considerably more challenging. The results for advanced-stage mergers are therefore less well-constrained, but are nonetheless all consistent with a modest but significant enhancement in SFR.

2.4.2 What fraction of star formation is triggered by major interactions?

I can now combine my estimates for the SFR enhancement, the fraction of galaxies in projected close pairs, the average SFR, and the amount of SFR

in recognizable merger remnants to quantify what fraction of star formation at $0.4 < z < 0.8$ is *directly triggered* by major interactions. I will not include systematics such as the uncertainty in conversion of $24\mu\text{m}$ to total IR, or the effect of the $24\mu\text{m}$ flux limit, but I will consider the systematics driving the difference between the SSFR enhancement and the SFR enhancement. I make the cross-correlation between star forming galaxies as primaries and all galaxies as secondaries my default case because it includes the residual SFR in red galaxies and also traces the SF enhancement in disk galaxies during the encounter with a non star forming galaxy. I will also show the values obtained for the SF-SF autocorrelation. I use the values 1.80 ± 0.30 and 1.50 ± 0.25 found in § 2.3.1 in $r_P < 40$ kpc systems, for the cross-correlation and the autocorrelation respectively.

The fraction of galaxies in close physical pairs within a separation r_f can be derived using the following approximation (Patton et al. 2000; Masjedi et al. 2006; Bell et al. 2006b):

$$P(r < r_f) = \frac{4\pi n}{3 - \gamma} r_0^\gamma r_f^{3-\gamma}. \quad (2.7)$$

Here $P(r < r_f)$ is the fraction of galaxies in the parent sample in pairs with real separations of $r < r_f$, n is the number density of galaxies satisfying the pair selection criteria, and r_0 and γ are the parameters of the power-law real-space correlation function of the parent sample, subjected to the pair selection criteria (i.e., I use a stellar mass ratio of 1:1 to 1:4 as a requirement for a pair to enter into the correlation function).

Note that because in this chapter I typically impose criteria for matching and forming pairs (e.g., a mass ratio between 1:1 and 4:1), the number density n used is not the number density of the larger parent sample n_{parent} . The number of possible pairs at any projected separation range is lower than in the case in which no mass ratio criteria is imposed because many pairs with mass ratios beyond the allowed limit are automatically rejected. As the fraction of galaxies in close physical pairs is directly related to the number density of galaxies n , this parameter has to be fine-tuned in order to get the right fraction. The number density used in Eq. 2.7 has to be corrected for the effect that the mass ratio criteria introduces on the total number of potential pairs. Then, the number density of the larger parent sample n_{parent} is not used here, instead I use $n = n_{\text{parent}} N_{\text{pairs}} / [0.5 N_{\text{parent}} (N_{\text{parent}} - 1)]$, where N_{pairs} is the number of pairs that can be formed in the parent sample given the matching criteria, and N_{parent}

is the number of galaxies in the parent sample ($N(N-1)/2$ is the expression for the number of possible pairs in the case of simply pairing up the parent sample).

I tested this approximation using the semi-analytic galaxy catalog of De Lucia et al. (2006), derived from the Millennium N -body simulation. At $z \sim 0.6$ these simulations matched well the stellar mass function and correlation function of $M_* > 10^{10} M_\odot$ galaxies. I find that at $r < 50$ kpc Equation 2.7 is a good approximation to the actual fraction of galaxies in close pairs in the simulation; at larger separation Equation 2.7 is increasingly incorrect.

From fits to the projected two-point cross-correlation function of my sample, I determine $r_0 = 1.8 \pm 0.2$ Mpc, $\gamma = 2.2 \pm 0.1$ for the real-space correlation function, and $n = 0.0152$ galaxies per cubic Mpc⁹; the latter gives a sample of $N_{\text{gal}} = nV = 1913$ galaxies in the volume probed by this study. This yields $P(r < 40 \text{ kpc}) = 0.06 \pm 0.01$ (i.e., 6% of sample galaxies are in close pairs with real-space separations < 40 kpc). With this real-space two-point correlation function, $75 \pm 10\%$ of all projected close pairs should be real close physical pairs¹⁰ (Eq. 6 of Bell et al. 2006b and confirmed using the Millennium Simulation at the redshift of interest). Thus the fraction of objects in projected close pairs will be $f_{\text{pair,proj}} = 0.06/0.75 = 0.08 \pm 0.02$. This fraction includes projections due to real structures like clusters or filaments, but not the purely random projections due to redshift uncertainties which would be present if I would just count the galaxies in projected close pairs in my catalogue.

When considering *all pairs* at all separations in my sample with $M_* > 10^{10} M_\odot$, mass ratios between 1 : 1 and 1 : 4, and primary galaxies with $24 \mu\text{m}$ fluxes $> 83 \mu \text{ Jy}$ and/or blue, the average SFR is $\langle SFR \rangle_{\text{typical,pair}} = 13.2 \pm 0.6 M_\odot \text{ yr}^{-1}$. The total SFR in the $N_{\text{rem}} = 38 \pm 5$ recognizable merger remnants is $SFR_{\text{remnants}} = 753 \pm 97 M_\odot \text{ yr}^{-1}$. Thus, I can calculate the fraction of SFR occurring in pairs with separations < 40 kpc:

$$\frac{N_{\text{gal}} f_{\text{pair,proj}} 0.5 \epsilon \langle SFR \rangle_{\text{typical,pair}} + SFR_{\text{remnants}}}{N_{\text{gal}} 0.5 \langle SFR \rangle_{\text{typical,pair}}} = 20 \pm 3\% \quad (2.8)$$

for the SF–All correlation. A similar analysis with the SF–SF correlation yields

⁹The correlation function is calculated in proper coordinates, because the process of interest is galaxy merging and close pairs of galaxies have completely decoupled from the Hubble flow.

¹⁰This is only valid after removing the effect introduced by purely random projections with the correlation function method.

$16 \pm 3\%$. What I have done in the numerator of Eq. 2.8 is to take the typical SFR in my pairs and divide by two in order to get the typical SFR of a galaxy contributing to such pairs. This number is different from the typical SFR in my galaxy sample for two reasons: first, I have imposed a mass–ratio criterion (only allow pairs with mass ratios between 1:1 and 1:4), which makes the averaged SFR in all pairs to be slightly biased high respect random pairs without any mass ratio criterion, and second, the fact that I force the primary galaxy to be a star former (in the case of the cross-correlation) has a similar effect. Then I have multiplied it by the enhancement ϵ in order to take into account the excess SFR triggered by major interactions and introduced the factor N_{gal} to account for all the SFR occurring in those galaxies. A key piece of Eq. 2.8 is the different treatment of merger remnants. The correlation function can tell us what is the fraction with separations between $r_P = 40$ kpc and $r_P = 0$ kpc but I have defined merger remnants as objects which have *already* coalesced, so if we think in terms of the duration of the interaction instead of the separation between the galaxies, these objects would be *beyond* the reach of the correlation function, and have to be treated separately. In the denominator I have only divided by the total SFR occurring in *all* the galaxies contributing to any pair I can form with the already mentioned criteria. The difference between this factor and the total SFR calculated simply adding up the SFR of all galaxies in the sample is 5% and is a consequence of the few galaxies which are not paired with any other galaxy in the sample.

Yet, the fraction of the total SFR that occurs in pairs and remnants with < 40 kpc separation does not immediately characterize the SFR *triggered* by interactions, because $\sim 12\%$ of SF should happen at $r_P < 40$ kpc anyway, as I show below. Only the *excess* star formation in pairs and remnants should be attributed to triggering by interactions:

$$\frac{N_{gal} f_{pair,proj} 0.5(\epsilon - 1) \langle SFR \rangle_{typical,pair} + (SFR_{remnants} - N_{rem} \langle SFR \rangle_{typical,pair})}{N_{gal} 0.5 \langle SFR \rangle_{typical,pair}} = 8 \pm 3\%. \quad (2.9)$$

Again, a similar analysis for the SF–SF autocorrelation yields $5 \pm 3\%$. These values for the excess are 12% lower than those in Eq. 2.8 due to the total number of interacting systems, which is higher than the 8% of galaxies in close pairs mentioned before because it includes the merger remnants that are not taken into account by the correlation function method.

Taking all this together, this analysis shows that only $\sim 8\%$ of the star formation at $0.4 < z < 0.8$ is triggered by major mergers/interactions. This may seem in

disagreement with previous results from 'morphological' studies. I therefore compare my results with those of Bell et al. (2005) and Wolf et al. (2005), who found that $\sim 30\%$ of the global SFR at $z = 0.7$ is taking place in morphologically perturbed systems and with Jogee et al. (2009), where we find a similar result at $0.24 < z < 0.8$.

Both Bell et al. (2005) and Wolf et al. (2005) performed a study of the total SFR occurring in visually-classified interacting galaxies in a thin redshift slice $0.65 < z < 0.75$ without imposing a lower mass limit (only an apparent magnitude limit). That is the key difference between those earlier works and mine. I impose a mass cut in this chapter of $10^{10}M_{\odot}$ and $2 \times 10^{10}M_{\odot}$ for galaxies and visually-classified interactions respectively. E.g. the fraction of SFR in galaxies with $M_* > 1 - 2 \times 10^{10}M_{\odot}$ that Bell et al. (2005) and Wolf et al. (2005) identified as interacting/peculiar is 15-21%, compared to 20% in Eq. 2.8. Only 1/6 of the star formation in the interacting/peculiar galaxies from Bell et al. (2005) and Wolf et al. (2005) occurs in what I would designate as merger remnants, with the other 5/6 occurring in galaxy pairs. Jogee et al. (2009) argued that 30% of star formation was in systems that they classified as major or minor interactions, with mass limits different from those used in this work. This value is an upper limit to the fraction of star formation in major mergers where each galaxy has mass $> 10^{10}M_{\odot}$, both because of the effect of mass limits, and because minor mergers host much of the star formation in systems that they classified to be interacting. Accounting for these differences, my result is in qualitative agreement with theirs.

However, the key difference is that neither Bell et al. (2005), Wolf et al. (2005) nor Jogee et al. (2009) try to quantify the *excess* of SF in interacting systems, as I do in going from Eq. 2.8 to Eq. 2.9. In summary, my new results here pose no inconsistency with earlier studies, but refine them by quantifying the physically more relevant quantity of SF excess.

I have presented the average enhancement in SFR caused by major mergers of galaxies with masses above $10^{10}M_{\odot}$ at $0.4 < z < 0.8$, deriving that approximately 8% of the SF in the volume is *directly* triggered by major merging. As I have mentioned before, the SFR enhancement ϵ seems to be roughly independent of the quiescent SFR ground level present in the galaxy population, that is, insensitive to the drop in the SFR density of the Universe since $z=1$. If this is true, it means that the fraction of star formation directly triggered by galaxy interactions (given a mass cut) would depend only on the number of galaxies undergoing interactions. Using the evolution of pair fraction found in

Kartaltepe et al. (2007) I can infer a directly-triggered SF fraction of 1-2% in the local Universe, as well as a fraction of 14-18% at $z=1$. On the other hand, assuming no evolution in the pair fraction would keep the merger-triggered fraction at 8% between $z = 0$ and $z = 1$. These numbers have to be taken extremely carefully by the reader, as I present here only a crude extrapolation of my results to different redshifts in order to get an idea of the importance of the merger-driven star formation in the Universe.

There are a number of limitations of my result that should be borne in mind. First, I can only include star formation rates $> 5 M_{\odot}\text{yr}^{-1}$ for $z \sim 0.6$ galaxies. Therefore, my estimates of the SF contribution from merging may be an upper limit because the merger-driven boost in SFR will cause more objects to satisfy this criterion. Second, there are uncertainties in the conversion of $24\mu\text{m}$ to total IR, which could influence the excess star formation in close pairs or mergers by $\sim 30\%$ (Papovich & Bell 2002; Zheng et al. 2007b); this could be addressed once longer-wavelength, deep *Herschel* PACS observations become available. I can only calculate an absolute upper limit by using the value of the enhancement found in the extreme case in which the $24\mu\text{m}$ to TIR conversion in all the interactions, independently of their luminosity, is calculated using an Arp220 template. Using as input $\epsilon = 3.1 \pm 0.6$ for Eq. 2.9 I would find a directly triggered fraction of $19 \pm 5\%$, consistent with an scenario in which the underlying level of SF is basically negligible and most of the new stars are being formed in the burst mode. Third, it is conceivable that some enhanced star formation occurs in very late-stage merger remnants that were no longer recognized as remnants and hence were not included in this census. This is both a practical (classification) and conceptual issue: when does one declare a merger remnant a normal galaxy again? Nonetheless, despite these points, the analysis presented here has made it very clear that only a small fraction of star formation in galaxies with $M_* > 10^{10} M_{\odot}$ at $0.4 < z < 0.8$ is triggered by major interactions/mergers.

2.4.3 Comparison with theoretical expectations

Star formation enhancement in mergers has been studied extensively with hydrodynamical N-body simulations (e.g., Barnes & Hernquist 1991; Mihos & Hernquist 1994, 1996b; Springel 2000; Cox et al. 2006, 2008; Di Matteo et al. 2007). However, large-scale cosmological simulations lack the dynamic range to resolve the internal dynamics of galaxies, crucial for modeling the

gas inflows and the associated enhancement in star formation. Therefore, the majority of these studies (except Tissera et al. 2002) have been of binary galaxy mergers with idealized initial conditions, typically bulgeless or late-type disks. In most studies, the properties of these progenitor disks are chosen to be representative of present-day, relatively massive spiral galaxies such as the Milky Way. These studies have shown that the burst efficiency in mergers is sensitive to parameters such as merger mass ratio and orbit, and progenitor gas fraction and bulge content. Therefore, any attempt to use these results in an ensemble comparison must somehow convolve these dependencies with a redshift dependent, cosmologically motivated distribution function for these quantities. In addition, Cox et al. (2006) have shown that star formation enhancement in mergers can also depend on the treatment of supernova feedback in the simulations. Furthermore, the detailed star formation history during the course of a merger, particularly in the late stages, may depend on the presence of an accreting supermassive black hole (Di Matteo et al. 2005).

Let us consider the results from representative examples of such binary merger simulations, by Cox et al. (2008), who studied a broad range of merger mass ratios, gas fractions, and progenitor B/T ratios, as well as exploring the effects of two different SN feedback recipes. The 1:1 merger of two “Milky Way”-like progenitors (shown in their Figure 12) shows an average factor of ~ 1.5 enhancement in SF over about 2.5 Gyr, and a larger enhancement of a factor of 2–10 for a shorter period of about 0.6 Gyr. The overall average enhancement over the whole merger is about a factor of 2.5, depending on the precise timescale one averages over. Very large enhancements ($\sim 5 - 10$) occur over a very short timescale, $\lesssim 100$ Myr. This particular simulation represents the largest expected SF enhancement, as the burst efficiency increases strongly towards equal merger mass ratio. For mergers with 1:2.3 mass ratio (Figure 10 of Cox et al. 2008), there is an enhancement of a factor of ~ 1.5 for 2.5–3 Gyr, and of 2.5 for about 0.6 Gyr. It is also interesting to note that the star formation rate in the late stages of the merger, when the galaxy still appears morphologically disturbed (see Fig. 7 of Cox et al. 2008) is *depressed* with respect to the isolated case. A diverse set of progenitor morphologies, ranging from ellipticals to late-type spirals, was studied by Di Matteo et al. (2007). Overall, their results are qualitatively similar to those from Cox et al. (2008).

The simulations discussed so far aimed to reflect progenitor disks with gas fractions, sizes, and morphologies typical of relatively massive, low-redshift late-type spirals such as the Milky Way: gas fraction $f_g \sim 0.2$; $B/T \sim 0.2$; scale

length $r_d \sim 3$ kpc. However, Hopkins et al. (2009) show that the burst efficiency is strong function of progenitor gas fraction, in the sense that higher gas fraction progenitors have *weaker* fractional enhancements. The burst efficiency is a factor of eight lower for a gas fraction of 90 % than for the canonically-used value of 20%. It is worth noting here that I find the same level of SF enhancement in major mergers at $z \sim 0.6$ and $z \sim 0.1$, where the gas fractions of the two samples are expected to be rather different (see §2.4.1). Whether or not this is quantitatively at odds with the expectations of Hopkins et al. (2009) remains to be seen. On the other hand, recent results from Di Matteo et al. (2008) show no difference between the strength or duration of tidally-triggered bursts of star formation in local Universe and their higher redshifts counterparts, in good agreement with the present study.

To place results in a cosmological context, Somerville et al. (2008) used the results from a large suite of hydrodynamic merger simulations (Cox et al. 2006; Robertson et al. 2006) to parameterize the dependence of burst efficiency and timescale on merger mass ratio, gas fraction, progenitor circular velocity, redshift, and the assumed effective equation of state. They implemented these scalings within a cosmological semi-analytic merger tree model. I applied my selection criteria to mock catalogs from Somerville et al. (2008), by comparing the fraction of SFR produced in the triggered mode in galaxies with $M_* > 2 \times 10^{10} M_\odot$ in my redshift range which suffered a major merger in the last 500 Myr with the total SFR occurring in galaxies $M_* > 10^{10} M_\odot$. I found that approximately 7% of the SFR in the volume is produced in the burst mode triggered by major mergers. This is in excellent agreement with the $8 \pm 3\%$ of the overall SFR being directly triggered by major interactions I showed in the previous section.

2.5 Conclusions

To quantify the *average* effect of major mergers on SFRs in galaxies, I have studied the enhancement of SF caused by major mergers between galaxies with $M_* > 10^{10} M_\odot$ at $0.4 < z < 0.8$. I combined redshifts and stellar masses from COMBO-17 with high-resolution imaging based on HST/ACS data for two fields (ECDFS/GEMS and A901/STAGES) and with star formation rates that draw on UV and deep $24\mu\text{m}$ data from *Spitzer* to form a sample a factor of two larger than previous studies in this redshift range. I then applied robust

two-point correlation function techniques, supplemented by morphologically-classified very close pairs and merger remnants to identify interacting galaxies. My main findings are as follows:

1. Major mergers and interactions between star-forming massive galaxies trigger, on average, a mild enhancement in the SFR in pairs separated by projected distances $r_P < 40$ kpc; I find an enhancement of $\epsilon = 1.80 \pm 0.30$ considering the SF-All cross-correlation, where only one galaxy in the pair is required to be forming stars. For a similar analysis using the autocorrelation of star forming galaxies I find $\epsilon = 1.50 \pm 0.25$.
2. My results agree well with previous studies of SF enhancement using close pairs at $z < 1$. In particular, the behavior of SF enhancement at $z = 0.1$, $z = 0.6$ and $z = 1$ appear to be rather similar, indicating that the average SFR enhancement in galaxy interactions is independent of the ‘pre-existing’ SFR in the population.
3. I combine my estimate of the average SFR enhancements in major mergers with the global SFR to show that overall, $8 \pm 3\%$ of the total star formation at these epochs is *directly* triggered by major interactions. I conclude that major mergers are an insignificant factor in stellar mass growth at $z < 1$.
4. Major interactions do, however, play a key role in triggering the most intense dust-obscured starbursts: I find that the majority of galaxies with IR-luminosities in excess of $3 \times 10^{11} L_\odot$ are visually classified as ongoing mergers or found in projected pairs within < 40 kpc separation. This is not in disagreement with the small *average* SFR enhancement if the most intense SF bursts last only ~ 100 Myr.
5. My results for the SF enhancement appear to be in qualitative agreement with the extensive suite of hydrodynamical simulations by Di Matteo et al. (2007, 2008) and Cox et al. (2008), who produce both intense, short-lived bursts of SF in some interactions, but yet produce average enhancements of only 25-50% averaged over the ~ 2 Gyr timescale taken to complete the merger. Furthermore, I find excellent agreement between the fraction of the total SFR directly triggered by major merging measured here and the 7% calculated from mock catalogues obtained from Somerville et al. (2008).

Chapter 3

Systematic Errors in Weighted 2–point Correlation Functions

Correlation functions (2-point and higher order ones) have proved to be powerful statistical tools in order to address the study of the galaxy clustering (e.g. Peebles & Groth 1976; Groth & Peebles 1977; Peebles 1980; Davis & Peebles 1983) and are still widely used in both local (Connolly et al. 2002; Eisenstein et al. 2005; Masjedi et al. 2006) and high-redshift Universe (Giavalisco et al. 1998; Blain et al. 2004). Study of the two point correlation function have matured to the point that one can study how galaxies populate dark matter halos in detail (e.g., Zehavi et al. 2004), the typical halo masses of galaxy populations as a function of redshift (e.g., Lyman breaks - Giavalisco et al. 1998), the relative clustering of different populations (e.g., the tendency of AGN to cluster like the massive galaxy population as a whole; Li et al. 2006b), and the use of clustering measures on the smallest scale to constrain the merger history of galaxies (e.g., Patton et al. 2000, Bell et al. 2006b).

Furthermore, the correlation function method allows me not only to study the clustering of the galaxies themselves, but also how some of their properties are clustered. Weighted correlation functions (Boerner et al. 1989) or in a general sense, marked statistics (Beisbart & Kerscher 2000; Gottlöber et al. 2002; Faltenbacher et al. 2002; Skibba et al. 2006) have been widely used in the last ten years in order to study how observables depend on the separation between galaxies. In particular, weighted correlation functions are frequently used to study the dependence of star formation rate (SFR) on separation between galaxies, in great part to explore the influence of galaxy interactions on enhancing a galaxy pair’s SFR (e.g., Li et al. 2006 or Chapter 2 in this thesis).

The goal of this chapter is to explore the application of weighted correlation

functions to study the variation of SFR in galaxy pairs as a function of separation, but the results can be extrapolated to other observables like color, morphologies, mass, etc. I briefly introduce weighted 2 point correlation functions in § 3.1. I then construct a toy model with which I study the behavior of the inferred weighted quantities relative to the input behavior (§ 3.2). This toy model is primarily to illustrate some general features of how weighted correlation functions recover input behavior, and I stress that the framework discussed in this work applies generally to any application of weighted correlation function analysis, while noting that I choose to present a case that is most directly analogous to the study of SFR enhancement in close pairs of galaxies. I show the results of this analysis in § 3.3. In § 3.4, I briefly compare with observational results of SF enhancement derived using the Sloan Digital Sky Survey (Li et al. 2008). In § 3.5, I present my conclusions. When necessary, I have assumed $H_0 = 70 \text{ km s}^{-1}$, $\Omega_{m0} = 0.3$, $\Omega_{\Lambda 0} = 0.7$.

3.1 Background

In this chapter, I explore the possible artifacts that the use of a marked correlation function could introduce when studying the clustering of galaxy properties. A full explanation of the methodology followed in this work has been already presented in Chapter 2, and is similar to the methodology adopted by Skibba et al. (2006) and Li et al. (2008); I summarize here the basics of the method.

The 2–point correlation function $\xi(r)$ is the *excess* probability of finding a galaxy at a given distance r from another galaxy:

$$dP = n[1 + \xi(r)]dV, \quad (3.1)$$

where dP is the probability of finding a galaxy in volume element dV at a distance r from a galaxy, and n is the galaxy number density. A simple estimator of the unweighted correlation function is $\xi(r) \simeq DD/RR - 1$, where DD is the histogram of separations between galaxies and RR is the histogram of separations between galaxies in a randomly-distributed catalog. In a similar way, one can estimate the weighted correlation function as $W(r) \simeq PP/PP_R - 1$, where PP is the weighted histogram of real galaxies and PP_R the weighted histogram of separations from the catalog with randomized coordinates.

I choose to use an additive weighting scheme (the weight of the pair is the sum of the weights of individual galaxies) for concreteness (Chapter 2), while noting that a multiplicative weighting would yield a qualitatively similar result. Then, I can define the ‘mark’ $E(r)$ as the excess clustering of the weighted correlation function compared to the unweighted correlation function:

$$E(r) = \frac{1 + W(r)}{1 + \xi(r)}. \quad (3.2)$$

3.2 An idealized experiment

I use De Lucia et al. (2006) catalog at $z = 0$ derived from the Millenium simulation (Springel et al. 2005) in order to study how the enhancement in a physical quantity caused by a galaxy–galaxy interaction (e.g., a SF enhancement) would be recovered by weighted 2–point correlation function techniques. I manually assign a weight (I refer to it as the mark) to every galaxy in the sample, giving a mark=1 to galaxies which are *not* closer than $r_c = 35$ kpc to any other galaxy and mark= ϵ (with $\epsilon > 1$) to those galaxies which are in close, 3D pairs with separation $r < r_c$ kpc. For concreteness, I consider simulated galaxies with stellar masses $M_* > 2.5 \times 10^{10} M_\odot$, noting that the conclusions reached in this work are generally applicable, in a qualitative sense.

I now examine how the marks of galaxy pairs relate to the actual behavior of the enhancement as a function of separation from their nearest neighbor. The mark is estimated by dividing the weighted correlation function by its unweighted counterpart, and recall that the correlation function relates every galaxy to every other galaxy in the sample¹. The weight is additive, and since every galaxy with a companion closer than r_c has weight ϵ , the mark of a close pair is 2ϵ . Yet, the galaxies in this close pair will be matched also to every other galaxy in the sample. Therefore, when a galaxy in the same group or cluster at a distance $r > r_c$ from the enhanced pair is matched with a galaxy in the pair, the mark of that pair will be $\epsilon + 1$ (1 being the default weight of non-enhanced galaxies). I see that a pair with $r > r_c$ will show an enhancement when, in reality, there is no physical interaction-induced enhancement at that radius. As that third galaxy will be matched with *both* galaxies in the neighbor close

¹Even in the case in which some criteria for pair-matching are imposed, like line-of-sight constraints, mass ratio, etc., one particular galaxy will be matched with many secondaries at very different separations.

pair, two pairs with $\text{mark}=\epsilon + 1$ will be contributed. Furthermore, imagine now that there is another real close pair of galaxies placed at several Mpc from the first close pair, in which both galaxies will also have $\text{mark}=\epsilon$. From matching all those 4 galaxies, the final product will be 6 galaxy pairs displaying $\text{mark}=2\epsilon$. This will clearly affect both the normalization of the mark and the recovered value for the enhancement, producing a tail of false enhancement in the regions where more companions would be found (representing dense regions of the Universe) and decreasing the enhancement found at $r < r_c$.

3.3 Results

I show this effect in Fig. 3.1. Clearly, a relatively weak tail of enhancement is recovered out to large separations. The amplitude of this tail has a radial dependence, as close pairs of galaxies tend to be found in dense regions of the Universe (Barton et al. 2007), where more neighbors are available. As the magnitude of this tail depends on the distribution of neighbors as a function of the separation it will be more relevant for galaxy samples in which the clustering is stronger (e.g., massive galaxies, or non star-forming galaxies).

Also visible in Fig. 3.1 is the dilution of the recovered enhancement compared with the actual enhancement ϵ for pairs with $r < r_c$; $E(r < r_c)$, is lower than the "real" enhancement ϵ by a factor which increases with ϵ . This effect is better seen in Fig.3.2, where I show the relative discrepancy between $E(r < r_c)$ and ϵ , as a function of ϵ . In this idealized case, this discrepancy can be exactly recovered by accounting carefully for the different pairs formed by galaxies in the sample. The relationship between $E(r < r_c)$ and ϵ is:

$$E(r < r_c) = \frac{\epsilon N_{p,tot}}{W_{cp,max}N_{cp,max} + W_{mp}N_{mp} + W_{fp}N_{fp}}, \quad (3.3)$$

where $N_{p,tot}$ is the total number of pairs which can be formed from the galaxy sample², $N_{cp,max}$ is the total number of pairs which can be formed with galaxies belonging to close pairs³, $W_{cp,max}$ is the weight associated with those pairs, N_{mp} is the number of pairs in which only one galaxy belongs to a close pair, W_{mp} is the weight associated with them, and W_{fp} and $N_{p,far}$ are respectively the weight

²When performing an autocorrelation, the total number of unique pairs would be $N(N-1)/2$, N being the number of galaxies in the sample.

³This is *not* the same as the number of close pairs, as I already explained.

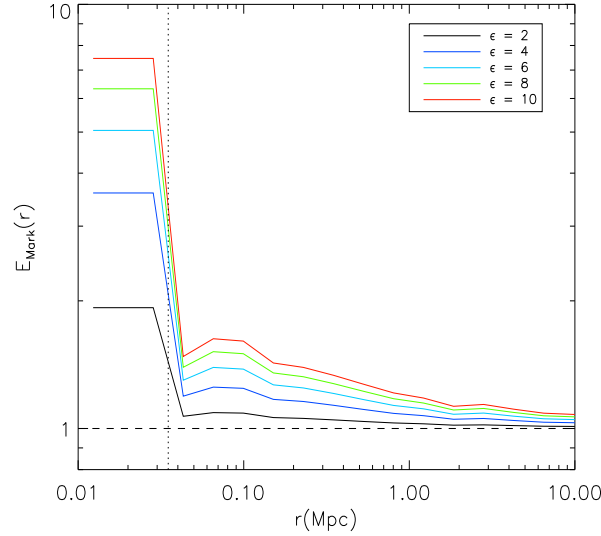


Figure 3.1 Apparent enhancement as a function of distance and "real" enhancement ϵ (which acts only at $r < r_c$ kpc) computed for a sample with a minimum stellar mass of $2.5 \times 10^{10} M_\odot$ and different values of ϵ . The vertical dotted line shows the separation r_c (35 kpc in this case). A tail of artificial enhancement extending to large separations is produced as an artifact of the weighted correlation function method. The enhancement recovered in the close pairs $r < r_c$ kpc is reduced respect to ϵ and the level of reduction is a strong function of ϵ (see text and Fig 3.2 for more details).

and the number of pairs in which none of the galaxies belongs to a close pair.

In the particular case of an additive weight, this expression reduces to:

$$E(r < r_c) = \frac{2\epsilon}{(f^2 + f)(\epsilon - 1) + 2}, \quad (3.4)$$

where f is the fraction of galaxies in close pairs. The degree of clustering of the sample is reflected in the value of f , so this expression is valid under different clustering conditions. For the purposes of this work, I calculate f *directly* from the mock catalogue, but real galaxy surveys lack of accurate 3D information. In principle f can be calculated from the 2-point correlation function by integrating Eq.3.1 out to the distance one considers a pair to be close (r_c). If the correlation function is parametrized as a power law $\xi(r) = (r/r_0)^{-\gamma}$, then:

$$P(r < r_c) = f = \int_0^{r_c} n[1 + \xi(r)]dV \quad (3.5)$$

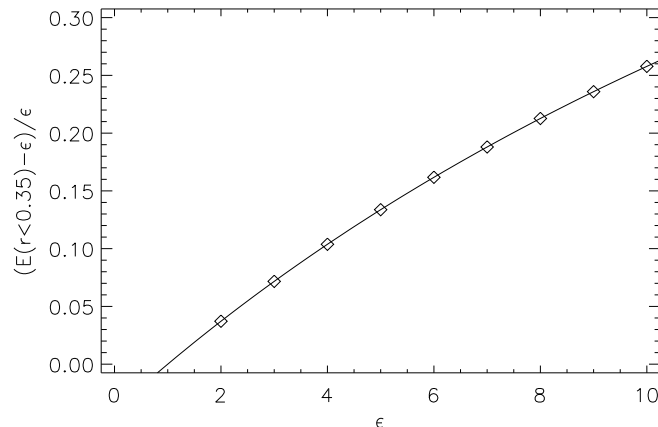


Figure 3.2 Relative error in $E(r < r_c)$, the enhancement recovered by the marked correlation function in close pairs as a function of the "real" enhancement ϵ in those pairs. For this example I have used, as in Fig. 3.1 a lower mass cut of $2.5 \times 10^{10} M_\odot$. *Diamonds*: Recovered values from the method. *Solid line*: Expected value using the proper normalization shown in Eq. 3.4. The error when the intrinsic enhancement is small is modest; when $\epsilon < 4$ then the discrepancy between $E(r < r_c)$ and ϵ is $< 10\%$.

$$f \simeq \frac{4\pi n}{3 - \gamma} r_0^\gamma r_c^{3-\gamma}. \quad (3.6)$$

In a work in preparation, I explore the validity of Eqn. 3.6, finding that it is a reasonable approximation for $r_c < 50$ kpc for realistic degrees of clustering, but that Eqn. 3.6 is increasingly inaccurate for larger r_c or stronger clustering.

It is worth noting that in the above example I have studied the simple case in which the enhancement is present only in close galaxy pairs, with the enhancement represented by a step function. When applying weighted correlation functions to more complex problems, like those involving clustering of the mass or color, the function describing the behavior of the weight on separation would be much more complex. In that case, an expression for the behavior of the weight as a function of separation will have to be derived on a case-by-case basis and matched with the data. Yet, even in that more complex case, the underlying problem is very similar: the magnitude of any radial dependence in properties will be diluted and smeared out in radius by the use of weighted 2 point correlation function methods.

3.4 An example application to observations

In order to test the relevance of this analysis to the real Universe, I compare my predictions with a well-established phenomenon: the enhancement of the star formation rate (SFR) in galaxy interactions. This observable has two obvious advantages. Firstly, apart from my results in the previous chapter there are a number of works in which this enhancement has been studied (Barton et al. 2000; Lambas et al. 2003; Li et al. 2008) Second, the SFR is expected to be enhanced only at scales at which galaxy-galaxy interactions are relevant; beyond that scale star formation is not only not expected to be enhanced, but should be depressed because of the well known SFR-density anticorrelation (e.g., Balogh et al. 2002). From the above mentioned works I choose to compare with Li et al. (2008) for three reasons: a) they use marked statistics, b) their large sample allowed an accurate estimate of enhancement to be made, and c) SDSS clustering has been shown to be similar to the one present in the De Lucia et al. (2006) mock catalogue from the Millenium Simulation in the local Universe (Springel et al. 2005).

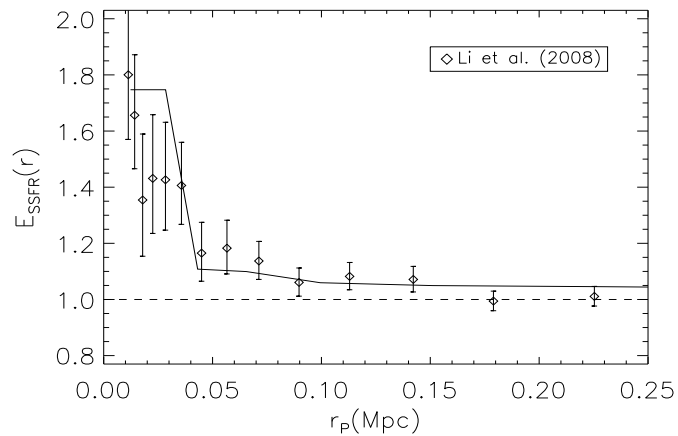


Figure 3.3 Specific SFR enhancement in (massive) galaxy pairs as function of the projected separation as measured by Li et al. (2008) (diamonds) and my prediction including the tail of artificial enhancement out to several hundred kiloparsecs (solid line). In this example a value of $\epsilon = 1.8$ has been used. The galaxy sample has been selected to be consistent with the massive sample in Li et al. (2008).

Real galaxy surveys, even spectroscopic surveys, have no access to the real space separation of galaxies. Li et al. (2008) used a projected correlation function $w(r_p)$ to circumvent this difficulty, where the projected correlation

function is related to the 3D correlation function via:

$$w(r_p) = \int_{-\infty}^{\infty} \xi([r_p^2 + \pi^2]^{1/2}) d\pi, \quad (3.7)$$

where π is the coordinate along the line of sight, and r_p is the projected separation transverse to the line of sight. I use for this exercise galaxies more massive than $3 \times 10^{10} M_{\odot}$ in order to match the selection criteria in Li et al. (2008). Moreover, they did not use an additive weight but used the SSFR of the primary galaxy as the weight of the pair. I also use such a scheme here to perform my weighted analysis in the simulation. Li et al. (2008) calculated the cross-correlation between a subsample of galaxies which are forming stars (primaries) and all the galaxies in the sample (secondaries). As I lack of such information I run a correlation using all the galaxies as both primaries and secondaries. I choose to model the data with a constant enhancement $\epsilon = 1.8$ at $r < r_c$, with $r_c = 35$ kpc. I also neglect any environmental suppression of star formation at separations $r > r_c$ (Barton et al. 2000; Balogh et al. 2002). These are clearly oversimplifications, as the real dependence of enhancement (and suppression at large radii) on separation will be considerably more complex. Yet, this simple model suffices to illustrate the recovered enhancement signature expected from a model in which SF is enhanced only at small radii.

Notwithstanding these limitations, I compare the results of my simple model with the data in Fig. 3.3. Strikingly, I find that the tail of enhanced SF out to ~ 200 kpc seen in the data may, in great part, be a reflection of the use of marked correlation functions statistics to explore the radial dependence of SF enhancement in galaxies. This has direct relevance in the interpretation of the results from Li et al. (2008). If one argued that the enhancement at ~ 100 kpc (or much of it) was real, one would need to fulfil two criteria to produce such an effect. Firstly, assuming that the triggering event is the first pass, one would need an enhancement lifetime of at least 300 Myr (longer than the internal dynamical time) for typical orbital velocities of 300 km/s or less. Secondly, a significant fraction of the secondaries would need to have near-radial orbits in order to produce such an enhancement. If, as I suggest instead, the enhanced SF at ~ 100 kpc is an artifact of the use of the 2 point correlation function, then one would argue that enhancement happens only for close pairs and shorter interaction-induced SF timescales and a greater diversity of orbits would be permitted. While developing a model that realistically reproduces the data is beyond the scope of this thesis, one can clearly see that this effect needs to be

accounted for in order to robustly interpret the behavior of marked correlation functions.

3.5 Conclusions

Weighted correlation functions are an increasingly important tool for understanding how galaxy properties depend on their separation from each other. I use a mock galaxy sample drawn from the Millenium simulation, assigning weights using a simple prescription to illustrate and explore how well a weighted correlation function recovers the true radial dependence of the input weights. I find that the use of a weighted correlation function results in a dilution of the magnitude of any radial dependence of properties and a smearing out of that radial dependence in radius, compared to the input behavior. I present a quantitative discussion of the dilution in the magnitude of radial dependence in properties in the special case of a constant enhancement ϵ for pairs separated by $r < r_c$. In this particular case the matching of one member of an enhanced pair with an unenhanced galaxy in the same group gives an artificial enhancement $\sim 0.1\epsilon$ out to large radii $< 5r_c$, and matches of one member of an enhanced pair with a member of another very distant enhanced pair pulls down the value of the recovered enhancement, with the discrepancy between the input and recovered enhancement being a function of the fraction of galaxies in close pairs and the value of the input enhancement. This systematic error is $< 10\%$ for enhancements $\epsilon < 4$, but precision measurements should account for this effect. I compare these results with observations of SFR enhancement from the SDSS Li et al. (2008), finding very similar behavior — a significant enhancement at radii < 40 kpc and a weak enhancement out to more than 150 kpc, lending credibility to the notion that weak enhancement in SFR seen out to large radii is an artifact of the use of weighted correlation function statistics. While I explored a particular case in this chapter, it is easy to see that the phenomenon is general.

Given this difference between input weights and those recovered by the weighted 2 point correlation function, one might ask if one shouldn't use a different method to explore radial trends in observables. I would argue that most different methods boil down to weighted 2 point correlation functions implicitly anyway, and that one is stuck at least at the qualitative level with the differences between input and recovered weights that I have discussed above.

For example, partnering projected pairs into different 'pairs' (i.e., not matching every galaxy with every other galaxy) suffers from two drawbacks: this is still a projected analysis, and many projected close pairs will be separated by significant distances along the line of sight; and second, one may choose the wrong galaxy to partner with, a particularly acute issue for triplets or groups of galaxies. One can see that such a method will suffer from a similar suppression of enhancement from the inclusion of non-pairs in the pair sample; of course, radial smearing is not possible in such a case, as there is only one radial bin. I conclude that those wishing to quantitatively analyze weighted correlation functions (or related observables) will need to account carefully for this effect using an analysis of simulated mock catalogs.

Chapter 4

The Merger–Driven Evolution of Massive Red Galaxies

In the introduction of this thesis (Chapter 1) I have mentioned that galaxy mergers are expected to be one of the main modes of massive galaxy growth in a hierarchical Universe. Now I focus on the impact of mergers on the build–up of massive red galaxies.

While the stellar populations of such massive red galaxies were already formed at redshift $z > 1$, these galaxies are expected to continue their mass–assembly at later times by the addition of stellar mass through merging. A factor $\sim 2 - 3$ evolution in number density has been observed around the knee of the luminosity function (LF) of red galaxies at $\sim 10^{11}M_{\odot}$ since $z = 1$ (Bell et al. 2004; Faber et al. 2007; Brown et al. 2007), but studies of much more massive galaxies have found results compatible with no evolution in that redshift range when accounting for passive luminosity evolution (Cimatti et al. 2006; Cool et al. 2008).

The goal of this chapter is to estimate the impact of galaxy mergers on the evolution of massive, red galaxies from $z = 1$ to the present day. The main challenge in observational studies of merger statistics is the identification of such systems. Galaxy mergers are found either in an early phase of the interaction, when the two galaxies have not yet coalesced and are found in a close pair (Patton et al. 2000; Le Fèvre et al. 2000; Lin et al. 2004, 2008; Bell et al. 2006b; Kartaltepe et al. 2007), or in a later phase, when they display signatures of gravitational interaction and are just prior to or after coalescence (Abraham et al. 1996; Conselice et al. 2003; Lotz et al. 2004; Bell et al. 2005; McIntosh et al. 2008; Jogee et al. 2009). A wide range of results have been found for the merger fraction evolution, parameterized as $(1 + z)^m$, with m ranging from 0 to 4 (e.g., Patton et al. 2000; Le Fèvre et al. 2000; Lin et al.

2004; Kartaltepe et al. 2007).

Here, I use robust 2–point correlation function techniques on a sample of galaxies with $0.2 < z < 1.2$ with masses in excess of $5 \times 10^{10} M_{\odot}$ selected from the COSMOS and COMBO–17 surveys to quantify the merger rate of massive galaxies and its evolution. I augment the statistical significance of my analysis by using an estimate of the pair fraction found in Sloan Digital Sky Survey (SDSS) at $z \sim 0.1$. The total volume probed by this study at intermediate redshifts is at least 4 times larger than any previous mass–selected study on the evolution of the merger fraction, and reduces dramatically the systematic uncertainties related to cosmic variance by the use of four independent fields. Then I compare the inferred galaxy merger rate with the observed number density evolution of massive ($M_* > 10^{11} M_{\odot}$), red galaxies from $z \sim 1$ to the present day, which I obtain by converting Brown et al. (2007) LFs to stellar–mass functions. I assume $H_0 = 70$ km/s, $\Omega_m = 0.3$ and $\Omega_{\Lambda} = 0.7$.

4.1 Sample and method

The bulk of my sample is drawn from the ~ 2 sq. degree COSMOS survey (Scoville et al. 2007). I use photometric redshifts calculated from 30-band photometry by Ilbert et al. (2009); comparison with spectroscopic redshifts shows excellent accuracy. I use those redshifts to derive rest-frame quantities and stellar masses by using the observed broad-band photometry in conjunction with a non-evolving template library derived using Pégase stellar population model (see Fioc & Rocca-Volmerange 1999) and a Chabrier (2003) stellar initial mass function (IMF). The use of a Kroupa et al. (1993) or a Kroupa (2001) IMF would yield similar stellar masses to within $\sim 10\%$. The reddest templates are produced through single exponentially–declining star formation episodes, intermediate templates also have a low-level constant star formation rate (SFR) and the bluer templates have superimposed a recent burst of star formation. A full description of the stellar masses will be provided in a future paper; comparison with Pannella et al. (2009) masses shows agreement at the 0.1 dex level.

To combat the sample variance of a single 2 sq. degree field, I augment the COSMOS sample with a sample drawn from three widely-separated 0.25 sq. degree fields from COMBO-17. COMBO–17 photo- z 's, colors and stellar masses have been extensively described in Wolf et al. (2003), Wolf et al. (2004),

Borch et al. (2006) and Gray et al. (2009). Given the different depths of the two surveys I only include galaxies from the COMBO-17 catalog at $z < 0.8$, where it is complete for my mass limit. The final sample comprises ~ 18000 galaxies with $M_* \geq 5 \times 10^{10} M_\odot$ over an area of ~ 2.75 sq. deg. in the redshift range $0.2 < z < 1.2$.

I use the fraction of galaxies with a companion closer than 30 kpc (close pairs) as a proxy for the merger fraction, as those systems are very likely to merge in a few hundred Myr¹. As redshift errors translate into line-of-sight (l.o.s.) distance uncertainties of the order of $\sim 50 - 100$ Mpc I use projected 2-point correlation functions (2pcf) to find the number of projected close pairs and then deproject into the 3D space.

The projected correlation function $w(r_p)$ is the integral along the line of sight of the real-space correlation function:

$$w(r_p) = \int_{-\infty}^{\infty} \xi([r_p^2 + \pi^2]^{1/2}) d\pi, \quad (4.1)$$

where r_p is the distance between the two galaxies projected on the plane of sky and π the line-of-sight separation. A convenient and simple estimator of the 2pcf at small scales is $w(r_p) = \Delta(DD/RR - 1)$ (e.g. Bell et al. 2006b), where Δ is the path length being integrated over, $DD(r_p)$ is the histogram of separations between real galaxies and $RR(r_p)$ is the histogram of separations between galaxies in a randomly-distributed catalog. As shown in the literature (e.g. Davis & Peebles 1983; Li et al. 2006a), the real-space 2pcf can be reasonably well fit by a power-law. Assuming $\xi(r) = (r/r_0)^{-\gamma}$, then $w(r_p) = Cr_0^\gamma r_0^{1-\gamma}$, with $C\sqrt{\pi}\{\Gamma[(\gamma - 1)/2]/\Gamma(\gamma/2)\}$. I fit the latter expression to my data to find the parameters γ and r_0 and use them in the real-space 2pcf to find the fraction of galaxies in close pairs.

As I wish to preserve S/N I did not integrate along the entire l.o.s. when calculating $w(r_p)$. Instead I allowed galaxies to form a pair only if the redshift difference was smaller than $\sigma_{pair} = \sqrt{2} \times \sigma_z$, with σ_z being the redshift error of the primary galaxy. As the photo- z errors follow a Gaussian distribution with width σ_z (Wolf et al. 2003, 2004) a fraction of the pairs would be missing by simply imposing the l.o.s. criteria. Thus, following Bell et al. (2006b) the fraction of galaxy pairs is

¹As the lower mass limit of my sample is $5 \times 10^{10} M_\odot$, I am automatically selecting both members of the pair to be above that mass.

$$f = \int_{-\sigma_{pair}}^{\sigma_{pair}} \frac{1}{\sqrt{2\pi}\sigma_z} e^{-z^2/2\sigma_z^2} dz. \quad (4.2)$$

Then, $w(r_P)$ is multiplied by $1/f$ in order to account for missing pairs; in my case a correction factor of 1.19.

Given the 3D correlation function $\xi(r)$, the differential probability of finding a galaxy occupying a volume δV at a distance r of another galaxy is $\delta P = n[1 + \xi(r)]\delta V$, where n is the number density of secondary galaxies. Then, by a simple integration of this expression, I obtain the probability of a galaxy being within a distance r_f of any other galaxy (Patton et al. 2000; Bell et al. 2006b; Masjedi et al. 2006):

$$P(r \leq r_f) = \int_0^{r_f} n[1 + \xi(r)]dV \quad (4.3)$$

Because $\xi(r) = (r/r_0)^{-\gamma}$ and $\xi(r) \gg 1$ at the small scales, I obtain:

$$P(r \leq r_f) = f_{pair} = \frac{4\pi n}{3 - \gamma} r_0^\gamma r_f^{3-\gamma}, \quad (4.4)$$

where f_{pair} is the fraction of *galaxies* in close pairs. As galaxy interactions are completely decoupled from the Hubble flow, I calculate probabilities as a function of the proper (physical) separation between the two galaxies. Errors in the correlation function are calculated by means of bootstrap resampling.

4.2 Results and discussion

In Fig. 4.1 I show the fraction of massive galaxies found in pairs with separations $r < 30$ kpc as a function of z . To augment the data at $z \sim 0.1$, I calculate the SDSS close pair fraction using γ and r_0 given by Li et al. (2006a). I adjust their r_0 by $\sim 5\%$ (an empirical adjustment based on the COSMOS+COMBO-17 sample) to account for different lower mass limits and binning. I also use the number density of galaxies fulfilling my mass criteria, adopting the g-band selected stellar-mass function in Bell et al. (2003) after correcting for stellar IMF and H_0 .

I perform an error-weighted least-squares fit of the form $F(z) = f(0) \times (1 +$

Table 4.1 3D correlation function parameters and close pair fractions

z	γ	r_0	f_{pair} ($r < 30$ kpc)
$0.2 < z \leq 0.4^a$	2.03 ± 0.05	3.50 ± 0.50	0.0171 ± 0.0050
$0.4 < z \leq 0.6^a$	2.06 ± 0.04	3.60 ± 0.50	0.0238 ± 0.0043
$0.6 < z \leq 0.8^a$	1.94 ± 0.04	3.80 ± 0.30	0.0241 ± 0.0038
$0.8 < z \leq 1.0^b$	1.93 ± 0.03	2.85 ± 0.25	0.0277 ± 0.0031
$1.0 < z \leq 1.2^b$	1.96 ± 0.03	2.55 ± 0.20	0.0315 ± 0.0030

^a Combined COSMOS+COMBO-17 sample

^b COSMOS-only sample

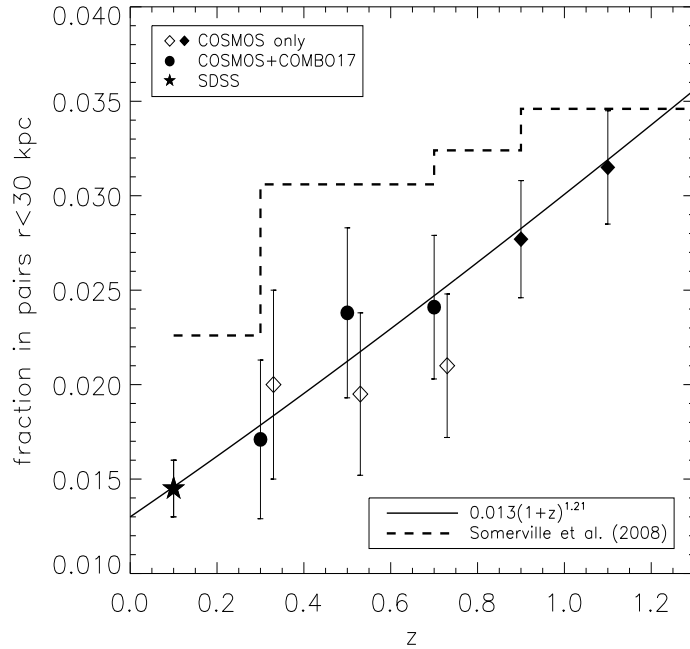


Figure 4.1 Fraction of $M_* > 5 \times 10^{10} M_\odot$ galaxies in close (3D) pairs ($r < 30$ kpc) as a function of redshift. *Diamonds*: Pair fraction found using only the COSMOS catalog. *Black circles*: Pair fraction found when adding galaxies from the COMBO-17 survey at $z < 0.8$ (I do not include galaxies from the COMBO-17 catalog in the two higher z bins). *Star*: Pair fraction from SDSS. The line shows the best fit to a real space pair fraction evolution with shape $F(z) = f(0) \times (1+z)^m$, with $f(0) = 0.0130 \pm 0.0019$ and $m = 1.21 \pm 0.25$ (fit to all black-filled points: star, circles and diamonds). *Dashed line*: Predicted fraction of galaxies above $M_* > 5 \times 10^{10} M_\odot$ involved in mergers, from the Somerville et al. (2008) model.

$z)^m$ to the filled points in Fig. 4.1, i.e., the SDSS pair fraction, the combined COSMOS+COMBO–17 pair fraction at $0.2 < z < 0.8$ and the COSMOS pair fraction at $0.8 < z < 1.2$. I find $f(0) = 0.0130 \pm 0.0019$ and $m = 1.21 \pm 0.25$. These associated uncertainties are at the same level as the systematic uncertainties in the overall M/L scale and its evolution since $z = 1$.

In my correlation function I do not impose an specific mass ratio criteria, but given the shape of the mass function above $M_* > 5 \times 10^{10} M_\odot$, I expect most of the mergers to be majors; i.e., with mass ratios between 1:1 and 1:4. I find between 70 and 90 percent of the purely projected close pairs have such a mass ratio.

Galaxies from the COSMOS survey represent 70% of my sample in the bins ranging from $z = 0.2$ to $z = 0.8$, however, the addition of COMBO–17 galaxies helps to decrease the sample variance. From the work by Moster et al. (in prep), I estimate that the sample variance is reduced by a factor of $\sim 30\%$ by including the three ~ 0.25 sq. deg independent fields from COMBO–17. This effect is clearly seen in Fig. 4.1. Considering only galaxies from COSMOS, there is an abrupt transition between $z = 0.7$ and $z = 0.9$, which is smoothed by the inclusion of COMBO–17 galaxies.

In Fig. 4.1 I include the close pair fractions found using mock catalogs from the Somerville et al. (2008) semi-analytic model (SAM). There is qualitative agreement between the slow evolution and overall normalization between models and observations, and given the difficulty that all models have in matching the shape of the stellar mass function in detail (which affects both the numerator and denominator of the close pair fraction; De Lucia et al. 2006; Somerville et al. 2008), I find this match encouraging. Predictions from other SAMs tend to agree reasonably well with Somerville et al. (2008) as shown in Fig. 11 of Joglee et al. (2009; see also Guo & White 2008).

4.2.1 Comparison with previous works

Very few studies of close pair fraction evolution use mass-limited samples. Bell et al. (2006b) used COMBO–17 data (0.75 sq. deg., the same catalog I use here to complement my COSMOS catalog) to find a fraction of galaxies in close major pairs ($r < 30$ kpc) of 2.8% for galaxies more massive than $3 \times 10^{10} M_\odot$ at $0.4 < z < 0.8$, in excellent agreement with my result despite the slightly different mass limit. They also performed an autocorrelation of all galaxies

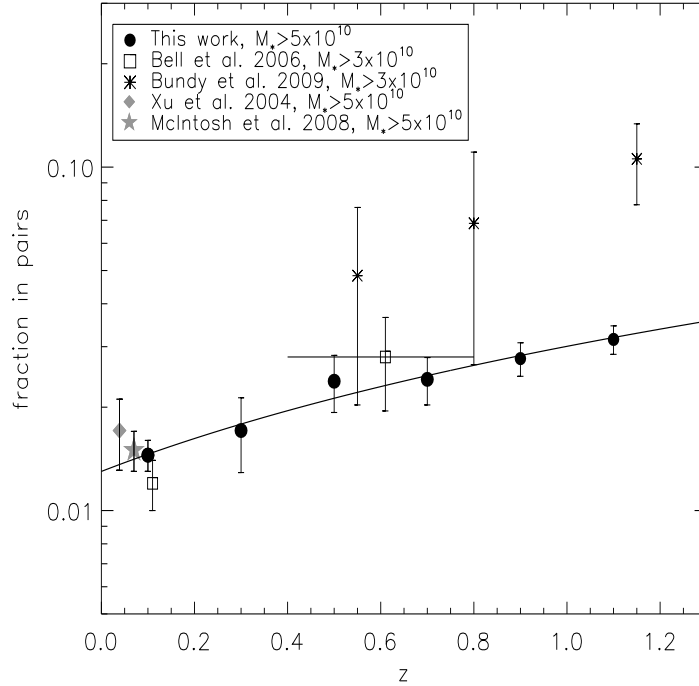


Figure 4.2 Evolution of the number of galaxies in close pairs. The estimate for major pair fraction of galaxies $M > 3 \times 10^{10} M_{\odot}$ from Bell et al. (2006b) is shown as empty squares. The results from Bundy et al. (2009) are represented by the asterisks. The point by Xu et al. (2004) is shown as the grey diamond. McIntosh et al. (2008) is shown as the grey star.

with $M_* > 2.5 \times 10^{10} M_{\odot}$ finding a pair fraction of $\sim 5\%$. This mismatch in pair fraction is entirely a consequence of the lower mass limit of the sample; adopting in my analysis instead a mass limit of $M_* > 2.5 \times 10^{10} M_{\odot}$ I recover a pair fraction of $\sim 5\%$. The main driver of this higher pair fraction is that $\sim 50\%$ of pairs in a sample limited to have $M_* > 2.5 \times 10^{10} M_{\odot}$ have mass ratios between 1:4 and 1:10; i.e., the major merger fraction is similar, but the close pair fraction is boosted by a considerable contribution from minors.

Recently, Bundy et al. (2009) found a higher pair fraction by studying a sample of galaxy pairs from the GOODS fields (total area ~ 0.36 sq. deg.). In Fig. 4.2 I show their results for the mass range $> 3 \times 10^{10} M_{\odot}$ after converting their fraction of pairs to the fraction of *galaxies in pairs*. I cannot explain why their results are so different from mine. I also show the estimate from Xu et al. (2004), who used a combined sample from the 2MASS and 2dFGRS surveys, after converting their results to my IMF and H_0 , and the result from McIntosh et al.

(2008), who measured the pair fraction in galaxy groups. I further correct the pair fractions found by Xu et al. (2004) and Bundy et al. (2009) down by 30% to account for pairs in their analyses that are genuinely associated with each other (so are not random projections), have projected separations of < 30 kpc but are separated by more than 30kpc in real space (i.e., galaxies in groups that are projected along the line of sight; Bell et al. 2006b)².

I can not compare my measurements with morphological studies of merger fractions because of uncertainties with the nature of the progenitors, and selection effects related to orbital parameters, galaxy structure and gas fractions. It is also hazardous to compare with close pair measurements based on luminosity-selected samples. Lin et al. (2008) used a sample of galaxies with B-band magnitudes (corrected for passive luminosity evolution) $-21 < M_B < -19$. For red galaxies, this is roughly compatible with my mass-selected sample, but it includes many low-mass blue galaxies, which makes a comparison impossible because their clustering properties are very different. Furthermore, as merging can enhance the star formation activity (see Chapter 2), selecting galaxies in rest-frame blue bands is biased in favor of mergers, as such a selection would recover merging systems with lower mass given the decreased M/L ratio induced by the interaction. All of these effects will be more pronounced in gas-rich galaxies, and gas fractions were likely higher in the past, leading to a redshift dependent bias.

Kartaltepe et al. (2007) derived the evolution of the pair fraction from a luminosity-selected sample from a similar dataset as analyzed in this chapter. Their very different result (they find $m = 3.1 \pm 0.1$) is caused at least in part by the difference between mass- and luminosity-selected samples, as described above. In addition, they identify pairs in both the ground-based and HST/ACS-based catalogues. Because their sample is selected by ground-based luminosity, very close pairs that are only resolved by ACS can be as bright as a single galaxy in a more widely separated pair that is resolved in the ground-based imaging. This artificially raises that close pair fraction, especially at high redshift.

²This effect is present also in pair fractions determined from spectroscopic redshifts as long as a deprojection to the 3D space is not performed.

4.2.2 The impact of galaxy merging on the creation of red $M_* > 10^{11}M_\odot$ galaxies.

My measured fraction of $M_* > 5 \times 10^{10}M_\odot$ galaxies in close pairs as a function of redshift constrains the impact that merging-induced mass assembly has on the creation rate of $M_* > 10^{11}M_\odot$ systems.

As only $\sim 6\%$ of my galaxies with a projected companion at $r < 30$ kpc has a *second* companion at such separation, I assume that the number of close pairs is simply one half of the number of galaxies in close pairs. The fraction of newly created $M_* > 10^{11}M_\odot$ galaxies due to merging is $f_{rem} = N_{cp}/N_{11}$, where N_{cp} is the number of close pairs of galaxies above $5 \times 10^{10}M_\odot$ each and N_{11} is the total number of galaxies with stellar masses in excess of $10^{11}M_\odot$.

Following Patton & Atfield (2008) or Bell et al. (2006b), the merger timescale for galaxy pairs at this separation is approximately $\tau = 0.5$ Gyrs, so I compute the creation rate of newly assembled galaxies, R_{rem} , as $R_{rem} = f_{rem}/\tau$. I integrate the merger rate over cosmic time finding that, on average, present day galaxies with stellar masses larger than $10^{11}M_\odot$ have undergone 0.5 (0.7) mergers since $z = 0.6$ (1.2) from interactions between galaxies more massive than $5 \times 10^{10}M_\odot$.

Now I want to address the question whether my observed merger rate evolution can explain the observed number density evolution of $M_* > 10^{11}M_\odot$ red galaxies. I assume that mergers of massive galaxies quench the star formation activity and the remnants will be red systems in order to compare with the number density evolution of red galaxies.

I convert the evolution of the B-band luminosity function of red galaxies as measured by Brown et al. (2007) to the evolution in the number density of galaxies more massive than $10^{11}M_\odot$. For this conversion I use the typical stellar mass-to-light ratio of nearby red galaxies ($M/L_B = 3.4 \pm 0.6$, e.g., Bell et al. 2003; Kauffmann et al. 2003) and apply a correction to account for its evolution with redshift, derived from the evolution of the fundamental plane zero point ($\Delta \log(M/L_B) = 0.555 \pm 0.042$, van Dokkum & van der Marel 2007). I repeat the process 10000 times allowing the luminosity function parameters, as well as the M/L_B constraints, to vary randomly within their uncertainties. I estimate the final uncertainty by estimating the typical dispersion of those 10000 realizations.

In Fig. 4.3 I show the observed evolution on the number density of massive, red

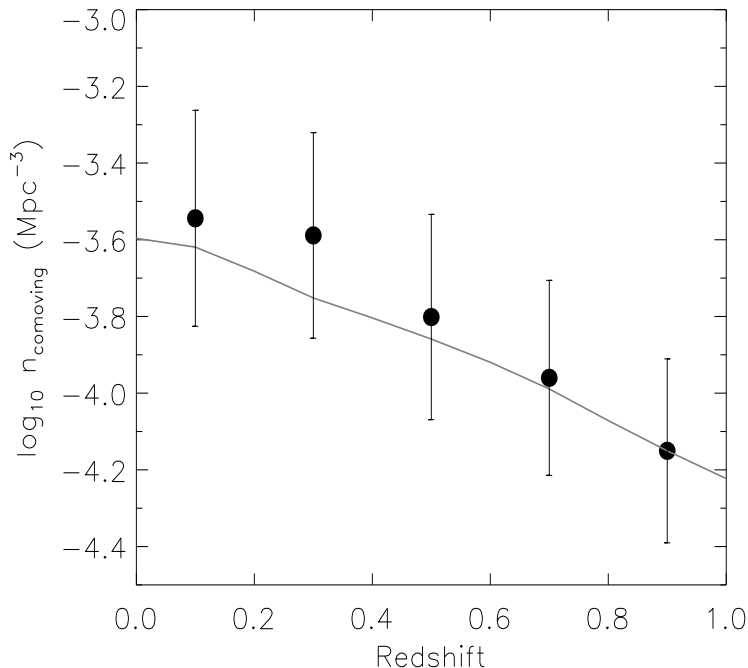


Figure 4.3 Number density evolution of red galaxies with $M_* > 10^{11} M_\odot$. Filled points represents the observed evolution by Brown et al. (2007) (see text for details). The solid line shows the expected growth implied by my measurement of the close pair fraction.

galaxies together with the evolution implied by my merger rate measurement. I stress that both measurements are *completely independent* except for the fact that I use the observed density at $z \sim 0.9$ as the zeropoint where I anchor the evolution predicted by my close pair fractions. I find that mergers of massive galaxies can explain the evolution in the observed number density of massive, red galaxies since $z = 1$. I have used $\tau = 0.5$ Gyrs, but using the $\tau \sim 1$ Gyr timescale from Kitzbichler & White (2008) yields a somewhat slower evolution that is still compatible within the error bars.

There are two caveats I would like to mention. Firstly, given the nature of my method, some of the progenitor galaxies have masses above $10^{11} M_\odot$, so strictly speaking they are not *newly formed* massive galaxies. Second, because I adopt a lower mass limit of $5 \times 10^{10} M_\odot$, I underestimate the number of major mergers that could lead to the formation of a massive galaxy. For example, a pair with individual masses $M_* = 6 \times 10^{10} M_\odot$ and $M_* = 4 \times 10^{10} M_\odot$ would not make it into my pair sample but would produce a major merger remnant of $10^{11} M_\odot$. Assuming that the merging population has a composition similar to my overall

sample, I estimate that this latter lower mass limit issue has an impact a factor ~ 2 larger on the creation of $> 10^{11}M_{\odot}$ galaxies than the overestimate caused by double counting already massive red galaxies (i.e., for each pair in which a progenitor was already above my mass limit I have ~ 2 pairs which will form a massive remnant that I am not counting because of my mass limit). Thus, if anything, I underestimate the real creation rate of massive galaxies induced by merging.

4.3 Conclusions

I have studied the impact of galaxy mergers on the evolution of massive red galaxies by using 2pcfs to measure the fraction of galaxies in close pairs from a sample of ~ 18000 galaxies more massive than $5 \times 10^{10}M_{\odot}$ drawn from the COSMOS and COMBO-17 surveys and a pair fraction estimate from SDSS. I have also used constraints from the observed evolution of the fundamental plane to calculate the number density evolution of $> 10^{11}M_{\odot}$ red galaxies from Brown et al. (2007) LFs. My main findings are:

- The fraction of galaxies in close pairs evolves as $F(z) = (0.0130 \pm 0.0019) \times (1+z)^{1.21 \pm 0.25}$. When assuming a merging timescale of $\tau = 0.5$ Gyr it implies that galaxies more massive than $10^{11}M_{\odot}$ have undergone, on average, 0.5(0.7) major mergers since $z = 0.6(1.2)$.
- The evolution implied by this merger rate is sufficient to explain the observed number density evolution of red galaxies with masses above $10^{11}M_{\odot}$. This result, together with the recent finding by van der Wel et al. (2009) that *all* massive quiescent galaxies in the local Universe have been formed by mergers, points to a scenario in which mergers are the dominant mechanism responsible for the formation of the red sequence above such stellar mass.

In this thesis I have studied the impact of major galaxy mergers on the evolution of galaxies over the last ~ 8 Gyrs. I have used ground-based and space-based photometry from the UV to the MIR to constrain, specifically, how mergers influence the creation of new stars in the Universe and how much they contribute to the assembly of stellar mass in massive, elliptical galaxies from already formed stars. I also had to develop statistical tools which will improve the reliability of future studies on the clustering of physical properties of galaxies.

In Chapter 2 I have made use of COMBO-17 survey redshifts and stellar masses, together with $24\mu\text{m}$ photometry from *Spitzer* in order to study the SF enhancement induced by galaxy interactions. This study has produced three main results: a) When averaged over all interactions and all phases of the interaction, the star formation activity is enhanced by a factor of 1.8 ± 0.3 ; b) Most of the interactions do not induce a ULIRG phase, but nevertheless, it seems that in order to reach the highest levels of SFR observed, interactions are required; and c) Over the redshift range $0.4 < z < 0.8$, roughly 20% of the star formation density is found in major interacting systems, but only a $8 \pm 3\%$ of such star formation is *directly triggered* by the interaction.

While working on the already mentioned problem of the SFR enhancement in galaxy interactions I found that the statistical tool I was using, the weighted 2-point correlation function, could introduce a bias in the shape of the recover enhancement. In Chapter 3 I used the Millennium Simulation in order to estimate the magnitude of the bias that the use of such a tool would introduce on my results. My findings were that the nature of the 2-point analysis, in which every point is matched with every other point, was causing that galaxies close to a physical close pair were inheriting a fraction of the enhancement

even if a causal relation does not exist. My simulations show that in those cases where the enhancement is relatively small (< 4), the overall uncertainty is negligible. On the other hand, studies of physical properties which strongly correlate with galaxy clustering should correct for this bias.

In Chapter 4 I have addressed one of the big open questions in modern studies of galaxy evolution, this is, the contribution from galaxy mergers to the build-up of the red sequence at large stellar masses. I have used catalogs from the COSMOS and COMBO-17 surveys in order to estimate the merger rate evolution from $z = 0$ to $z = 1.2$ and constrain the implications for the formation of red galaxies with stellar masses larger than $10^{11}M_{\odot}$. I found that the fraction of $M_{*} \geq 5 \times 10^{10}M_{\odot}$ galaxies found in close pairs at separations $r < 30$ kpc evolves as $F(z) = (0.0130 \pm 0.0019) \times (1 + z)^{1.21 \pm 0.25}$. By assuming a pair timescale of $\tau = 0.5$ Gyr this pair fraction implies that, on average, galaxies more massive than $10^{11}M_{\odot}$ have undergone 0.5(0.7) major mergers since redshift 0.6(1.2).

I have also used the luminosity functions of red galaxies in the rest-frame B band from Brown et al. (2007) to measure the number density evolution of $M_{*} > 10^{11}M_{\odot}$ red galaxies. I transformed those luminosity functions to mass functions by using constraints on the M/L_B ratio evolution from the fundamental plane of elliptical galaxies from $z = 1$ to $z = 0$ (van Dokkum & van der Marel 2007) and a normalization of such ratio in the local Universe from SDSS (Bell et al. 2003; Kauffmann et al. 2003). I found that the number density of massive red galaxies has increased by a factor of ~ 4 since $z = 1$ and that the merger rate of massive galaxies can, under the assumption that all merger remnants will be red galaxies, explain such evolution.

Overall, this thesis has helped to understand the role that galaxy mergers play in the big picture of galaxy evolution in the last 8 gyrs. Cosmologically speaking, major mergers are not an important factor in the formation of new stars since $z = 1$, since less than 10% of the star formation has a causal relation with such events. On the other hand, I have argued that major galaxy interactions play a crucial role in the build-up of stellar mass in massive red galaxies. These two results, which could seem mutually exclusive at first sight are rather complementary, i.e., major mergers are irrelevant for the generation of new stellar mass in the Universe, but they cause the reorganization of the *already existent* stellar mass transforming disks into bulges and adding-up galaxies to form more massive systems.

Ten or fifteen years ago we started to witness the high redshift Universe and

realized that the galaxy populations looked somehow different at different times. Nowadays, it is clear that the global properties of galaxies not only depend on the age of the Universe at which we observe them but also on the environment in which the galaxy is found. Galaxies in dense environments have, on average, different global properties (morphology, SF activity, color, etc.) than galaxies in the field and that might have some impact in the global evolution of galaxy populations. As an example, I have shown how galaxy mergers drive the evolution of the massive end of the red sequence but we do not know if the merger rate is dominated by galaxies in groups/clusters or by galaxies in the field. Furthermore, we still do not have a definitive answer to the question of what is driving the decline of the cosmic star formation density, neither we know what quenches the star formation and force galaxies to migrate from the blue cloud to the red sequence.

I have argued that mergers move galaxies in the mass axis of the color–mass diagram, but more detailed studies are needed in order to understand if the new formed very massive galaxies are assembled from a population of already red galaxies on the red sequence or from the quenching of the star formation in mergers involving blue galaxies. For example, mergers have been predicted to trigger nuclear activity by driving large amounts of gas to the very central region of the galaxy, where the supermassive black hole is expected to lie, but not conclusive observational evidence has been found so far. Given the relations linking the mass of the black hole with some properties of the galaxies, coevolution is expected. I believe that it is not a minor problem for us as a community that we have failed to confirm or refute such scenario.

We also need to understand what is driving the quenching in the lower mass galaxies since $z = 1$. Mergers do certainly account for a fraction of the quenched systems, but in the regime of $M_* < 10^{11} M_\odot$ galaxies, Ram-pressure stripping and other environmental mechanisms are expected to play also an important role, so does the gradual depletion of available gas. All these questions need to be answered in order to understand the last 8 Gyrs of galaxy evolution.

But, indeed, the Universe does extend beyond $z = 1$. We are at the beginning of the era in which NIR instrumentation has become sensitive enough to start large galaxy surveys at $z > 1$, or in other words, we are starting to harvest the desert. For example, massive elliptical galaxies at $z \sim 2$ were 5 times smaller than present day galaxies of equivalent stellar mass. Arguments in favor and against mergers driving the evolution in the mass–size relation have been published in the last two years, but I believe that we do not fully understand

the process behind such an evolution. Another major breakthrough in the last years has been the realization of the importance that the so-called clumpy disk galaxies could have on galaxy evolution. The clumpiness of those disks is expected to be related to massive flows of cold gas from the cosmic web. We do not know what dominates the star formation density at $z > 1$ but we do know that clumpy galaxies were relatively common at $z > 1$ and very rare at lower redshifts. If the decline of the cosmic SFR since $z \sim 1$ turns out to be related with the absence of cold inflows, the study of these galaxies could provide a huge step in the direction of understanding the star formation properties of the Universe.

It is clear, then, that the knowledge about galaxy evolution has advanced at an incredible rate over the last 15 years, but there are still many issues to be solved before we can claim a profound comprehension of the field. In the next 10–20 years, thanks to powerful new instrumentation, we will collect new information which will greatly help to reach a better understanding of our Universe.

The most exciting fact is that we might not have yet asked ourselves the questions that we will answer over the next two decades.

Acknowledgements

I would like to thank all the people who have helped me in some way during my thesis.

First of all, Eric Bell, my thesis advisor. He has not only guided me through these years of research, saved my scientific life when the political side of research was exceeding the limits of what I can take and been extremely patient when I did come down to his office every second day with my newest crazy idea about how to unveil the mysteries of the Universe, but also taught me what might be the most important thing I have learned about Astronomy: There are millions of questions out there to be answered, but only some are worth a good astronomer's time.

Arjen van der Wel is a postdoc at MPIA who has been helping me a great deal during the last year of this thesis. He did not have any formal responsibility on me but he has been extremely helpful for the development of this thesis, to the point that I am not sure if I would have made it on time without him. Thanks for that.

Hans-Walter Rix, Alejo Martínez Sansigre, Yolanda Sestayo de la Cerra, Dan McIntosh, Isabel Franco Rico, Ros Skelton and Christine Ruhland have also played an important role in the development of my research.

Christian Fendt, Ingrid Apfel and Heide Seifert for performing with exquisite

efficiency their work and helping in so many different issues during these years.

Uli Hiller and Marco Piroth. Every institute or university would be lucky to have such great professionals and so willing-to-help technicians.

On the personal side, my wife Yolanda deserves the biggest acknowledgement of all, because she has been the other half of the fine-tuned researcher-parental machine we have formed in our little family. I remember how we used to discuss about our thesis when we got to Heidelberg, later during the pregnancy and more recently while we were playing with Silvia on the carpet. We have gone through very hard times being so far from our families and now that we are so close to the end I cannot believe we have made it. Thanks for all those moments.

I take the opportunity to apologize to my wife for my (many and frequent) jokes on “How can you know that if you haven’t detected one single high-energy neutrino so far?”

My parents, M. Dolores and Octavio, are responsible for half of what I am. I can only admire the great efforts they have made to create the basis on which we (my two brothers and myself) are building our lives. This thesis, as little thing as it might be, is evidence for how well you have done your job. Thanks for everything.

Silvia will be one day old enough to read these words. I want her to know that in spite of the many sleepless nights, her temper when she loses the pacifier and the permanent attention she requires because of her tendency to run faster than what her short legs permit, she has been the light at the end of the tunnel, the air that we deeply breathe when we had to run the final sprint.

She is my North Star.

Aday Robaina Rapisarda.
Heidelberg, 30th October 2009

Bibliography

- Abraham, R. G., Tanvir, N. R., Santiago, B. X., Ellis, R. S., Glazebrook, K., & van den Bergh, S. 1996, MNRAS, 279, L47**
- Aguirre, A. N. 1999, ApJ, 512, L19
- Alonso-Herrero, A., Pérez-González, P. G., Alexander, D. M., Rieke, G. H., Rigopoulou, D., Le Floch, E., Barmby, P., Papovich, C., Rigby, J. R., Bauer, F. E., Brandt, W. N., Egami, E., Willner, S. P., Dole, H., & Huang, J. 2006, ApJ, 640, 167
- Babcock, H. W. 1939, Lick Observatory Bulletin, 19, 41
- Balogh, M. L., Couch, W. J., Smail, I., Bower, R. G., & Glazebrook, K. 2002, MNRAS, 335, 10
- Barnes, J. E., & Hernquist, L. 1996, ApJ, 471, 115
- Barnes, J. E., & Hernquist, L. E. 1991, ApJ, 370, L65
- Barton, E. J., Arnold, J. A., Zentner, A. R., Bullock, J. S., & Wechsler, R. H. 2007, ApJ, 671, 1538
- Barton, E. J., Geller, M. J., & Kenyon, S. J. 2000, ApJ, 530, 660
- Baugh, C. M., Lacey, C. G., Frenk, C. S., Granato, G. L., Silva, L., Bressan, A., Benson, A. J., & Cole, S. 2005, MNRAS, 356, 1191

- Beisbart, C., & Kerscher, M. 2000, *ApJ*, 545, 6
- Bell, E. F., & de Jong, R. S. 2001, *ApJ*, 550, 212
- Bell, E. F., McIntosh, D. H., Katz, N., & Weinberg, M. D. 2003, *ApJS*, 149, 289
- Bell, E. F., Naab, T., McIntosh, D. H., Somerville, R. S., Caldwell, J. A. R., Barden, M., Wolf, C., Rix, H.-W., Beckwith, S. V., Borch, A., Häussler, B., Heymans, C., Jahnke, K., Jogee, S., Kuposov, S., Meisenheimer, K., Peng, C. Y., Sanchez, S. F., & Wisotzki, L. 2006a, *ApJ*, 640, 241
- Bell, E. F., Papovich, C., Wolf, C., Le Floch, E., Caldwell, J. A. R., Barden, M., Egami, E., McIntosh, D. H., Meisenheimer, K., Pérez-González, P. G., Rieke, G. H., Rieke, M. J., Rigby, J. R., & Rix, H.-W. 2005, *ApJ*, 625, 23
- Bell, E. F., Phleps, S., Somerville, R. S., Wolf, C., Borch, A., & Meisenheimer, K. 2006b, *ApJ*, 652, 270
- Bell, E. F., Wolf, C., Meisenheimer, K., Rix, H.-W., Borch, A., Dye, S., Kleinheinrich, M., Wisotzki, L., & McIntosh, D. H. 2004, *ApJ*, 608, 752
- Bell, E. F., Zheng, X. Z., Papovich, C., Borch, A., Wolf, C., & Meisenheimer, K. 2007, *ApJ*, 663, 834
- Birnboim, Y., & Dekel, A. 2003, *MNRAS*, 345, 349
- Blain, A. W., Chapman, S. C., Smail, I., & Ivison, R. 2004, *ApJ*, 611, 725
- Blanton, M. R. 2006, *ApJ*, 648, 268
- Blanton, M. R., Hogg, D. W., Bahcall, N. A., Baldry, I. K., Brinkmann, J., Csabai, I., Eisenstein, D., Fukugita, M., Gunn, J. E., Ivezić, Ž., Lamb, D. Q., Lupton, R. H., Loveday, J., Munn, J. A., Nichol, R. C., Okamura, S., Schlegel, D. J., Shimasaku, K., Strauss, M. A., Vogeley, M. S., & Weinberg, D. H. 2003, *ApJ*, 594, 186
- Boerner, G., Mo, H., & Zhou, Y. 1989, *A&A*, 221, 191
- Bond, J. R., Cole, S., Efstathiou, G., & Kaiser, N. 1991, *ApJ*, 379, 440
- Borch, A., Meisenheimer, K., Bell, E. F., Rix, H.-W., Wolf, C., Dye, S., Kleinheinrich, M., Kovacs, Z., & Wisotzki, L. 2006, *A&A*, 453, 869
- Brown, M. J. I., Dey, A., Jannuzi, B. T., Brand, K., Benson, A. J., Brodwin, M., Croton, D. J., & Eisenhardt, P. R. 2007, *ApJ*, 654, 858

- Bundy, K., Fukugita, M., Ellis, R. S., Targett, T. A., Belli, S., & Kodama, T. 2009, *ApJ*, 697, 1369
- Caldwell, J. A. R., McIntosh, D. H., Rix, H., Barden, M., Beckwith, S. V. W., Bell, E. F., Borch, A., Heymans, C., Häußler, B., Jahnke, K., Jogee, S., Meisenheimer, K., Peng, C. Y., Sánchez, S. F., Somerville, R. S., Wisotzki, L., & Wolf, C. 2008, *ApJS*, 174, 136
- Chabrier, G. 2003, *ApJ*, 586, L133
- Chapman, S. C., Smail, I., Windhorst, R., Muxlow, T., & Ivison, R. J. 2004, *ApJ*, 611, 732
- Cimatti, A., Daddi, E., & Renzini, A. 2006, *A&A*, 453, L29
- Colless, M., Dalton, G., Maddox, S., Sutherland, W., Norberg, P., Cole, S., Bland-Hawthorn, J., Bridges, T., Cannon, R., Collins, C., Couch, W., Cross, N., Deeley, K., De Propriis, R., Driver, S. P., Efstathiou, G., Ellis, R. S., Frenk, C. S., Glazebrook, K., Jackson, C., Lahav, O., Lewis, I., Lumsden, S., Madgwick, D., Peacock, J. A., Peterson, B. A., Price, I., Seaborne, M., & Taylor, K. 2001, *MNRAS*, 328, 1039
- Connolly, A. J., Scranton, R., Johnston, D., Dodelson, S., Eisenstein, D. J., Frieman, J. A., Gunn, J. E., Hui, L., Jain, B., Kent, S., Loveday, J., Nichol, R. C., O'Connell, L., Postman, M., Scoccimarro, R., Sheth, R. K., Stebbins, A., Strauss, M. A., Szalay, A. S., Szapudi, I., Tegmark, M., Vogeley, M. S., Zehavi, I., Annis, J., Bahcall, N., Brinkmann, J., Csabai, I., Doi, M., Fukugita, M., Hennessy, G. S., Hindsley, R., Ichikawa, T., Ivezić, Ž., Kim, R. S. J., Knapp, G. R., Kunszt, P., Lamb, D. Q., Lee, B. C., Lupton, R. H., McKay, T. A., Munn, J., Peoples, J., Pier, J., Rockosi, C., Schlegel, D., Stoughton, C., Tucker, D. L., Yanny, B., & York, D. G. 2002, *ApJ*, 579, 42
- Conselice, C. J., Bershady, M. A., Dickinson, M., & Papovich, C. 2003, *AJ*, 126, 1183
- Cool, R. J., Eisenstein, D. J., Fan, X., Fukugita, M., Jiang, L., Maraston, C., Meiksin, A., Schneider, D. P., & Wake, D. A. 2008, *ApJ*, 682, 919
- Cox, T. J., Dutta, S. N., Di Matteo, T., Hernquist, L., Hopkins, P. F., Robertson, B., & Springel, V. 2006, *ApJ*, 650, 791
- Cox, T. J., Jonsson, P., Somerville, R. S., Primack, J. R., & Dekel, A. 2008, *MNRAS*, 384, 386
- Davis, M., & Peebles, P. J. E. 1983, *ApJ*, 267, 465
- De Lucia, G., Springel, V., White, S. D. M., Croton, D., & Kauffmann, G. 2006, *MNRAS*, 366, 499

- Dekel, A., & Birnboim, Y. 2008, MNRAS, 383, 119
- Devriendt, J. E. G., Guiderdoni, B., & Sadat, R. 1999, A&A, 350, 381
- Di Matteo, P., Bournaud, F., Martig, M., Combes, F., Melchior, A., & Semelin, B. 2008, A&A, 492, 31
- Di Matteo, P., Combes, F., Melchior, A., & Semelin, B. 2007, A&A, 468, 61
- Di Matteo, P., Jog, C. J., Lehnert, M. D., Combes, F., & Semelin, B. 2009, A&A, 501, L9
- Di Matteo, T., Springel, V., & Hernquist, L. 2005, Nature, 433, 604
- Eisenstein, D. J., Zehavi, I., Hogg, D. W., Scoccamarro, R., Blanton, M. R., Nichol, R. C., Scranton, R., Seo, H., Tegmark, M., Zheng, Z., Anderson, S. F., Annis, J., Bahcall, N., Brinkmann, J., Burles, S., Castander, F. J., Connolly, A., Csabai, I., Doi, M., Fukugita, M., Frieman, J. A., Glazebrook, K., Gunn, J. E., Hendry, J. S., Hennessy, G., Ivezić, Z., Kent, S., Knapp, G. R., Lin, H., Loh, Y., Lupton, R. H., Margon, B., McKay, T. A., Meiksin, A., Munn, J. A., Pope, A., Richmond, M. W., Schlegel, D., Schneider, D. P., Shimasaku, K., Stoughton, C., Strauss, M. A., SubbaRao, M., Szalay, A. S., Szapudi, I., Tucker, D. L., Yanny, B., & York, D. G. 2005, ApJ, 633, 560
- Emsellem, E., Cappellari, M., Peletier, R. F., McDermid, R. M., Bacon, R., Bureau, M., Copin, Y., Davies, R. L., Krajnović, D., Kuntschner, H., Miller, B. W., & de Zeeuw, P. T. 2004, MNRAS, 352, 721
- Faber, S. M., Willmer, C. N. A., Wolf, C., Koo, D. C., Weiner, B. J., Newman, J. A., Im, M., Coil, A. L., Conroy, C., Cooper, M. C., Davis, M., Finkbeiner, D. P., Gerke, B. F., Gebhardt, K., Groth, E. J., Guhathakurta, P., Harker, J., Kaiser, N., Kassin, S., Kleinheinrich, M., Konidaris, N. P., Kron, R. G., Lin, L., Luppino, G., Madgwick, D. S., Meisenheimer, K., Noeske, K. G., Phillips, A. C., Sarajedini, V. L., Schiavon, R. P., Simard, L., Szalay, A. S., Vogt, N. P., & Yan, R. 2007, ApJ, 665, 265
- Faltenbacher, A., Gottlöber, S., Kerscher, M., & Müller, V. 2002, A&A, 395, 1
- Ferrarese, L., Côté, P., Jordán, A., Peng, E. W., Blakeslee, J. P., Piatek, S., Mei, S., Merritt, D., Milosavljević, M., Tonry, J. L., & West, M. J. 2006, ApJS, 164, 334
- Fioc, M., & Rocca-Volmerange, B. 1997, A&A, 326, 950
- . 1999, ArXiv Astrophysics e-prints

- Ford, H. C., Clampin, M., Hartig, G. F., Illingworth, G. D., Sirianni, M., Martel, A. R., Meurer, G. R., McCann, W. J., Sullivan, P. C., Bartko, F., Benitez, N., Blakeslee, J., Bouwens, R., Broadhurst, T., Brown, R. A., Burrows, C. J., Campbell, D., Cheng, E. S., Feldman, P. D., Franx, M., Golimowski, D. A., Gronwall, C., Kimble, R. A., Krist, J. E., Lesser, M. P., Magee, D., Miley, G., Postman, M., Rafal, M. D., Rosati, P., Sparks, W. B., Tran, H. D., Tsvetanov, Z. I., Volmer, P., White, R. L., & Woodruff, R. A. 2003, in *Society of Photo-Optical Instrumentation Engineers (SPIE) Conference Series*, Vol. 4854, *Society of Photo-Optical Instrumentation Engineers (SPIE) Conference Series*, ed. J. C. Blades & O. H. W. Siegmund, 81–94
- Giavalisco, M., Steidel, C. C., Adelberger, K. L., Dickinson, M. E., Pettini, M., & Kellogg, M. 1998, *ApJ*, 503, 543
- Gottlöber, S., Kerscher, M., Kravtsov, A. V., Faltenbacher, A., Klypin, A., & Müller, V. 2002, *A&A*, 387, 778
- Gray, M. E., Wolf, C., Barden, M., Peng, C. Y., Häußler, B., Bell, E. F., McIntosh, D. H., Guo, Y., Caldwell, J. A. R., Bacon, D., Balogh, M., Barazza, F. D., Böhm, A., Heymans, C., Jahnke, K., Jogee, S., van Kampen, E., Lane, K., Meisenheimer, K., Sánchez, S. F., Taylor, A., Wisotzki, L., Zheng, X., Green, D. A., Beswick, R. J., Saikia, D. J., Gilmour, R., Johnson, B. D., & Papovich, C. 2009, *MNRAS*, 393, 1275
- Groth, E. J., & Peebles, P. J. E. 1977, *ApJ*, 217, 385
- Hammer, F., Flores, H., Elbaz, D., Zheng, X. Z., Liang, Y. C., & Cesarsky, C. 2005, *A&A*, 430, 115
- Holmberg, E. 1940, *ApJ*, 92, 200
- . 1941, *ApJ*, 94, 385
- Hopkins, A. M. 2004, *ApJ*, 615, 209
- Hopkins, A. M., & Beacom, J. F. 2006, *ApJ*, 651, 142
- Hopkins, P. F., Cox, T. J., Younger, J. D., & Hernquist, L. 2009, *ApJ*, 691, 1168
- Hubble, E. 1937, *Ciel et Terre*, 53, 194
- Ilbert, O., Capak, P., Salvato, M., Aussel, H., McCracken, H. J., Sanders, D. B., Scoville, N., Kartaltepe, J., Arnouts, S., Floc'h, E. L., Mobasher, B., Taniguchi, Y., Lamareille, F., Leauthaud, A., Sasaki, S., Thompson, D., Zamojski, M., Zamorani, G., Bardelli, S., Bolzonella, M., Bongiorno, A., Brusa, M., Caputi, K. I., Carollo, C. M., Contini, T., Cook, R., Coppa, G., Cucciati, O., de la Torre, S., de Ravel, L., Franzetti, P., Garilli,

- B., Hasinger, G., Iovino, A., Kampczyk, P., Kneib, J., Knobel, C., Kovac, K., LeBorgne, J. F., LeBrun, V., Fèvre, O. L., Lilly, S., Looper, D., Maier, C., Mainieri, V., Mellier, Y., Mignoli, M., Murayama, T., Pellò, R., Peng, Y., Pérez-Montero, E., Renzini, A., Ricciardelli, E., Schiminovich, D., Scodreggio, M., Shioya, Y., Silverman, J., Surace, J., Tanaka, M., Tasca, L., Tresse, L., Vergani, D., & Zucca, E. 2009, *ApJ*, 690, 1236
- Jogee, S., Miller, S. H., Penner, K., Skelton, R. E., Conselice, C. J., Somerville, R. S., Bell, E. F., Zheng, X. Z., Rix, H., Robaina, A. R., Barazza, F. D., Barden, M., Borch, A., Beckwith, S. V. W., Caldwell, J. A. R., Peng, C. Y., Heymans, C., McIntosh, D. H., Häußler, B., Jahnke, K., Meisenheimer, K., Sanchez, S. F., Wisotzki, L., Wolf, C., & Papovich, C. 2009, *ApJ*, 697, 1971
- Jonsson, P., Cox, T. J., Primack, J. R., & Somerville, R. S. 2006, *ApJ*, 637, 255
- Kahn, F. D., & Woltjer, L. 1959, *ApJ*, 130, 705
- Kartaltepe, J. S., Sanders, D. B., Scoville, N. Z., Calzetti, D., Capak, P., Koekemoer, A., Mobasher, B., Murayama, T., Salvato, M., Sasaki, S. S., & Taniguchi, Y. 2007, *ApJS*, 172, 320
- Kauffmann, G., & Haehnelt, M. 2000, *MNRAS*, 311, 576
- Kauffmann, G., Heckman, T. M., White, S. D. M., Charlot, S., Tremonti, C., Brinchmann, J., Bruzual, G., Peng, E. W., Seibert, M., Bernardi, M., Blanton, M., Brinkmann, J., Castander, F., Csábai, I., Fukugita, M., Ivezić, Z., Munn, J. A., Nichol, R. C., Padmanabhan, N., Thakar, A. R., Weinberg, D. H., & York, D. 2003, *MNRAS*, 341, 33
- Kaviraj, S., Peirani, S., Khochfar, S., Silk, J., & Kay, S. 2009, *MNRAS*, 394, 1713
- Kitzbichler, M. G., & White, S. D. M. 2008, *MNRAS*, 391, 1489
- Kormendy, J., Fisher, D. B., Cornell, M. E., & Bender, R. 2009, *ApJS*, 182, 216
- Kroupa, P. 2001, *MNRAS*, 322, 231
- Kroupa, P., Tout, C. A., & Gilmore, G. 1993, *MNRAS*, 262, 545
- Lacey, C., & Cole, S. 1993, *MNRAS*, 262, 627
- . 1994, *MNRAS*, 271, 676
- Lambas, D. G., Tissera, P. B., Alonso, M. S., & Coldwell, G. 2003, *MNRAS*, 346, 1189

- Le Fèvre, O., Abraham, R., Lilly, S. J., Ellis, R. S., Brinchmann, J., Schade, D., Tresse, L., Colless, M., Crampton, D., Glazebrook, K., Hammer, F., & Broadhurst, T. 2000, *MNRAS*, 311, 565
- Le Floch, E., Papovich, C., Dole, H., Bell, E. F., Lagache, G., Rieke, G. H., Egami, E., Pérez-González, P. G., Alonso-Herrero, A., Rieke, M. J., Blaylock, M., Engelbracht, C. W., Gordon, K. D., Hines, D. C., Misselt, K. A., Morrison, J. E., & Mould, J. 2005, *ApJ*, 632, 169
- Lehmer, B. D., Brandt, W. N., Alexander, D. M., Bell, E. F., Hornschemeier, A. E., McIntosh, D. H., Bauer, F. E., Gilli, R., Mainieri, V., Schneider, D. P., Silverman, J. D., Steffen, A. T., Tozzi, P., & Wolf, C. 2008, *ApJ*, 681, 1163
- Li, C., Kauffmann, G., Heckman, T. M., Jing, Y. P., & White, S. D. M. 2008, *MNRAS*, 385, 1903
- Li, C., Kauffmann, G., Jing, Y. P., White, S. D. M., Börner, G., & Cheng, F. Z. 2006a, *MNRAS*, 368, 21
- Li, C., Kauffmann, G., Wang, L., White, S. D. M., Heckman, T. M., & Jing, Y. P. 2006b, *MNRAS*, 373, 457
- Lilly, S. J., Le Fevre, O., Hammer, F., & Crampton, D. 1996, *ApJ*, 460, L1+
- Lin, L., Koo, D. C., Weiner, B. J., Chiueh, T., Coil, A. L., Lotz, J., Conselice, C. J., Willner, S. P., Smith, H. A., Guhathakurta, P., Huang, J., Le Floch, E., Noeske, K. G., Willmer, C. N. A., Cooper, M. C., & Phillips, A. C. 2007, *ApJ*, 660, L51
- Lin, L., Koo, D. C., Willmer, C. N. A., Patton, D. R., Conselice, C. J., Yan, R., Coil, A. L., Cooper, M. C., Davis, M., Faber, S. M., Gerke, B. F., Guhathakurta, P., & Newman, J. A. 2004, *ApJ*, 617, L9
- Lin, L., Patton, D. R., Koo, D. C., Casteels, K., Conselice, C. J., Faber, S. M., Lotz, J., Willmer, C. N. A., Hsieh, B. C., Chiueh, T., Newman, J. A., Novak, G. S., Weiner, B. J., & Cooper, M. C. 2008, *ApJ*, 681, 232
- Lisker, T. 2008, *ApJS*, 179, 319
- Lotz, J. M., Primack, J., & Madau, P. 2004, *AJ*, 128, 163
- Madau, P., Ferguson, H. C., Dickinson, M. E., Giavalisco, M., Steidel, C. C., & Fruchter, A. 1996, *MNRAS*, 283, 1388

- Markevitch, M., Gonzalez, A. H., Clowe, D., Vikhlinin, A., Forman, W., Jones, C., Murray, S., & Tucker, W. 2004, *ApJ*, 606, 819
- Masjedi, M., Hogg, D. W., & Blanton, M. R. 2008, *ApJ*, 679, 260
- Masjedi, M., Hogg, D. W., Cool, R. J., Eisenstein, D. J., Blanton, M. R., Zehavi, I., Berlind, A. A., Bell, E. F., Schneider, D. P., Warren, M. S., & Brinkmann, J. 2006, *ApJ*, 644, 54
- McIntosh, D. H., Guo, Y., Hertzberg, J., Katz, N., Mo, H. J., van den Bosch, F. C., & Yang, X. 2008, *MNRAS*, 388, 1537
- Melbourne, J., Koo, D. C., & Le Floch, E. 2005, *ApJ*, 632, L65
- Mihos, J. C., & Hernquist, L. 1994, *ApJ*, 431, L9
- . 1996a, *ApJ*, 464, 641
- . 1996b, *ApJ*, 464, 641
- Miller, S. H., Jogee, S., Conselice, C., Penner, K., Bell, E., Zheng, X., Papovich, C., Skelton, R., Somerville, R., Rix, H., Barazza, F., Barden, M., Borch, A., Beckwith, S., Caldwell, J., Häussler, B., Heymans, C., Robaina, A., Sanchez, S., Zheng, X., Borch, A., Peng, C., Papovich, C., Beckwith, S., McIntosh, D., Caldwell, J., Conselice, C., Haeussler, B., Rix, H., Wolf, C., Somerville, R., Meisenheimer, K., & Wisotzki, L. 2008, in *Astronomical Society of the Pacific Conference Series*, Vol. 393, *New Horizons in Astronomy*, ed. A. Frebel, J. R. Maund, J. Shen, & M. H. Siegel, 235–+
- Noeske, K. G., Weiner, B. J., Faber, S. M., Papovich, C., Koo, D. C., Somerville, R. S., Bundy, K., Conselice, C. J., Newman, J. A., Schiminovich, D., Le Floch, E., Coil, A. L., Rieke, G. H., Lotz, J. M., Primack, J. R., Barmby, P., Cooper, M. C., Davis, M., Ellis, R. S., Fazio, G. G., Guhathakurta, P., Huang, J., Kassin, S. A., Martin, D. C., Phillips, A. C., Rich, R. M., Small, T. A., Willmer, C. N. A., & Wilson, G. 2007, *ApJ*, 660, L43
- Ostriker, J. P., & Peebles, P. J. E. 1973, *ApJ*, 186, 467
- Pannella, M., Gabasch, A., Goranova, Y., Drory, N., Hopp, U., Noll, S., Saglia, R. P., Strazzullo, V., & Bender, R. 2009, *ApJ*, 701, 787
- Papovich, C., & Bell, E. F. 2002, *ApJ*, 579, L1
- Papovich, C., Dole, H., Egami, E., Le Floch, E., Pérez-González, P. G., Alonso-Herrero, A., Bai, L., Beichman, C. A., Blaylock, M., Engelbracht, C. W., Gordon, K. D., Hines, D. C., Misselt, K. A., Morrison, J. E., Mould, J., Muzerolle, J., Neugebauer, G.,

- Richards, P. L., Rieke, G. H., Rieke, M. J., Rigby, J. R., Su, K. Y. L., & Young, E. T. 2004, *ApJS*, 154, 70
- Patton, D. R., & Atfield, J. E. 2008, *ApJ*, 685, 235
- Patton, D. R., Carlberg, R. G., Marzke, R. O., Pritchett, C. J., da Costa, L. N., & Pellegrini, P. S. 2000, *ApJ*, 536, 153
- Peebles, P. J. E. 1980, *The large-scale structure of the universe*, ed. P. J. E. Peebles
- Peebles, P. J. E., & Groth, E. J. 1976, *A&A*, 53, 131
- Pérez-González, P. G., Trujillo, I., Barro, G., Gallego, J., Zamorano, J., & Conselice, C. J. 2008, *ApJ*, 687, 50
- Perlmutter, S., Aldering, G., Goldhaber, G., Knop, R. A., Nugent, P., Castro, P. G., Deustua, S., Fabbro, S., Goobar, A., Groom, D. E., Hook, I. M., Kim, A. G., Kim, M. Y., Lee, J. C., Nunes, N. J., Pain, R., Pennypacker, C. R., Quimby, R., Lidman, C., Ellis, R. S., Irwin, M., McMahon, R. G., Ruiz-Lapuente, P., Walton, N., Schaefer, B., Boyle, B. J., Filippenko, A. V., Matheson, T., Fruchter, A. S., Panagia, N., Newberg, H. J. M., Couch, W. J., & The Supernova Cosmology Project. 1999, *ApJ*, 517, 565
- Press, W. H., & Schechter, P. 1974, *ApJ*, 187, 425
- Ramos Almeida, C., Pérez García, A. M., Acosta-Pulido, J. A., & Rodríguez Espinosa, J. M. 2007, *AJ*, 134, 2006
- Riess, A. G., Filippenko, A. V., Challis, P., Clocchiatti, A., Diercks, A., Garnavich, P. M., Gilliland, R. L., Hogan, C. J., Jha, S., Kirshner, R. P., Leibundgut, B., Phillips, M. M., Reiss, D., Schmidt, B. P., Schommer, R. A., Smith, R. C., Spyromilio, J., Stubbs, C., Suntzeff, N. B., & Tonry, J. 1998, *AJ*, 116, 1009
- Risaliti, G., Maiolino, R., & Salvati, M. 1999, *ApJ*, 522, 157
- Rix, H., Barden, M., Beckwith, S. V. W., Bell, E. F., Borch, A., Caldwell, J. A. R., Häussler, B., Jahnke, K., Jogee, S., McIntosh, D. H., Meisenheimer, K., Peng, C. Y., Sanchez, S. F., Somerville, R. S., Wisotzki, L., & Wolf, C. 2004, *ApJS*, 152, 163
- Robaina, A. R., & Cepa, J. 2007, *A&A*, 464, 465
- Robertson, B., Bullock, J. S., Cox, T. J., Di Matteo, T., Hernquist, L., Springel, V., & Yoshida, N. 2006, *ApJ*, 645, 986
- Roussel, H., Sauvage, M., Vigroux, L., & Bosma, A. 2001, *A&A*, 372, 427

- Ruhland, C., Bell, E. F., Häußler, B., Taylor, E. N., Barden, M., & McIntosh, D. H. 2009, *ApJ*, 695, 1058
- Sanders, D. B., Soifer, B. T., Elias, J. H., Madore, B. F., Matthews, K., Neugebauer, G., & Scoville, N. Z. 1988, *ApJ*, 325, 74
- Schweizer, F., & Seitzer, P. 1992, *AJ*, 104, 1039
- Scoville, N., Aussel, H., Brusa, M., Capak, P., Carollo, C. M., Elvis, M., Giavalisco, M., Guzzo, L., Hasinger, G., Impey, C., Kneib, J.-P., LeFevre, O., Lilly, S. J., Mobasher, B., Renzini, A., Rich, R. M., Sanders, D. B., Schinnerer, E., Schminovich, D., Shopbell, P., Taniguchi, Y., & Tyson, N. D. 2007, *ApJS*, 172, 1
- Silk, J., & Rees, M. J. 1998, *A&A*, 331, L1
- Silva, L., Maiolino, R., & Granato, G. L. 2004, *MNRAS*, 355, 973
- Skelton, R. E., Bell, E. F., & Somerville, R. S. 2009, *ApJ*, 699, L9
- Skibba, R., Sheth, R. K., Connolly, A. J., & Scranton, R. 2006, *MNRAS*, 369, 68
- Skibba, R. A., & Sheth, R. K. 2009, *MNRAS*, 392, 1080
- Somerville, R. S., Hopkins, P. F., Cox, T. J., Robertson, B. E., & Hernquist, L. 2008, *MNRAS*, 391, 481
- Somerville, R. S., Primack, J. R., & Faber, S. M. 2001, *MNRAS*, 320, 504
- Spergel, D. N., Bean, R., Doré, O., Nolta, M. R., Bennett, C. L., Dunkley, J., Hinshaw, G., Jarosik, N., Komatsu, E., Page, L., Peiris, H. V., Verde, L., Halpern, M., Hill, R. S., Kogut, A., Limon, M., Meyer, S. S., Odegard, N., Tucker, G. S., Weiland, J. L., Wollack, E., & Wright, E. L. 2007, *ApJS*, 170, 377
- Spinoglio, L., Malkan, M. A., Rush, B., Carrasco, L., & Recillas-Cruz, E. 1995, *ApJ*, 453, 616
- Springel, V. 2000, *MNRAS*, 312, 859
- Springel, V., White, S. D. M., Jenkins, A., Frenk, C. S., Yoshida, N., Gao, L., Navarro, J., Thacker, R., Croton, D., Helly, J., Peacock, J. A., Cole, S., Thomas, P., Couchman, H., Evrard, A., Colberg, J., & Pearce, F. 2005, *Nature*, 435, 629
- Taylor, E. N., Franx, M., G van Dokkum, P., Bell, E. F., Brammer, G. B., Rudnick, G., Wuyts, S., Gawiser, E., Lira, P., Urry, C. M., & Rix, H.-W. 2009, *ApJ*, 694, 1171

- Tissera, P. B., Domínguez-Tenreiro, R., Scannapieco, C., & Sáiz, A. 2002, *MNRAS*, 333, 327
- Toomre, A., & Toomre, J. 1972, *ApJ*, 178, 623
- Trager, S. C., Faber, S. M., Worthey, G., & González, J. J. 2000, *AJ*, 119, 1645
- van der Wel, A., Rix, H., Holden, B. P., Bell, E. F., & Robaina, A. R. 2009, ArXiv e-prints
- van Dokkum, P. G. 2005, *AJ*, 130, 2647
- van Dokkum, P. G., & van der Marel, R. P. 2007, *ApJ*, 655, 30
- Walcher, C. J., Lamareille, F., Vergani, D., Arnouts, S., Buat, V., Charlot, S., Tresse, L., Le Fèvre, O., Bolzonella, M., Brinchmann, J., Pozzetti, L., Zamorani, G., Bottini, D., Garilli, B., Le Brun, V., Maccagni, D., Milliard, B., Scaramella, R., Scodreggio, M., Vettolani, G., Zanichelli, A., Adami, C., Bardelli, S., Cappi, A., Ciliegi, P., Contini, T., Franzetti, P., Foucaud, S., Gavignaud, I., Guzzo, L., Ilbert, O., Iovino, A., McCracken, H. J., Marano, B., Marinoni, C., Mazure, A., Meneux, B., Merighi, R., Paltani, S., Pellò, R., Pollo, A., Radovich, M., Zucca, E., Lonsdale, C., & Martin, C. 2008, *A&A*, 491, 713
- Wolf, C., Bell, E. F., McIntosh, D. H., Rix, H., Barden, M., Beckwith, S. V. W., Borch, A., Caldwell, J. A. R., Häussler, B., Heymans, C., Jahnke, K., Jogee, S., Meisenheimer, K., Peng, C. Y., Sánchez, S. F., Somerville, R. S., & Wisotzki, L. 2005, *ApJ*, 630, 771
- Wolf, C., Meisenheimer, K., Kleinheinrich, M., Borch, A., Dye, S., Gray, M., Wisotzki, L., Bell, E. F., Rix, H., Cimatti, A., Hasinger, G., & Szokoly, G. 2004, *A&A*, 421, 913
- Wolf, C., Meisenheimer, K., Rix, H., Borch, A., Dye, S., & Kleinheinrich, M. 2003, *A&A*, 401, 73
- Xu, C. K., Sun, Y. C., & He, X. T. 2004, *ApJ*, 603, L73
- Zehavi, I., Weinberg, D. H., Zheng, Z., Berlind, A. A., Frieman, J. A., Scoccamarro, R., Sheth, R. K., Blanton, M. R., Tegmark, M., Mo, H. J., Bahcall, N. A., Brinkmann, J., Burles, S., Csabai, I., Fukugita, M., Gunn, J. E., Lamb, D. Q., Loveday, J., Lupton, R. H., Meiksin, A., Munn, J. A., Nichol, R. C., Schlegel, D., Schneider, D. P., SubbaRao, M., Szalay, A. S., Uomoto, A., & York, D. G. 2004, *ApJ*, 608, 16
- Zheng, X. Z., Bell, E. F., Papovich, C., Wolf, C., Meisenheimer, K., Rix, H., Rieke, G. H., & Somerville, R. 2007a, *ApJ*, 661, L41
- Zheng, X. Z., Dole, H., Bell, E. F., Le Floch, E., Rieke, G. H., Rix, H., & Schiminovich, D. 2007b, *ApJ*, 670, 301
- Zwicky, F. 1933, *Helvetica Physica Acta*, 6, 110